The Role of *N*-linked Glycosylation on the Structure and Function of Somatic Angiotensin-Converting Enzyme

Karabelo M. Nkoe

Thesis Presented for the degree of:

Masters of Science in Medicine

in the Division of Medical Biochemistry
University of Cape Town

February 2014

Supervisor: Prof. E.D. Sturrock

Acknowledgements

I would like to thank my supervisor, Prof. E.D Sturrock for his great leadership, guidance and mentorship. Completing a challenging project like this would not have been possible had it not been for his support, inappreciable help and patience through the trials and tribulations.

A very special mention has to go to Sylva Schwager. Her presence in the lab made it a very pleasant place to work, especially through the seemingly unbearable times. More importantly, the support and love I got from her has been cherishable.

I would like to thank the ACE lab members Kate, Nailah, Palesa, Albert, Lizelle, Vinasha, and Afolake for the invaluable advice, interesting talks and the occasional escape from reality.

I owe my deepest gratitude to my family, Mantoa, Katleho and Paballo and to my father, the late L.J Nkoe, whom I know, would have been very proud. Not forgetting Mafole, who has made his support, motivation and guidance available in a number of ways.

Many thanks go to my friends, Makhethe, Sihlalo, Boikokobetso, Rufaro, Itumeleng and everyone else for their active encouragement through the difficult times, the moral support, love and preservation of sanity. I certainly would not have made it this far if it were not for them.

A very special thank you goes to God, for without Him, none of this would have been possible.

Finally, I send my gratitude to my funders, The German Academic Exchange Service (DAAD), the National Research Foundation and the University of Cape Town.

Abbreviations

A-beta42 - amyloid-β protein1-42

ACE - angiotensin-I converting enzyme

AcSDKP - N-acetyl-Ser-Asp-Lys-Pro

AngI - angiotensin I

AngII - angiotensin II

Asn - asparagine

BK - bradykinin

CHO-K1 - Chinese hamster ovary K1

CRT - calreticulin

CNX - calnexin

CVD - cardiovascular disease

DMEM - Dulbecco's modified Eagle's medium

DMSO - dimethyl sulphoxide

E. coli - *Escherichia coli*

EDEM - ER degradation enhancing α-mannosidase-like protein

EDTA - ethylenediaminetetraacetic acid

ER - endoplasmic reticulum

ERAD - ER associated degradation pathway

ERGIC-53 - ER Golgi intermediate compartment

ERp57 - ER protein 57

FCS - fetal calf serum

Gal - galactose

Gln - glutamine

GlcNAc - N-acetyl glucosamines

GnRH - gonadotropin-releasing hormone

HEPES - N-2-hydroxyethylpiperazine-N'-2-ethanesulphonic Acid

KKS - kallikrein-kinin system

LH - luteinizing hormone

NeuAc - sialic acid

OST - oligosaccharidal transferase complex

PBS - phosphate-buffered saline

PCR - polymerase chain reaction

PDB - Protein Data Bank

PMSF - phenylmethylsulphonyl fluoride

PD – pixel density

RAAS - Renin angiotensin aldosterone system

sACE - somatic ACE

SDS-PAGE - sodium dodecyl sulphate polyacrylamide gel electrophoresis

tACE - testis ACE

Ser - Serine

Thr - Threonine

Tris - tris-(hydroxymethyl)-aminomethane

VIP36 - Vesicular integral protein 36

VIPL - VIP36-like protein

WT - wild-type

Z-FHL - Z-Phe-His-Leu

Abstract

Angiotensin converting enzyme (ACE) is a key regulator of blood pressure and comprised of two homologous domains (N- and C-domain), both of which are glycosylated. *N*-linked glycosylation is important for the processing, expression and stability of ACE, but it interferes with protein crystallization. Previously, the *N*-glycan site occupancy required for the expression and stability of the individual domains of ACE was determined using minimally glycosylated (MG) N- and C-domain isoforms. However the role of glycosylation in the structure and function of the full-length somatic ACE (sACE) has remained elusive. A novel MG-sACE mutant, comprised of previously characterized MG N- and C-domains was generated. Unfortunately, the protein was susceptible to limited proteolysis in the inter-domain linker region, suggesting that key glycans might shield the linker region from proteolysis. Furthermore, a loss in expression of MG-sACE was observed. These observations prompted the investigation of the effect of *N*-glycosylation on protection from inter-domain linker proteolysis, expression and overall stability of sACE. These aims were addressed by generating a panel of sACE glycosylation mutants. The minimal glycosylation requirements for an MG-sACE mutant that was least susceptible to inter-domain linker proteolysis was found to be six intact glycosylation sites (N25, N45, N416, N666 and N685). Furthermore, we determined that *N*-glycans on the C-domain confer most of sACE's resistance to proteolysis. Surprisingly, the presence of glycosylation site 2 (N25) resulted in a sharp increase in MG-sACE linker proteolysis, which was blunted significantly by the presence of site 6 (N131) and site 12 (N666). Additionally, while site 2 (N25) had no effect on MG-sACE expression, site 6 (N131) was found to be crucial for sACE expression and the thermal stability of sACE. Furthermore, site 6 (N131) was able to rescue the thermal stability of the least stable MG-sACE (from 9% to 20% remaining enzymatic activity). A combination of *N*-glycans N45, N131, N480, N666 and N685 produced an MG-sACE mutant with substantially reduced inter-domain linker proteolysis. We also determined that MG-sACE mutants were functionally comparable to wild-type sACE in terms of their K_m and k_{cat} values.

Finally, inter-domain linker proteolysis was found to occur intracellularly, evidenced by the secretion of the N-domain to the extracellular milieu, intracellular retention and degradation of both the N- and C-domains, and exportation of MG-sACE to the cell surface. This work enhances our understanding of the glycosylation requirements of somatic ACE and provides a solid foundation for obtaining a stable, high expressing MG-sACE mutant that has the potential to generate the first full-length sACE crystal structure.

Table of Contents

Chapter 1: Introduction

1.1 ANGIOTENSIN CONVERTING ENZYME (ACE)

Angiotensin-converting enzyme (ACE), also known as peptidyl-dipeptidase A, is a zinc metalloprotease grouped under the M2 family of the MA clan sharing a single evolutionary ancestor (Acharya *et al.*, 2003; Coates, 2003). ACE was first discovered in mid-1950s by Skeggs and colleagues (Skeggs, 1993; Skeggs, Kahn*, et al.*, 1956). This discovery arose from research that was being conducted on Renin, the first enzyme in the Renin angiotensin aldosterone system (RAAS) (see section 1.1.3). Here, Skeggs was able to purify two products, now known as angiotensin I (AngI) (hypertensin I) and angiotensin II (AngII) (hypertensin II) (Skeggs *et al.*, 1954). It was soon discovered that AngI was a product of Renin and AngII was a product of a hypertensin-converting enzyme (Skeggs, Kahn*, et al.*, 1956; Skeggs *et al.*, 1954), now known as ACE. Additional investigations resulted in a significant body of information on ACE, which facilitated a better understanding of the RAAS (Bumpus *et al.*, 1957; Elliott *et al.*, 1956; Rittel, 1957; Skeggs, Lentz*, et al.*, 1956). We now know that ACE displays its diversity by playing important roles in several physiological processes, the most notable of which are the kallikrein-kinin system (KKS) (E. G. Erdos, 2006; Yang *et al.*, 1967) and the abovementioned RAAS (Bernstein *et al.*, 2013; Campbell, 2001; Fyhrquist *et al.*, 2008).

1.1.1 The ACE Gene

The human ACE gene is located on the chromosomal locus 17q23, spanning 21 kilobases with 26 exons (Hakkarainen *et al.*, 2012). ACE has two isoforms, somatic ACE (sACE), expressed universally in somatic tissues and testis ACE (tACE), expressed only in the male spermatozoa (Tigerstedt *et al.*, 2009; Tigerstedt *et al.*, 2010). These isoforms are the result of two distinct promoter regions in the 4024 nucleotide ACE gene, the first of which is located upstream of the ACE gene, responsible for initiating the transcription of a 4.3-

kilobase sACE mRNA, and the second is located in intron 12, initiating the transcription of a 3.0-kilobase tACE mRNA (Langford *et al.*, 1991; Soubrier *et al.*, 1988) (Figure 1.1).

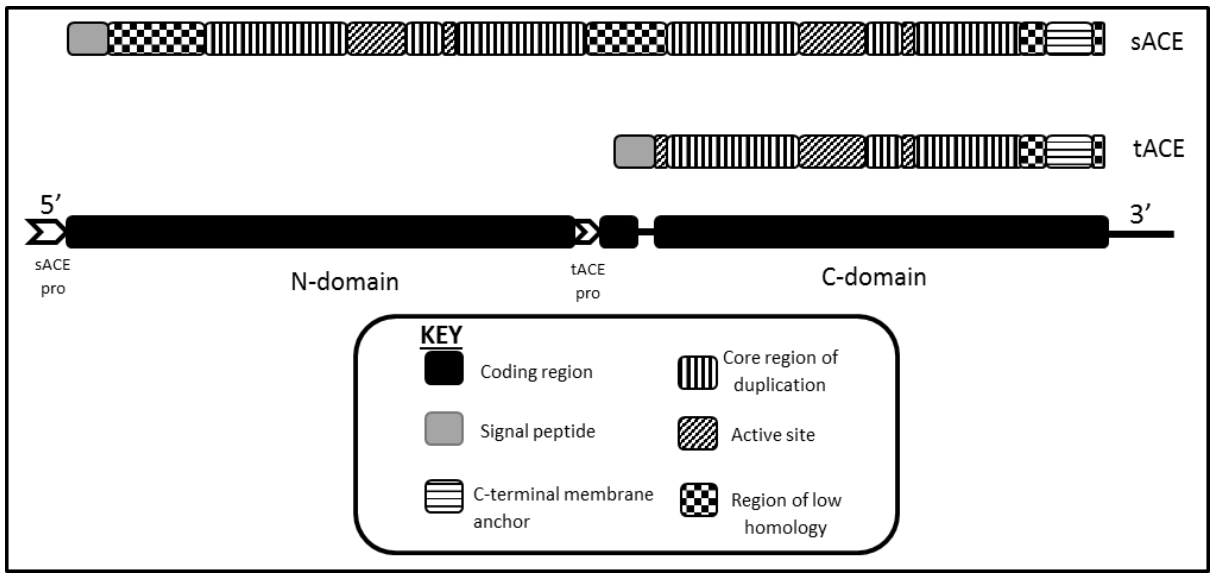

Figure 1.1: Diagrammatic representation of the ACE gene and protein structure. sACE is composed of two domains which are expressed off the somatic promoter region (sACE pro) upstream of the complete gene. tACE is the genetic and peptide equivalent of the C-domain of sACE and a result of an internal testis ACE promoter (tACE pro). Protein sequences that show high sequence homology are indicated with vertical stripes, active site(s) are indicated with diagonal stripes, in close proximity to the zinc binding site. N-terminal signalling peptides are indicated in grey and C-terminal hydrophobic membrane anchor region is indicated with horizontal stripes (Adapted from Coates et al. 2003.).

1.1.2 Structural properties

Human sACE cloning was first completed in 1988 by Soubrier and colleagues. It was found that immature human sACE is synthesized as a 1306 amino acid chain, with a 29 amino acid containing signal peptide (Soubrier *et al.*, 1988). The resultant mature enzyme is 146.6 kDA (predicted mass) and contains 1277 amino acids (Soubrier *et al.*, 1988). sACE is a highly conserved enzyme between eukaryotes, sharing protein sequence homology of 84.37% with porcine, 83.35% with rat, 82.21% with mouse, 83.80% with chimpanzee, and 84.49% with bovine sACE homologues (Figure 1.2). The sACE isoform is comprised of two homologous domains termed the N- and the C- domain, joined by a short inter-domain linker region. These domains display 60% amino acid sequence homology and both are catalytically active with a HEMGH, zinc dependent active site motif. However, they have different substrate, inhibitor, functional and chloride ion dependency profiles (Acharya *et al.*, 2003; Bernstein *et al.*, 2013; Coates, 2003; Lambert *et al.*, 2010). tACE is identical to the C-domain of sACE

with a short 36-amino acid peptide located at the N-terminus of the isoform (Acharya *et al.*, 2003; Coates, 2003; Lambert *et al.*, 2010; Langford *et al.*, 1991).

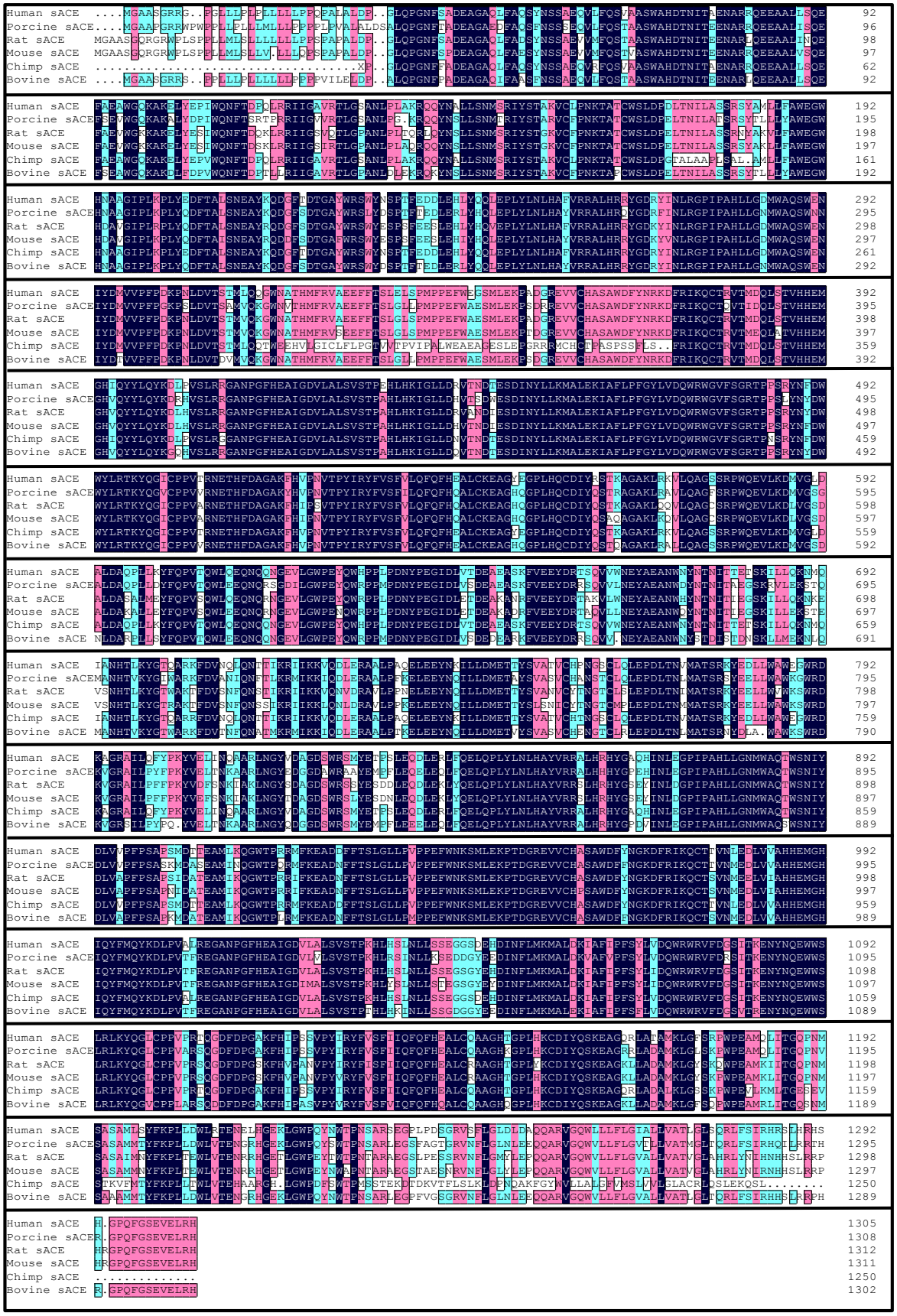

Figure 1.2 : Multiple sequence alignment of human, porcine, rat, mouse, chimp and bovine sACE's. Navy blue indicates regions of 100% homology, pink indicates regions of ≥ 75% and turquoise indicates regions of ≥ 50% across species.

1.1.1.2 N- and C-domain structures

The first N- and C-domain structures solved were obtained via the expression of the constructs in the presence of an α-glucosidase-I inhibitor (N-butyldeoxy-nojirimycin (NB-DNJ)), which prevents the post-translational addition of complex oligosaccharides, limiting it only to the *N*-glycan backbone and thus allowing sufficient processing of the protein (Corradi *et al.*, 2006; Natesh *et al.*, 2003) (see section 1.2.2). As successful as this approach was, the potential loss of protein expression and the elevated cost prompted the development of a cheaper and more reliable method of generating reproducibly crystallisable sACE constructs. To this end, minimally glycosylated individual domains (N-domain with glycosylation sites 3 (Asn45), 8 (Asn416) and 9 (Asn480) (Anthony *et al.*, 2010), and C-domain with glycosylation sites 11 (Asn648) and 13 (Asn685) (Gordon *et al.*, 2003)) were generated via site directed mutagenesis (SDM) and subsequently resulted in the high resolution crystal structures (Figure 1.3).

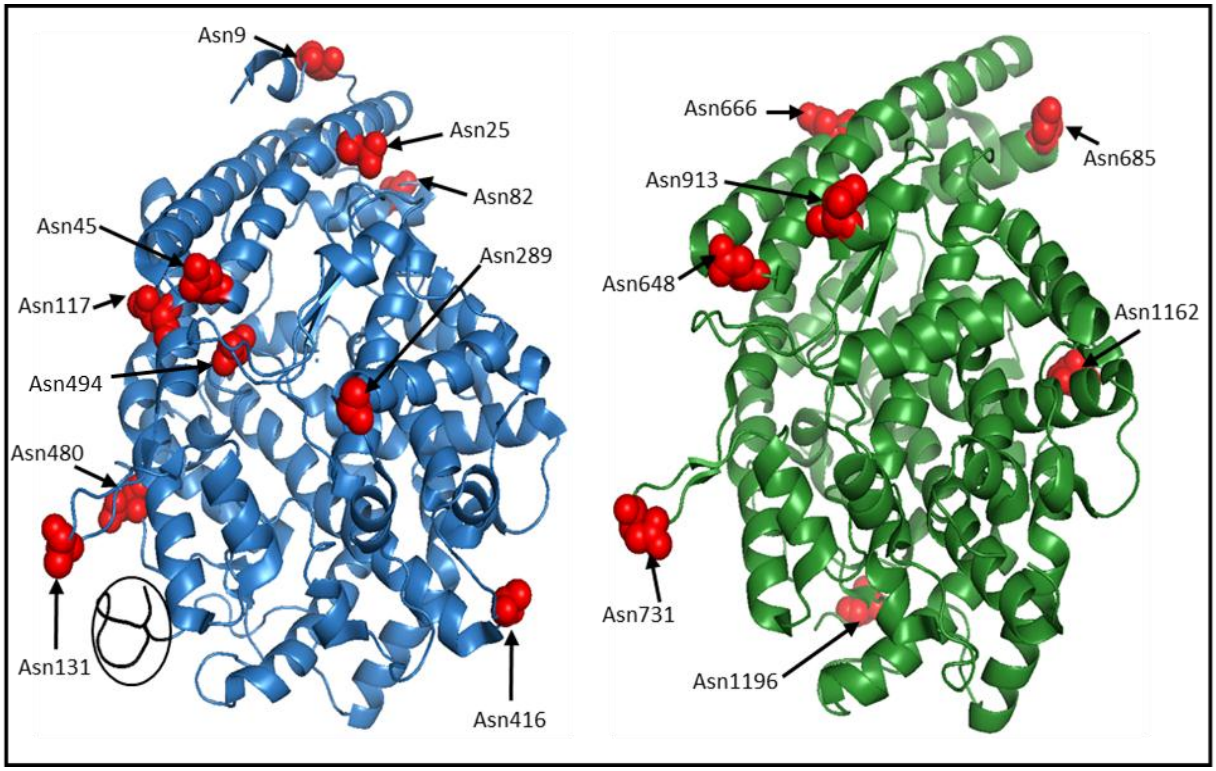

Figure 1.3: Three-dimensional X-ray crystal structures of the N-domain (blue) and the C-domain (green) (PDB accession numbers: 2C6F and 1O86, respectively). Potential *N*-glycosylation sites are indicated in red with their respective residue numbers. The inter-domain linker region is indicated in black (circle). *N*-glycans at positions Asn45, Asn416, Asn480, Asn648 and Asn685 are present in the crystal structures (somatic ACE numbering).

To date, a number of individual domain structures have been co-crystallized with synthetic and natural inhibitors of sACE (Akif, Masuyer*, et al.*, 2011; Akif, Schwager*, et al.*, 2011; Douglas *et al.*, 2014; Masuyer *et al.*, 2012; Watermeyer *et al.*, 2010).

1.1.1.3 Full-length sACE structural model

Although the high resolution 3D crystal structure of the full-length sACE has been elusive, Chen *et.al* have successfully solved a 3D electron microscope structure of porcine ACE fitted to the above mentioned human N- and C-domains (Chen *et al.*, 2010). As previously mentioned, human and porcine sACE share a high level of protein sequence homology, making the predicted reconstruction of sACE fairly reliable. In this study, the low resolution model of 2.3 nm was sufficient to show the spatial arrangement of the domains, including the inter-domain linker region (Chen *et al.*, 2010). Interestingly, the model also highlighted the proposed hinge-movement important during substrate binding (Towler *et al.*, 2004). This was particularly evident in the C-domain displaying it in its “open” conformation. Furthermore, the active sites of both domains were distinct in volume, and the domains were orientated at an incline of about 60°, separated by the approximately 2.0-2.5 nm long inter-domain linker. These data combined show sACE beginning with the N-domain residue Leu1 and spanning a further 600 residues to the beginning of the inter-domain linker region at Pro602 (Acharya *et al.*, 2003; Anthony, 2011) (Figure 1.4).

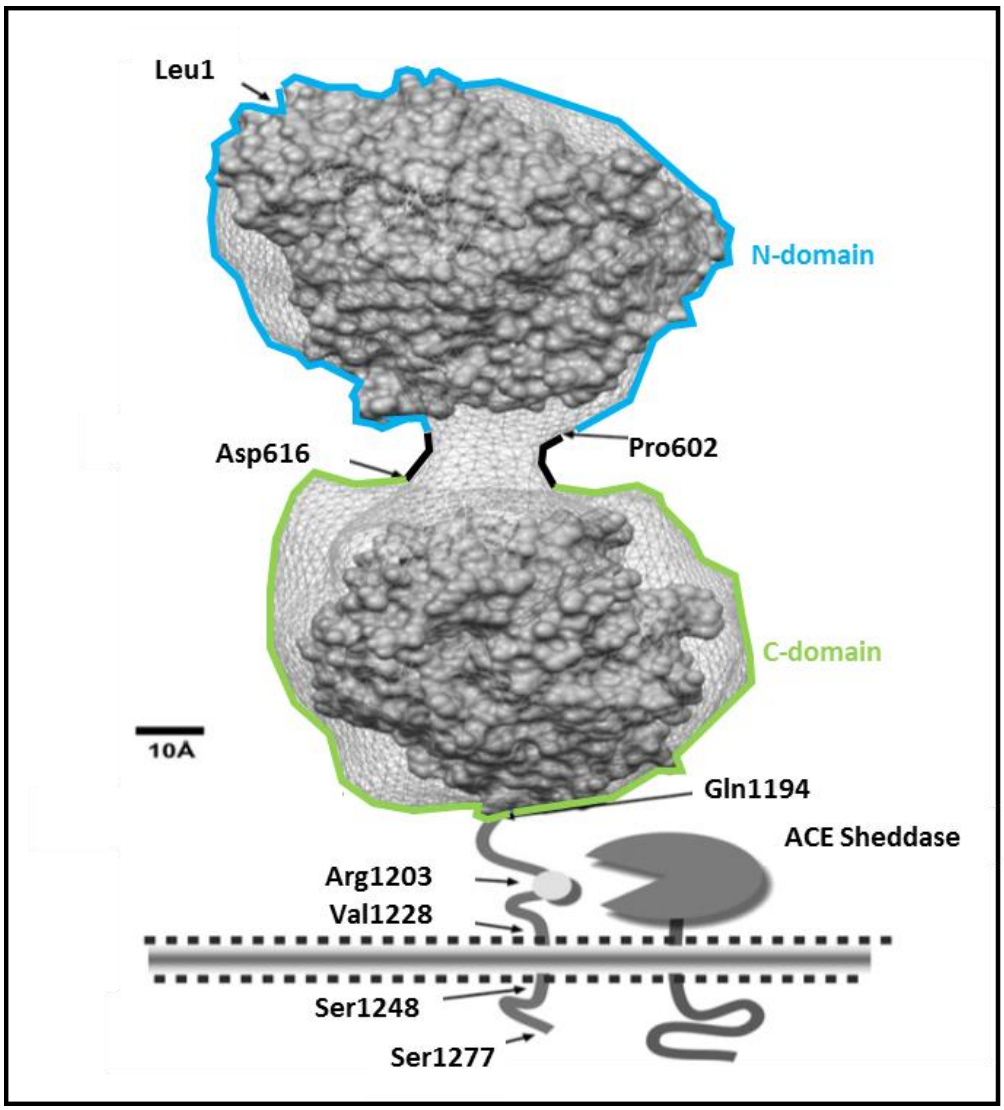

Figure 1.4: Three-dimensional reconstructed model of human sACE. The model was reconstructed from the electron microscopic structure (net) of porcine ACE combined with the individual X-ray crystal structures of human sACE (Chen, Lunsdorf et al. 2010, Danilov, Gordon et al. 2011). The N-domain is indicated in blue spanning from Leu1 to Pro601. The inter-domain linker region is indicated in black spanning from Pro602 to Asp616. The C-domain is indicated in green, spanning from Glu617 to Pro1193. The stalk region spans from Gln1194 to Arg1227. The transmembrane region spans from Val1228 to Ser1248. The cytoplasmic tail spans from Gln1249 to Ser1277. The ACE sheddase is also indicated on the diagram. (Adapted from Bernstein *et. al.* 2013).

The N-domain active site motif, HEMGH spans from 361-365, with the zinc coordinating residues His361 and His365, and the downstream Glu389. The inter-domain linker region spans a total of 15 amino acid residues, inclusive of the tripeptide, Leu613-Val614-Thr615, which is absent in the crystal structures of the individual domains. The C-domain begins at Glu617 and ends at Pro1193 (Corradi *et al.*, 2006; Gordon *et al.*, 2003; Natesh *et al.*, 2003).

This region includes the HEMGH (959-963) active site motif and the zinc coordinating residue Glu987. It is then followed by the 34-amino acid stalk region (Gln1194-Arg1227) which contains the Arg1203 sheddase cleavage site (Danilov *et al.*, 2011; Woodman *et al.*, 2005). A hydrophobic transmembrane region extends from Val1228 to Ser1248, followed by the cytoplasmic tail (Gln1249-Ser1277).

1.1.3 Biological roles of sACE

ACE's two domain structure make it versatile in the hydrolysis of diverse peptides. It's native structure and cellular location also allows for involvement in other important physiological roles. ACE is a zinc dependent (Wei *et al.*, 1991) dipeptidyl carboxypeptidase (Lentz *et al.*, 1956; Soffer *et al.*, 1978) and an endopeptidase (Jaspard *et al.*, 1993).

1.1.3.1 Traditional roles

The most notable role of ACE has been in blood pressure regulation through the RAAS and the KKS. Briefly, the aspartic protease, Renin, catalyses the cleavage of angiotensinogen to the decapeptide AngI. ACE then converts of AngI to the vasoconstrictive octapeptide AngII through its dipeptidyl peptidase function, while simultaneously converting the vasodilator bradykinin (BK) to its inactive fragment BK_{1-7} (Figure 1.5).

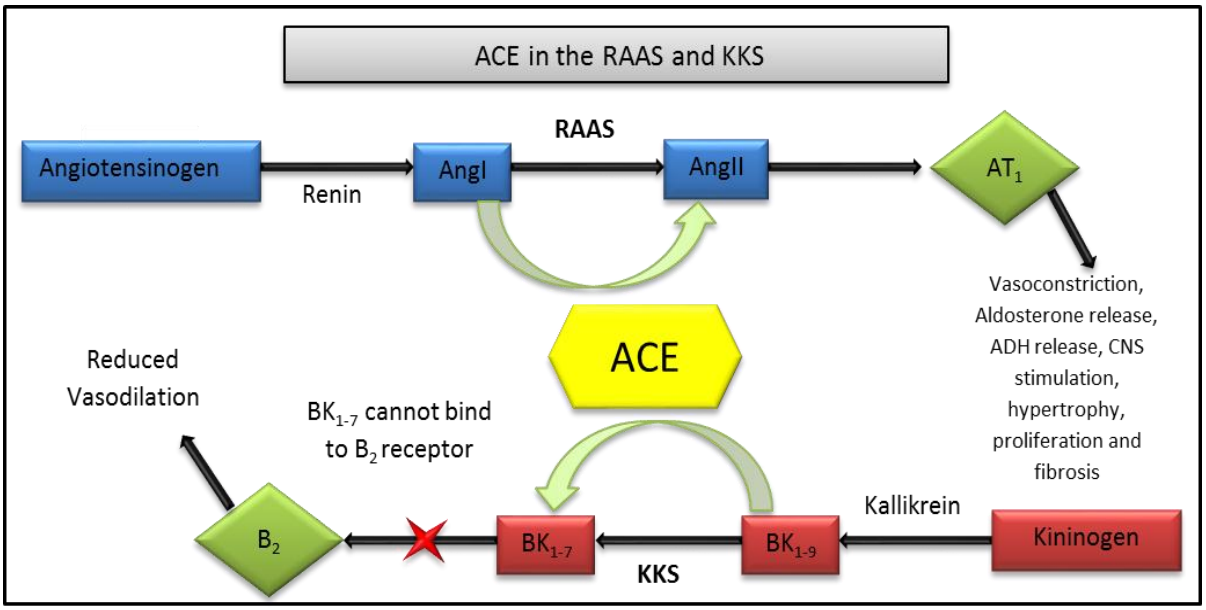

Figure 1.5: Overview of the central role of ACE in blood pressure regulation. AngI – Angiotensin I, AngII – Angiotensin II, AT_1 – Angiotensin II type I receptor, ADH- Antidiuretic Hormone, BK_{1-9} – Bradykinin (active), BK_{1-7} – Bradykinin (inactive) and B_2 – Bradykinin receptor 2.

It is now well known that the primary *in vivo* site of AngI hydrolysis is the C-domain, while both domains hydrolyse BK equally (Bernstein *et al.*, 2011; Fuchs *et al.*, 2004; Fuchs *et al.*, 2008; Junot *et al.*, 2001). Current non-domain selective ACE inhibitors result in BK associated side effects such as angioedema and persistent cough that hamper the efficient treatment of hypertension (Acharya *et al.*, 2003; Bernstein *et al.*, 2011; Ehlers *et al.*, 2013; Kroger *et al.*, 2009). As previously mentioned, tACE is solely synthesized in the testis and has been shown to be crucial for male fertility (Esther *et al.*, 1997; Hagaman *et al.*, 1998). Furthermore, recent evidence has revealed that ACE is essential for the production of fertile spermatozoa through the removal of the GPI-anchored protein TEX10 (Y. Fujihara *et al.*, 2013). The N-domain of sACE is known to hydrolyse a variety of substrates. The most notable of which is the hydrolysis of the naturally occurring anti-fibrotic peptide, *N*-acetyl-seryl-aspartyl-lysyl-proline (Ac-SDKP) (E. G. Erdos *et al.*, 1967; Li *et al.*, 2010; Skeggs, 1993). Gonadotropin-releasing hormone (GnRH), a mediator of the release of follicle stimulating hormone, has been shown to be inactivated by the activity of the N-domain (G. Erdos *et al.*, 2006; Papakyriakou *et al.*, 2007; Taaseh *et al.*, 2011). One striking function of the N-domain is the hydrolysis of the Alzheimer's disease related amyloid-β peptide$_{1\text{-}42}$ (aβ42) to the less detrimental aβ40 (Zou *et al.*, 2009; Zou *et al.*, 2007).

1.1.3.2 Non-traditional roles

A number of studies have recently focused on the non-traditional roles of sACE. A detailed review on this topic is beyond the scope of this thesis but it is covered elegantly by (Gonzalez-Villalobos *et al.*, 2013) and (Bernstein *et al.*, 2013). Briefly, sACE is involved in the in cytokine production evidenced by the reduced levels of TNFα in ACE-null mice (Ong *et al.*, 2012). sACE has also been implicated as a signalling molecule in a number of studies (Fleming, 2006; Guimaraes *et al.*, 2011; Kohlstedt *et al.*, 2004; Kohlstedt *et al.*, 2009; Kohlstedt *et al.*, 2002; Lucero *et al.*, 2010). Another interesting role lies within the immune response where sACE is believed to aid in antigen presentation to the major histocompatibility complex (MHC) class I (Kozlowski *et al.*, 1992; X. Z. Shen *et al.*, 2011; X.

Z. Shen *et al.*, 2008; Sherman *et al.*, 1992). sACE has also been shown to be an important factor in developing hematopoietic tissues of the human embryo and fetus (Jokubaitis *et al.*, 2008; Sinka *et al.*, 2012; Zambidis *et al.*, 2008). Finally myelopoiesis is thought to be regulated by sACE through the hydrolysis of its substrate, substance P (SP), and angiotensin receptor 1 (AT1) signalling, by the upregulation of CCAAT/enhancer-binding protein α, an important stimulator of myelopoiesis (Lin *et al.*, 2011).

1.1.4 ACE inhibitors

ACE inhibition has been used for decades to treat hypertension, with several ACE inhibitors being commercially available, the most widely used being lisinopril. Classic ACE inhibitors are non-selective for the domains of ACE. These have been associated with side effects such as angioedema, persistent cough, loss of taste and skin rash (Bicket, 2002; Coulter *et al.*, 1987; Slater *et al.*, 1988; Speirs *et al.*, 1998). The last two are a result of sulfhydryl group containing inhibitors such as captopril, leading to the rapid avoidance of the use of these inhibitors (Acharya *et al.*, 2003; Adam *et al.*, 2002; Dickstein *et al.*, 2002). Angioedema is an uncommon side effect, affecting up to 0.5% of patients, while persistent cough affects up to 20% of patients (Acharya *et al.*, 2003; Adam *et al.*, 2002; Dickstein *et al.*, 2002). These adverse side effects have been associated with the increased levels of BK, due to the non-selective inhibition of both the N- and C-domain (Acharya *et al.*, 2003; Adam *et al.*, 2002; Dickstein *et al.*, 2002). This has set the platform to develop ACE inhibitors that will selectively inhibit either the N- or the C-domain individually. The C-domain has been shown to be the major cleavage site of AngI, therefore, selective C-domain inhibition will allow the N-domain to continue BK hydrolysis while conversion of AngI to AngII is inhibited, reducing hypertension. While selective N-domain inhibition will result in the reduced hydrolysis of AcSDKP (see section 1.1.3.1) which can be useful in combination therapy with bleomycin, reducing lung fibrotic effects usually observed with this anti-cancer treatment while maintaining normotensive conditions mediated by the activity of the C-domain (Bernstein *et al.*, 2011). Currently, highly selective N- and C-domain inhibitors RXP407 (Junot *et al.*, 2001)

and RXPA380 (Georgiadis *et al.*, 2004) respectively, have been developed. However, RXP407 is not a good candidate due to its low bioavailability. Furthermore, new N- (Douglas *et al.*, 2014) and C-domain (Masuyer *et al.*, 2012) selective inhibitors are currently being studied.

1.2 PROTEIN GLYCOSYLATION

Protein glycosylation is one of the most important post-translational modifications in eukaryotes and has been shown to be involved in a number of key cellular processes such as protein solubility, folding, stability and localization, to name a few (Csala *et al.*, 2012; A. Helenius *et al.*, 2004; Yan *et al.*, 2005). Almost 50% of all eukaryotic proteins are predicted to be glycosylated and 90% of those are *N*-linked (Apweiler *et al.*, 1999).

1.2.1 *O*-linked glycosylation

This process of *O*-linked glycosylation is primarily initiated in the Golgi apparatus and secondarily in the endoplasmic reticulum (ER), resulting in the addition of *N*-acetyl-galactosamine (GlcNAc) to serine or threonine residue through the action of glycosyltransferases, using an activated membrane anchored polyisoprenoid lipid (dolichol (Dol)) bound monosaccharaides as substrates (An *et al.*, 2011; Gill *et al.*, 2010; Mitra *et al.*, 2006). *O*-linked glycans are often found at serine/threonine rich areas with no particular consensus motif.

1.2.2 *N*-linked glycosylation

N-linked glycans are found on the surface of many proteins forming bulkier side chains and occurring much more frequently than *O*-linked glycans (An *et al.*, 2011; Apweiler *et al.*, 1999; Csala *et al.*, 2012; A. Helenius *et al.*, 2004; Imperiali *et al.*, 1999; Mitra *et al.*, 2006). They occur only at the asparagine residue found in the conserved sequence, Asn-Xxx-Thr/Ser (Xxx being any amino acid except proline) (An *et al.*, 2011; Imperiali *et al.*, 1999). Three types of *N*-glycans exist: high mannose, complex and hybrid (Figure 1.6).

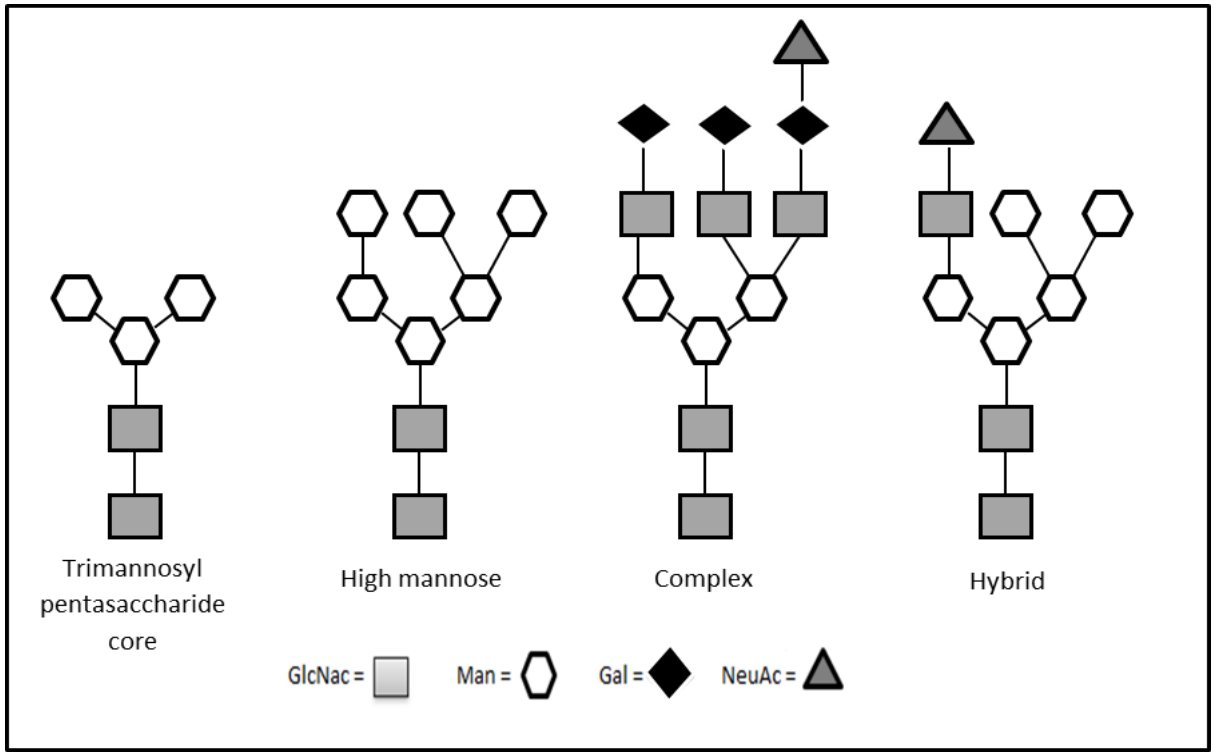

Figure 1.6: Three categories of *N*-linked glycans including the trimannosyl pentasaccharide core backbone. (Adapted from An *et al*. 2011).

High mannose glycans are composed of the trimannosyl pentasaccharide (GlcNac and Tri-Man) backbone bound to a variety of mannose residues (An *et al.*, 2011). Complex glycans include the typical backbone bound to varying residues such as galactose (Gal) or sialic acid (NeuAc) as well as additional GlcNAc residues, responsible for the complex nature (Figure 1.6) (An *et al.*, 2011). The glycan composition of these can be altered considerably due to the presence of a wide range of glycosyltransferases synthesized simultaneously with the

complex glycans. Hybrid glycans include the components of high mannose and complex glycans bound to the typical pentasaccharide backbone (Figure 1.6). However these glycans can have additional GlcNac, Gal, NeuAc and fucose residues added during synthesis (An *et al.*, 2011). *N*-linked glycans are synthesized partially in the cytosol and then in the ER by an oligosaccharyltransferase using dolichyl pyrophosphate (Dol-PP) bound nucleotide sugars as substrates to add residues to the glycan backbone (Jones *et al.*, 2005). When all residues of the glycan have been added, the intermediate $Man_5GlcNAc_2$-Dol-PP, is flipped into ER lumen by flippases that are very well characterized, but yet to be identified (J. Helenius *et al.*, 2002) (Figure 1.7).

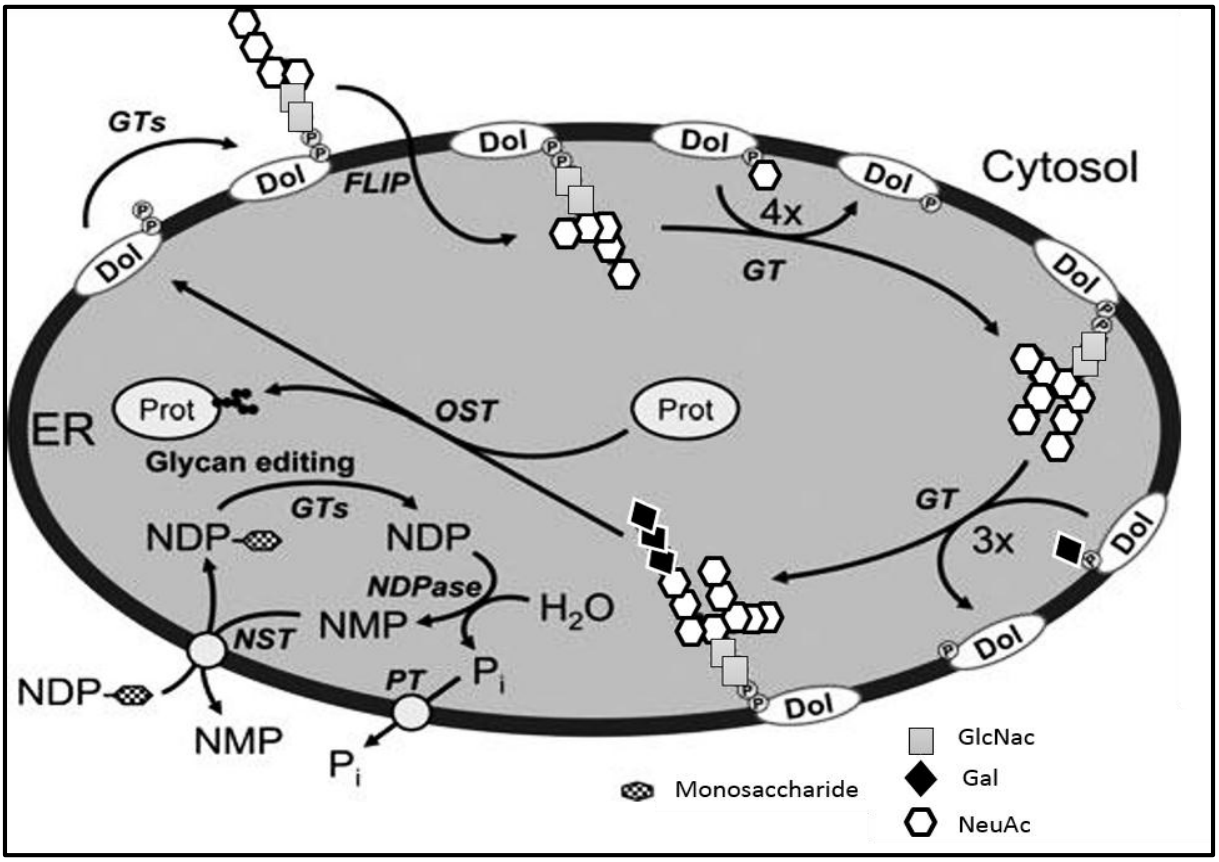

Figure 1.7: Protein glycosylation in the endoplasmic reticulum. The core glycan is partially assembled on dolichol pyrophosphate in the cytosol. The $Man_5GlcNAc_2$-PP-Dol glycan intermediate is "flipped" across the membrane by an unidentified flippase. Addition of glucose and mannose is catalysed by glycosyltranferases using Dol-P-Man and Dol-P-Glc as substrates. Finally, oligosaccharyltransferase adds the complete glycan en bloc to the asparagine residue in the glycosylation site. Dol = dolichol; ER = endoplasmic reticulum; FLIP = flippase; GT = glucosyltransferase; NDP = nucleoside diphosphate; NMP = nucleoside monophosphate; NST = nucleotide sugar transporter; OST = oligosaccharyltransferase; PT = phosphate transporter. (Adapted from Csala *et. al.* 2012).

Synthesis continues in the ER by addition of sugars from Dol-PP linked monosaccharaides, which are synthesized in the cytosol and subsequently flipped into the ER lumen. The complete *N*-glycan is then coupled to the nitrogen on the side chain of Asn (in the previously mentioned motif) in the growing nascent polypeptide through an *N*-glycosidic bond and promptly undergoes refinement through elongation by glycosyltransferases and trimming by glycosidases (A. Helenius *et al.*, 2004; Jones *et al.*, 2005). This continues until glycopeptide chains can be recognized by the calnexin-calreticulin cycle (see section 1.2.3.1).

1.2.3 Glycosylation and protein folding

N-Glycan mediated protein folding occurs co-translocationally when the polypeptide enters the Sec61 translocon channel in the ER lumen (Cheng, 2010; Osborne *et al.*, 2005), proceeding until complete dissociation of the peptide chain from the ribosome (Bergman *et al.*, 1979; Daniels *et al.*, 2003; A. Helenius *et al.*, 2004). The oligomeric nature of unfolded proteins requires conversion to their final folded state in this manner. Additionally, a number of proteins require the presence of glycans to allow efficient secretion, highlighting the importance of *N*-glycans in protein folding (Csala *et al.*, 2012; A. Helenius *et al.*, 2004). Some polypeptide chains that are synthesized lacking the presence of *N*-linked glycans fail to reach the oligomeric state and do not undergo the complex folding procedure. These are retained in the ER where they are degraded, preventing the accumulation of misfolded and potentially inactive proteins (Csala *et al.*, 2012; A. Helenius *et al.*, 2004). Clearly, protein folding is one of the most crucial roles of *N*-linked glycosylation in eukaryotes. In addition, *N*-linked glycosylation is known to affect protein folding both indirectly and directly.

1.2.3.1 Indirect effects of *N*-glycosylation on protein folding

The calnexin-calreticulin cycle is a molecular chaperone system that mediates complex *N*-linked glycosylation associated protein folding in the ER (Frenkel *et al.*, 2004; A. Helenius *et al.*, 2004; Lederkremer *et al.*, 2005; Trombetta *et al.*, 1998). The system comprises of calnexin, an ER-bound type I trans-membrane and the soluble calreticulin, found in the ER lumen. Protein folding and quality control via this cycle begins with the attachment of a

nascent polypeptide in the ER. This attachment occurs through monoglucosylated *N*-linked oligosaccharides on the polypeptide chain, found in the proline-rich area called the P-domain (Trombetta *et al.*, 1998). This monoglycosylation is a result of glucosidase I and II activity, which catalyse the stepwise removal of two outermost glucose residues, while glucosyltransferase promptly reglucosylates incompletely folded proteins cyclically until the correct protein conformation is reached (Figure 1.8) (Trombetta *et al.*, 1998).

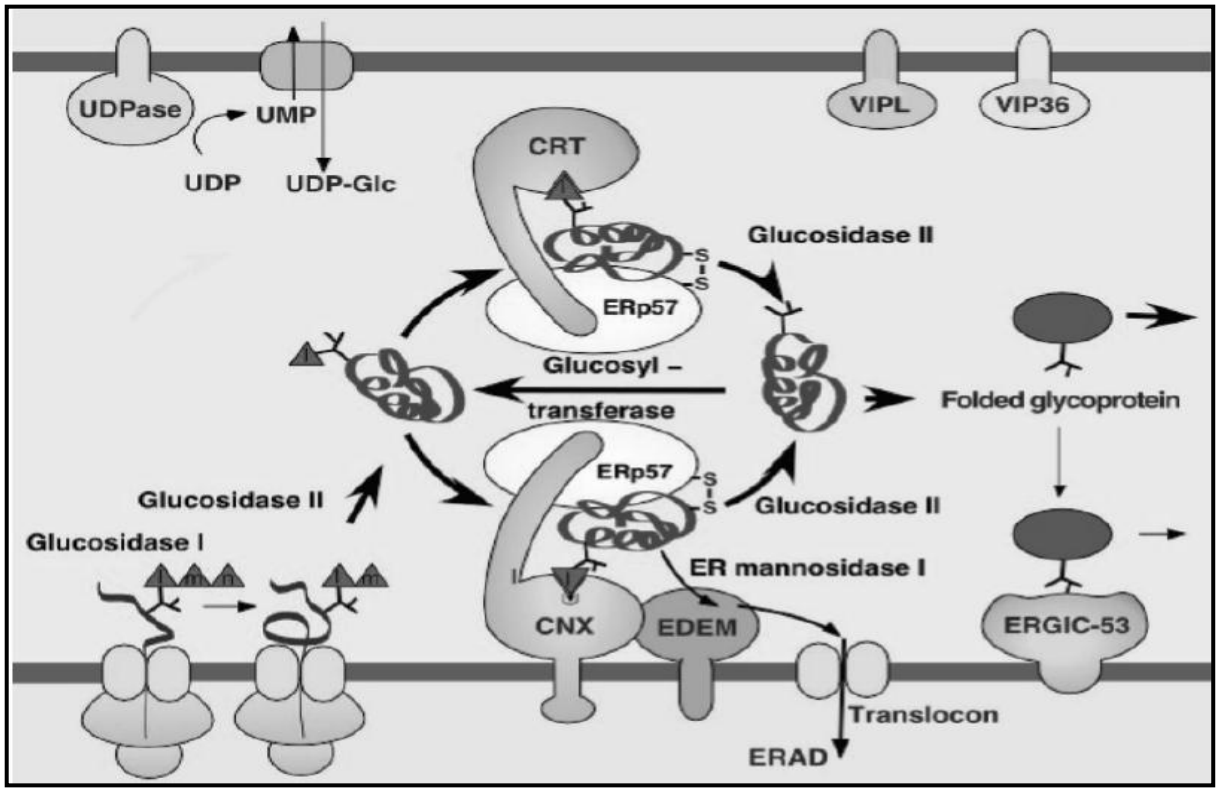

Figure 1.8: Calnexin-calreticulin mediated protein folding in the endoplasmic reticulum. Following addition of the core glycan to the polypeptide chain, the three outermost glucose residues (n) are removed by glucosidase I, followed by removal of the middle (m) glucose by glucosidase II, generating monoglucosylated glycans. These then bind to calnexin (CNX) and calreticulin (CRT) for presentation to ERp57. Glucosidase II removes the remaining glucose, leading to dissociation of the polypeptide-calnexin/calreticulin complex. The protein intermediate then goes through one of three steps; If properly folded, it leaves the ER via mannose lectins such as ERGIC-53, VIP36 and VIPL; If it is not completely folded, UDP-Glc (glycoprotein glucosyltransferase) uses UDP-glucose transported by a UDP-glucose/UMP exchanger to reglucosylate the incompletely folded protein; finally, misfolded proteins undergo ER-associated degradation (ERAD) by recognition of a putative lectin (EDEM) that have lost a mannose residue through the action of ER mannosidase I. Triangles – Glucose, VIP36 – vesicular integral protein 36, VIPL – VIP36-like protein, ERAD – ER-associated protein degradation, ERGIC-53 – ER-Golgi intermediate compartment 53, ERp57 – ER protein 57 (Adapted from Helenius et al. 2004.).

Calnexin and calreticulin present the monoglucosylated protein intermediate to ER protein 57 (ERp57), a thioldisulfide oxidoreductase responsible for assisting the formation of disulphide bridges to the protein being folded (Frenkel *et al.*, 2004; A. Helenius *et al.*, 2004; Trombetta *et al.*, 1998). Properly folded proteins can no longer bind to either calnexin or

calreticulin and are thus released from the ER via ER-Golgi intermediate compartment 53 (ERGIC-53), vesicular integral protein 36 (VIP36) and VIP36-like protein (VIPL) (A. Helenius *et al.*, 2004; Trombetta *et al.*, 1998; Yamaguchi *et al.*, 2007). ERGIC-53 is mainly responsible for the export of secretory and lysosomal proteins from the ER to the Golgi. VIP36 is more specific for proteins containing β-1,2 mannoses and it is proposed that it mediates forward transport of proteins for secretion (A. Helenius *et al.*, 2004). VIPL is specific for high mannose sugars and is also responsible for the glucosylation of the α-1,2 mannoses which it binds (Yamaguchi *et al.*, 2007). Incompletely folded protein intermediates are recognized and reglucosylated only by UDP-Glc-glycoprotein glucotransferase (GT) which is located at ER exit sites and also found in the ERGIC (A. Helenius *et al.*, 2004; Trombetta *et al.*, 1998). This process occurs via the transfer of a glucose residue from UDP-glucose to high mannose glycans bound to the protein intermediate (A. Helenius *et al.*, 2004; Trombetta *et al.*, 1998). Reglucoslated protein intermediates bind calnexin or calreticulin and go through the cycle again until complete folding is reached. Irreparably misfolded proteins are targeted for degradation by the ER-associated degradation (ERAD) pathway. These proteins are recognized by an intricate system involving ER mannosidase-1 which removes the terminal mannose residue from the trimannosyl pentapeptide backbone, resulting in the $Man_8GlcNac_2$ isoform (A. Helenius *et al.*, 2004; Trombetta *et al.*, 1998). Recognition of this isoform is mediated by a specific membrane-bound ER protein, Htm1/Mnl1 (an enzymatically inactive mannosidase homologue) also known as ER degradation-enhancing α-mannosidase-like protein (EDEM) which is thought to chaperone proteins into the degradation and retro-translocation pathway as well as promoting the less specific mannose trimming by the ERAD pathway (Marin *et al.*, 2012; Ron *et al.*, 2011). This pathway ensures the safe processing glycopeptides without exposure to sudden proteolysis (A. Helenius *et al.*, 2004).

1.2.3.2 Direct effects of *N*-glycosylation mediated protein folding

The direct involvement of *N*-glycans on protein folding has been reported extensively (A. Helenius, 1994; A. Helenius *et al.*, 2001; Imperiali *et al.*, 1999; Mitra *et al.*, 2006; O'Connor *et al.*, 1996; Wormald *et al.*, 1999). Addition of polar core oligosaccharide backbones (Figure 1.6) to glycoproteins increases their solubility. This results in the hydrophilic regions of the glycoprotein facing "outward" to the polar ER lumen, while the hydrophobic regions face "inward". This entropic force allows the hydrophobic and hydrophilic residues to interact with their respective environments for efficient folding (Anthony, 2011; A. Helenius, 1994). This essentially alters the folding pathway by stabilizing secondary structures during folding while limiting the formation of equilibrium intermediates (Mitra *et al.*, 2006). Furthermore, a direct effect by the *N*-acetyl group of the glycan residues of the attached glycan on the glycopeptide have been found to enhance β-turn formation (O'Connor *et al.*, 1996). Upon inhibition of glycosylation during protein expression, proteins display an aggregated, misfolded and non-functional state (A. Helenius, 1994; Varki, 1993). Interestingly, deglycosylation of a mature protein has no effect on functionality, but reduces protein stability (Hagaman *et al.*, 1998). This stabilization is thought to be due to the lack of mobility of unfolded conformations (A. Helenius *et al.*, 2004). When exploring the importance of individual glycosylation sites on this effect, some are found to be much more important than others, although a certain level of redundancy may be noticed, i.e. the importance of one site may be uncovered upon the removal of other sites (A. Helenius, 1994). Another interesting effect is the ability of *N*-glycans to cause a conformational shift upon glycan attachment (Imperiali *et al.*, 1995). This shift forces the glycopeptide into a more rigid, thus more stable structure, resembling that of the mature protein (Imperiali *et al.*, 1995).

1.2.4 Glycosylation and proteolysis

A number of studies have explored the ability of glycans to protect proteins from unregulated proteolysis (Beckham *et al.*, 2012; Bernard *et al.*, 1982; J. Fujihara *et al.*, 2008; Hsiao *et al.*, 2009; Kretz *et al.*, 1990; Nachon *et al.*, 2002; Olden *et al.*, 1982; Ripka *et al.*, 1993; van

Berkel *et al.*, 1995; Withka *et al.*, 1993). As previously mentioned, *N*-glycans are thought to promote the formation of β-turns (Mitra *et al.*, 2006; O'Connor *et al.*, 1996) and thus inducing a rigid conformation which may prevent proteolysis. An alternative mode of protection from proteolysis may be conferred by the presence of bulky glycans which may physically shield protease recognition sites (Anthony, 2011; Beckham *et al.*, 2012; Bernard *et al.*, 1982; J. Fujihara *et al.*, 2008; Kretz *et al.*, 1990; Nachon *et al.*, 2002; Olden *et al.*, 1982; Ripka *et al.*, 1993; van Berkel *et al.*, 1995; Withka *et al.*, 1993). Interestingly, *N*-glycans are thought to regulate the auto-proteolysis of the adhesion G protein-coupled receptor (GPCR), CD97 (Hsiao *et al.*, 2009). Thus, *N*-glycans may also be involved in the activation of adhesion-GPCR.

1.3 ACE GLYCOSYLATION

ACE is heavily glycosylated (30% glycosylation by weight) with a total of 17 N-linked glycosylation sites, 10 of which are located on the N-domain and seven on the C-domain (tACE) (Figure 1.9 A) (Acharya *et al.*, 2003; Anthony *et al.*, 2010; Deddish *et al.*, 1994; Gordon *et al.*, 2003; O'Neill *et al.*, 2008). Recombination studies have since shown that three N-terminal sites (sites 1, 2 and 3) are always glycosylated, sites 4, 5, 6 are partially glycosylated and site 7 is never glycosylated (Figure 1.9) (Anthony *et al.*, 2010; Gordon *et al.*, 2003). A study involving the construction of a wide range of tACE glycosylation mutants indicated that one or two of the N-terminal sites in tACE are important in secretion and folding of tACE (Figure 1.9 C) (Gordon *et al.*, 2003). From these glycosylation mutants, tACE with glycosylation sites 1 and 3 (corresponding to sACE glycosylation sites 11 and 13) was able to be crystalized reproducibly (Figure 1.9 C) (Gordon *et al.*, 2003). Another study on the N-domain indicated that glycosylation sites at C-terminus (sites 7, 8 and 9) were found to be crucial in the expression and folding of this domain. Notably, glycosylation mutant with only sites 3, 8 and 9 (Ndom3,8,9) was enzymatically active, while those with 7 and 9 (Ndom7,9), and 8 and 9 (Ndom8,9) were not, indicating a substantial degree of redundancy in

combination of glycosylation sites important for the expression of the N-domain (Figure 1.9 B) (Anthony *et al.*, 2010).

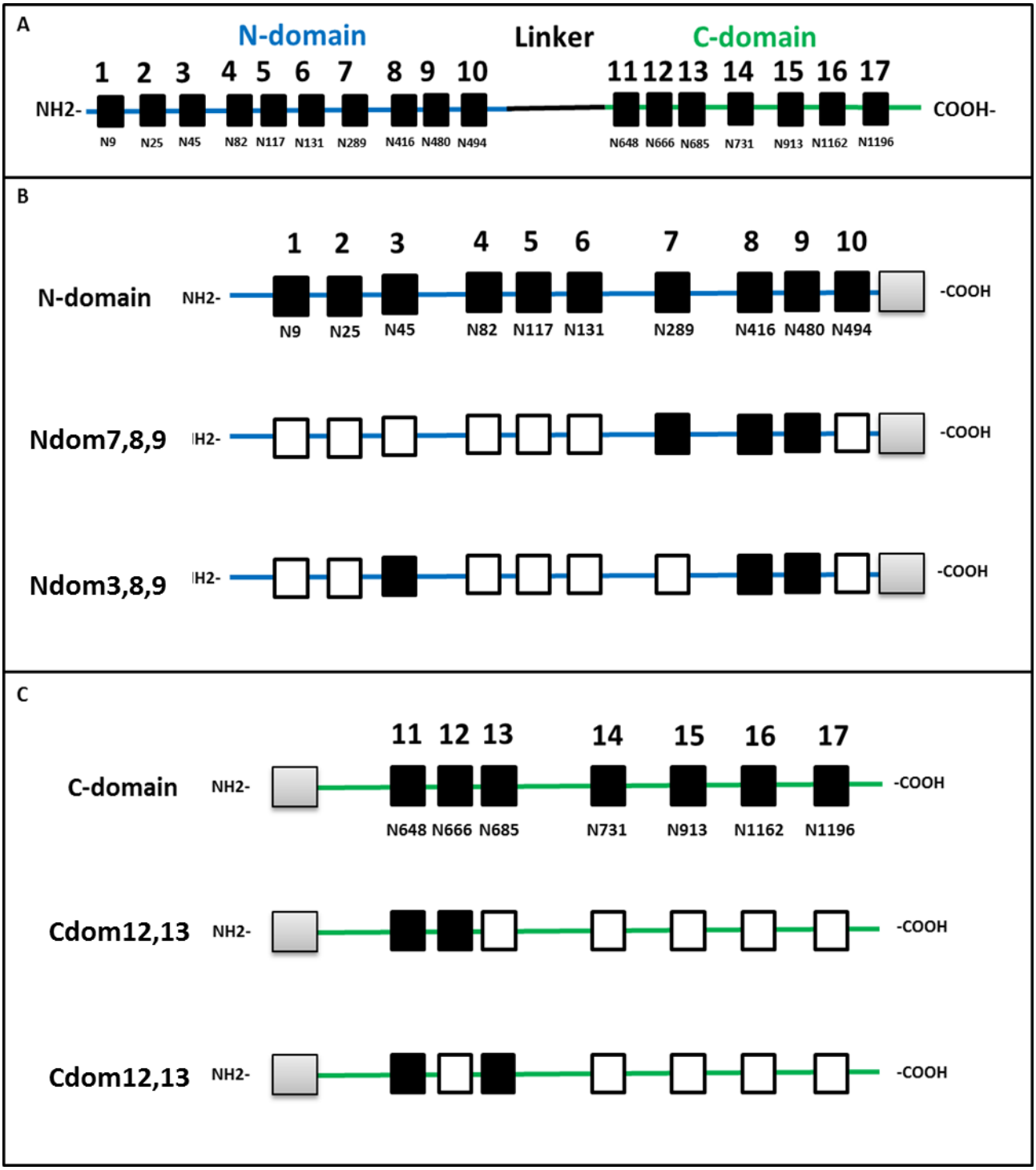

Figure 1.7: Schematic representation of glycosylation sites on sACE and the individual domains. (A), sACE (B), N-domain and (C) C-domain. In A, all glycosylation sites are indicated with their respective Asn (N) residue numbers on sACE. In B, minimally glycosylated N-domain mutants, Ndom7,8,9 and Ndom3,8,9 are indicated. In C, minimally glycosylated C-domain mutants, Cdom11,12 and Cdom11,13 are indicated. Glycosylation sites are numbered according to the sequence the full-length sACE. Black box – intact glycosylation site; open box – mutated glycosylation sites; grey box – Represents overlapping sequence common to both domains (inter-domain linker region, which is indicated by a black line in A).

1.3.1 ACE glycosylation and crystallization

Rational drug design relies heavily on protein crystallization for the structure-based design of potent and selective inhibitors. The degree of flexibility and heterogeneous composition of glycans often interferes with protein-crystal formation making glycosylation a major hurdle in crystallization studies (Butters *et al.*, 1999). As previously mentioned, glycosylation is crucial for protein expression. Manipulation of glycosylation sites is usually employed to obtain reproducibly crystallisable protein isoforms. However, lack of intact glycosylation sites may produce inactive or misfolded proteins which essentially cannot be purified for crystallography trials. Therefore, manipulation of glycoproteins in the aim to acquire the crystal structure is very limited as is the case with ACE. Currently, crystallization of the full-length somatic ACE has not yet been achieved, due to the high degree of glycosylation and also due to the flexibility conferred by the linker region between the two domains. One approach to develop the crystal structure of the individual domains of ACE has proved to be highly successful. As mentioned in section 1.1.1.2, crystal structures of the N- and C-domain have been solved through extensive manipulation of glycans on these domains, creating minimally glycosylated constructs (Anthony *et al.*, 2010; Gordon *et al.*, 2003).

1.3.2 ACE glycosylation and expression

Glycosylation is known to play a crucial role on the proper folding of ACE (see section 1.2.3). The glycosylation requirements sufficient for protein folding vary considerably among different cell types. Expression of ACE in *Escherichia coli* resulted in inactive protein (Sadhukhan *et al.*, 1996), due to the lack of glycosylation machinery in these cells. As mentioned in section 1.3, elegant recombination studies have identified the minimum glycosylation requirements of the N- and C-domains of ACE in Chinese hamster ovary (CHO) cells (Anthony *et al.*, 2010; Gordon *et al.*, 2003). However, not all mammalian cell types share the same protein glycosylation requirements (Croset *et al.*, 2012). Additionally, certain proteins have significant differences in the glycan composition, size, quantity and the general glycosylation pattern among CHO and HEK cells (Croset *et al.*, 2012). Expression of

tACE with mutated glycosylation sites or in the presence of a glycosylation inhibitor in HeLa cells resulted in inactive proteins that were rapidly degraded by the proteasome (Gordon *et al.*, 2003; Sadhukhan *et al.*, 1996). Interestingly, tACE with only glycosylation site 3, which suffered the same fate in HeLa cells, was properly processed in yeast cells (Sadhukhan *et al.*, 1996). Furthermore, a pilot study exploring the expression of the N-domain in yeast cells revealed very low levels of Ndom3,8,9 (unpublished data) (Figure 1.9). Interestingly Ndom3,8,9 was sufficiently expressed in CHO cells (Anthony *et al.*, 2010).

1.3.2 ACE glycosylation and stability

When looking at the stability of ACE, two points have to be considered; the thermal stability and; the apparent structural integrity. Focusing on the thermal stability, ACE has been shown to have two distinct melting temperatures (Tm) at 55°C and 72°C, corresponding to the Tm values of the individual domains, the higher value being that of the N-domain and the lower value being that of the C-domain (Voronov *et al.*, 2002). This difference in the Tm of the individual domains was initially thought to be a result of the high proline content present in 29-133 amino acid sequence of the N-domain, in comparison to corresponding amino acid sequence, 633-734 in the C-domain, and/or the α-helical content found in the same region which is much higher in the N-domain than in the C-domain (Voronov *et al.*, 2002). It is now known that the most critical contributor to the thermal stability of ACE, and thus the individual domains, is the presence of *N*-linked glycans (Anthony *et al.*, 2010; Gordon *et al.*, 2003; O'Neill *et al.*, 2008; Voronov *et al.*, 2002). This is evidenced by the sequential removal of glycosylation sites on the N- and C-domain showing that with decrease in the number of glycans, there is a subsequent decrease in the Tm (Anthony *et al.*, 2010; Gordon *et al.*, 2003; Natesh *et al.*, 2003; O'Neill *et al.*, 2008). It is now known that ACE relies on the N-domain to maintain a high Tm (Honours Thesis, 2011). With regards to the apparent structural integrity, ACE is known to be susceptible to minor levels of limited proteolysis in the inter-domain linker region (Deddish *et al.*, 1994; Sturrock *et al.*, 1997). A minimally glycosylated (MG) sACE resulted in increased inter-domain linker proteolysis (Anthony,

2011) suggesting that *N*-glycosylation plays a crucial role in protecting ACE from proteolysis (see section 1.3.4).

1.4 AIMS AND OBJECTIVES

The role *N*-linked glycosylation on the N- and C-domain has been well described, however, little is known about the relevance of glycosylation on the structure and function of sACE. Initial attempts to investigate the role of *N*-glycosylation on sACE resulted in an increased susceptibility to inter-domain linker proteolysis and reduction in the expression. The aim of this work was to a) strategically generate a panel of sACE glycosylation mutants that would be used to b) investigate the importance of *N*-linked glycosylation on the stability and functionality of sACE, and c) determine the minimal glycosylation requirements for a stable enzymatically active sACE construct.

These aims will be addressed by:

1) Generating sACE constructs of varying degrees of glycosylation (Chapter 2).
2) Investigating the role of *N*-glycan site occupancy on inter-domain linker proteolysis (Chapter 3).
3) Determining the cellular location and rate of inter-domain linker proteolysis (Chapter 4).
4) Investigating the role of *N*-glycans on the expression and thermal stability of sACE (Chapter 4).

Chapter 2: DNA Manipulation

2.1 INTRODUCTION

Elegant work has been done to study the individual domains of sACE by generating mutants lacking glycosylation sites using PCR-based SDM (see section 1.3) (Anthony *et al.*, 2010; Gordon *et al.*, 2003). Here, *N*-glycan attachment was prevented by converting the asparagine in the glycosylation site recognition motif (Asn-Xxx-Ser/Thr) to a glutamine. MG-sACE constructs were generated by combining some of these with previously generated individual domain glycosylation mutants (Figure 2.1).

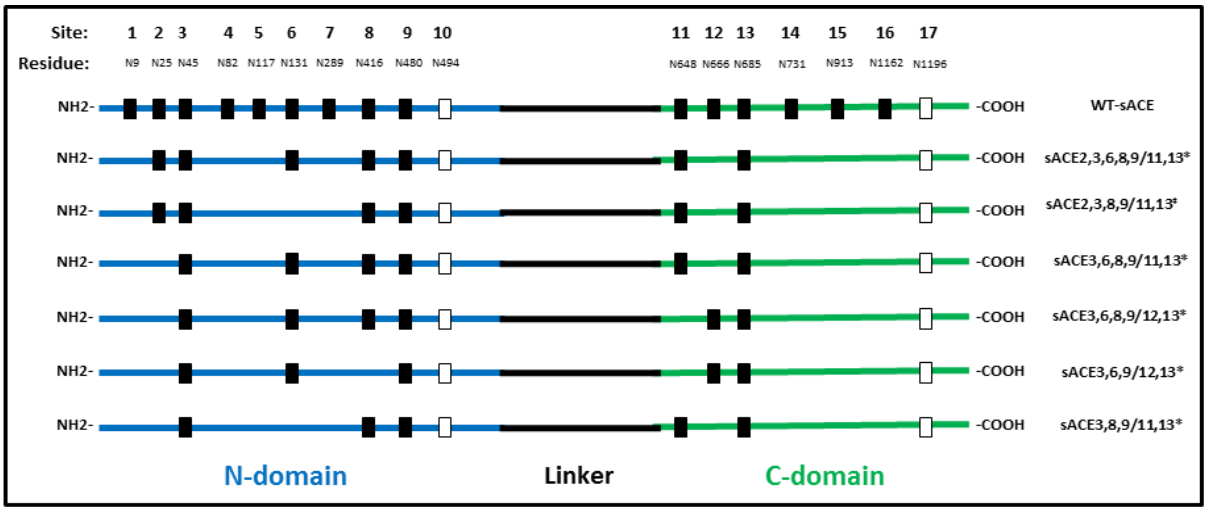

Figure 2.1: Diagrammatic representation of previously generated MG-sACE mutants. Black boxes indicate intact glycosylation sites and white boxes indicate sites that are not glycosylated. Numbers indicate glycosylation site positions.
*Mutants generated by Anthony (2011).
‡Mutant generated for Honours Thesis (2011).

These were used as subcloning templates for generating novel MG-sACE mutants for the purpose of investigating the effect of *N*-glycan site occupancy on protection from inter-domain linker proteolysis, expression and thermal stability. An sACE mutant with a H600C substitution has previously been generated and characterized (Gordon, 2011). This mutant formed a disulphide bridge between Cys600 and Cys474 located in the N-domain. This interaction limits flexibility caused by the linker region, and may prevent inter-domain linker

proteolysis in MG-sACE mutants. To this end, an MG-sACE mutant containing a H600C substitution was also generated.

2.2 EXPERIMENTAL METHODS

2.2.1 Materials

Restriction enzymes AgeI, KpnI, PvuI, Eco47III, SacI, EcoRI, BamHI, NotI, XbaI, Eco91I, T4 DNA ligase and O'GeneRuler™ DNA Ladder were obtained from Fermentas (Waltham, MA, USA). Restriction enzymes RcaI and EcoRV were obtained from Roche Ltd. (Basel, Switzerland). The GeneJET Gel Extraction Kit was purchased from Thermo Scientific (Wilmington, USA). *E.coli* DH5 α cells were purchased from Promega (Madison, WI, USA). Microcentrifuge 5424R (Eppendorf, Hamburg, Germany) was used for centrifugations.

2.2.2 Subcloning of novel MG-sACE constructs

ACE Plasmids sACE2,3,6,8,9/11,13; sACE2,3,8,9/11,13; sACE3,6,9/11,12; sACEH600C; Ndom3,8,9 all in pcDNA3.1(+) and WT-sACE in pBSK(+) were used as templates.

2.2.2.1 Restriction enzyme digest and agarose gel electrophoresis

Templates were digested with relevant restriction enzymes and DNA fragments were electrophoresed at 70 V for 1 hour. Vector and insert fragments were excised and purified using the GeneJET Gel Extraction Kit according to the manufacturer's instructions. DNA concentrations were determined using a NanoDrop™ 1000 spectrophotometer (Thermo Scientific, Wilmington, USA).

2.2.2.2 Ligation

Vector and insert fragments were ligated in a 3:1 insert to vector ratio using 1U T4 DNA ligase and 1X T4 DNA ligase buffer (Fermentas, Waltham, MA, USA) in a final volume of 20 µl, made up with nuclease free H_2O and incubated at 22°C for 1 hour.

2.2.2.3 Transformation of competent cells

From each ligation mix, 10 µl was added to 100 µl of competent DH5 α cells followed by a 20 minute incubation on ice. Cells were heat shocked at 42°C for 1 minute, followed by 1 minute incubation on ice. To the transformation mix, 450 µl of Luria broth (LB) was added and then incubated at 37°C for 1 hour. 100 µl of the LB-transformation mix was plated out on a Luria agar (LA) plate containing 50 µg/ml ampicillin and incubated overnight at 37°C.

2.2.2.4 Crude Plasmid DNA isolation and for positive clone screening

DNA was isolated from resistant clones using the STET boiling-mini lysate method (Ehrt *et al.*, 2003). Cultures were incubated at 37°C overnight and transferred to 1.5 ml Eppendorf tubes for centrifugation at 12000xg. The resultant supernatants were removed leaving the bacterial pellets which were resuspended in 250 µl of STET (8% (w/v) sucrose; 5% (w/v) triton X-100; 50 mM EDTA; 50 mM TRIS, pH 8.0) containing 1 mg/ml of lysozyme. Suspensions were boiled for 1 minute and promptly centrifuged for 15 minutes at 12000xg. The resultant pellet was removed with a sterile toothpick and discarded. An equal volume of isopropanol was then added to each of the tubes and mixed by inversion then centrifuged at 12000xg for 10 minutes. The resultant supernatants were removed and DNA pellets were left to air-dry for approximately 10 minutes. Plasmid DNA was then resuspended in 20 µl of 1/10 Tris EDTA (1.0 mM Tris-HCl, 0.1 mM EDTA, pH 7.4) and heated at 68°C for 10 minutes to ensure complete solubilisation. DNA constructs were screened by digestion to determine the presence/absence of introduced/removed restriction sites with the relevant restriction enzymes according to recommended conditions. Digest products were visualized on 1% (w/v) agarose gels containing 0.3 µg/ml ethidium bromide.

2.2.2.5 Plasmid DNA preparation for sequencing

Positive clones were picked into 3 ml LB containing 50 µg/ml ampicillin, and incubated at 37°C overnight with shaking. Plasmid DNA was isolated using the GeneJET Plasmid

Miniprep Kit (Thermo Scientific, Wilmington, USA) as per manufacturer's instructions. DNA concentrations were determined as described in section 2.2.2.1.

2.2.2.6 DNA sequencing to confirm the presence of mutations in recombinant sACE constructs

All novel sACE constructs were sequenced to confirm the presence of the engineered mutations. This was done by capillary sequencing conducted at the Central Analytical Facility (CAF) (Stellenbosch University, South Africa) with the 5500xl SOLiD™ System Genome analyser, using internal sACE sequencing primers (Appendix A1) and a T7 promoter primer.

2.2.2.7 Up-scaled plasmid DNA preparation for transfection

A 100 µl of positive plasmid containing DH5 α cultures were seeded into 50 ml LB containing 50 µg/ml ampicillin, and incubated at 37°C overnight with shaking. DNA was isolated using the Qiagen Plasmid Midi Kit (Qiagen, Hilden, Germany) as per manufacturer's instructions. DNA concentrations were determined as described in section 2.2.2.1.

2.3 RESULTS

MG-sACE constructs were assembled in pcDNA3.1(+) for expression in mammalian cells (Figure 2.2). Here, restriction sites previously engineered to facilitate subcloning of the N-domain (Anthony, 2011), intrinsic sACE restriction sites and the pcDNA3.1(+) multiple cloning sites were used to obtain fragments containing glycosylation sites of interest. Codons responsible for the translation of the asparagine to which a sugar will be attached are represented by AAC/T, those mutated to a glutamine to inhibit sugar attachment are represented by CAG while that of the H600C mutation is represented by TGC.

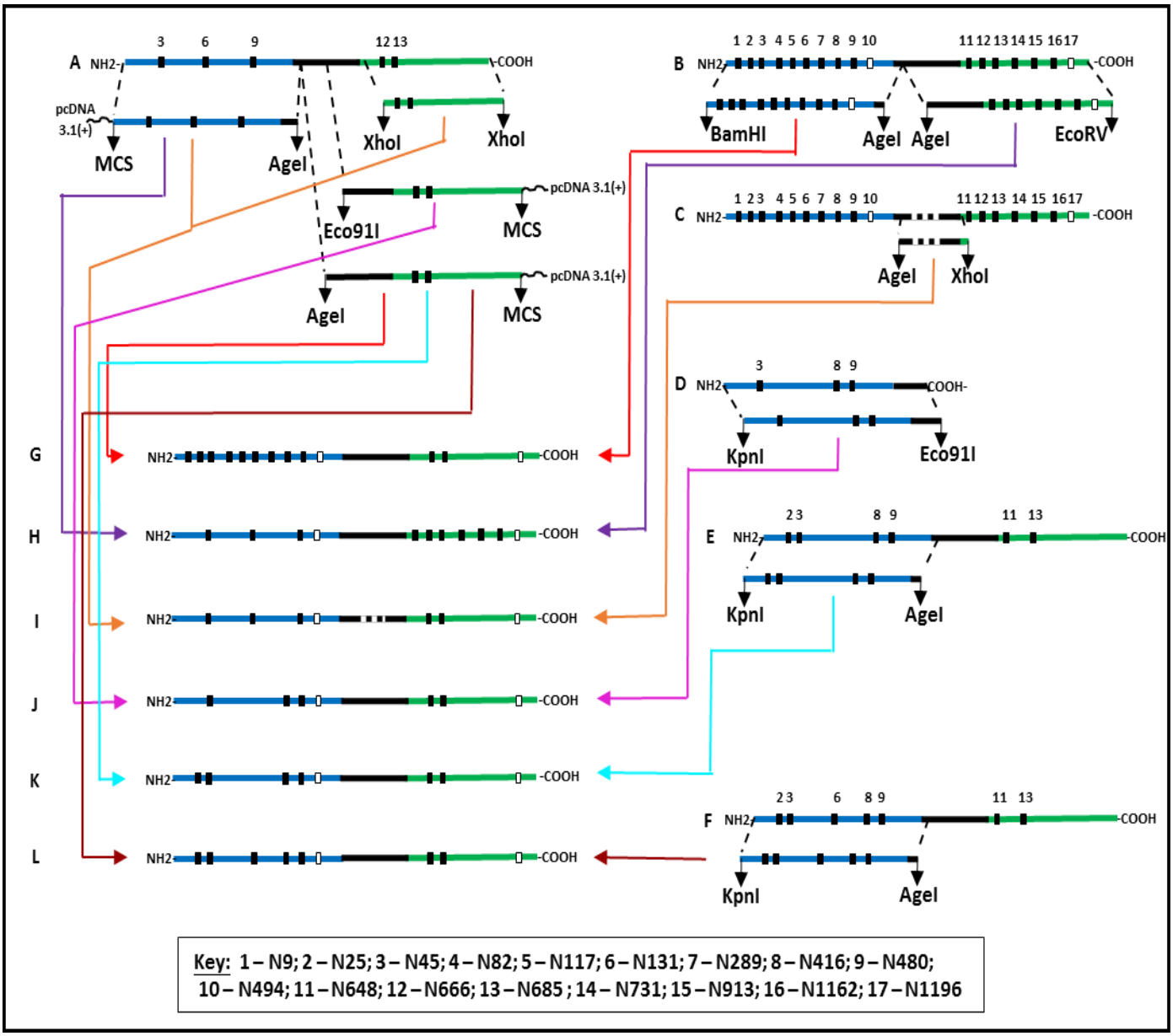

Figure 2.2: Cloning strategies used to generate MG-sACE isoforms. All constructs were assembled in pcDNA3.1(+). A) sACE3,6,9/12,13; B) WT-sACE, C) sACEH600C; D) Ndom3,8,9; E) sACE2,3,8,9/11,13 and F) sACE2,3,6,8,9/11,13 were used as templates to generate a total of six novel MG-sACE mutants. G) sACEWTNdom/12,13 was constructed using sACEWTNdom and sACE12,13pcDNA3.1(+) fragments obtained from a BamHI/AgeI digest. H) sACE3,6,9/WTCdom was constructed using sACEWTCdom and sACE3,6,9pcDNA3.1(+) fragments obtained from a AgeI/EcoRV digest. I) sACE3,6,9/H600C/12,13 was constructed using sACE3,6,9, H600C and sACE12,13pcDNA3.1(+) fragments obtained from a AgeI/XhoI digest. J) sACE3,8,9/12,13 was constructed using Ndom3,8,9 and sACE12,13pcDNA3.1(+) fragments obtained from a Eco91I/KpnI digest. K) sACE2,3,8,9/12,13 was constructed using sACE2,3,8,9 and sACE12,13pcDNA3.1(+) fragments obtained from a KpnI/Age/KpnI digest. L) sACE2,3,6,8,9/12,13 was constructed using sACE2,3,6,8,9 and sACE12,13pcDNA3.1(+) fragments obtained from a KpnI/Age/KpnI digest. Black boxes indicate intact glycosylation sites and white boxes indicate sites that are not glycosylated. MCS – Multiple cloning site in pcDNA3.1(+).

2.3.1 Cloning of minimally glycosylated sACE mutants to investigate the stability of the linker region

Firstly, wild-type domains were substituted with MG N- and C-domains to help give an indication of which domain contains protective *N*-glycans (see Chapter 3). MG-sACE constructs were then strategically generated by manipulating glycosylation sites proximal to the inter-domain linker region, while preserving sites that have been shown to be crucial for the expression of the individual domains. Of the available DNA recombination techniques available, subcloning was opted due to its simplicity and the reduced chances of introducing PCR-based spurious mutations (see section 2.4).

2.3.1.1 Construction of sACEWTNdom/12,13

As previously mentioned, to help identify in which domain resides the protective *N*-glycans, a MG N-domain was substituted with a WT N-domain to generate sACEWTNdom/12,13pcDNA3.1(+). Constructs WTsACEpBSK(+) and sACE3,6,9/12,13pcDNA3.1(+) were used as templates. These were digested as indicated in Figure 2.3.

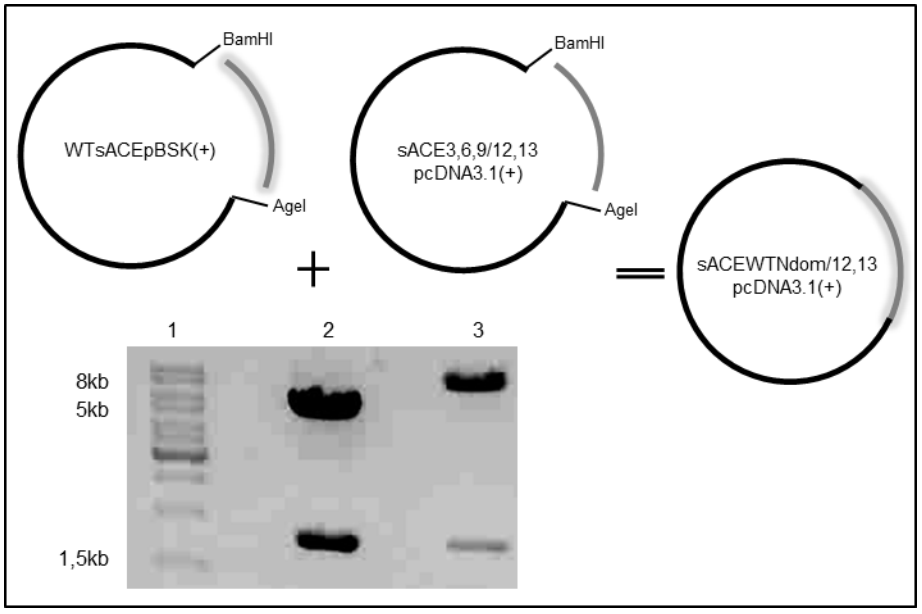

Figure 2.3 Schematic showing subcloning strategy of sACEWTNdom/12,13pcDNA3.1(+). Restriction enzymes BamHI and AgeI were used to cut out a 1717 bp WT N-domain insert and a 7724 bp vector fragment containing the C-domain and pcDNA3.1(+) with glycosylation sites 12 and 13. 1 - O'generuler DNA ladder mix; 2 – WTsACEpBSK(+); 3 – sACE3,6,9/12,13pcDNA3.1(+).

Successful subcloning was confirmed by restriction enzyme digests (Figure 2.4 A, B) and DNA sequencing (Figure 2.4 C, D), where the incorporation of site 5 results in the removal of an AflII restriction site at position 1401 while the absence of site 15 results in the addition of an EcoR1 restriction site at position 3787. All the expected bands were observed in Figure 2.4 A and B, although the 305 bp and 314 bp fragments appear to be approximately 500 bp. This is possibly due to an electrophoretic mobility shift caused by increased binding of the restriction enzyme to the DNA without dissociating before and/or during electrophoresis (Makela *et al.*, 2012), thus resulting in a band appearing higher than expected. However, DNA sequencing did confirm the presence of site 5 (Figure 2.4 C), indicating the fully-glycosylated status of the N-domain, and the absence of site 15 (Figure 2.4 D), indicating the hypo-glycosylated status of the C-domain. No discrepancies were found in the entire plasmid. An additional EcoRI restriction site is present at position 4656 and is a result of previous subcloning procedures for MG C-domain mutants (Gordon, 2011) (see section 2.4).

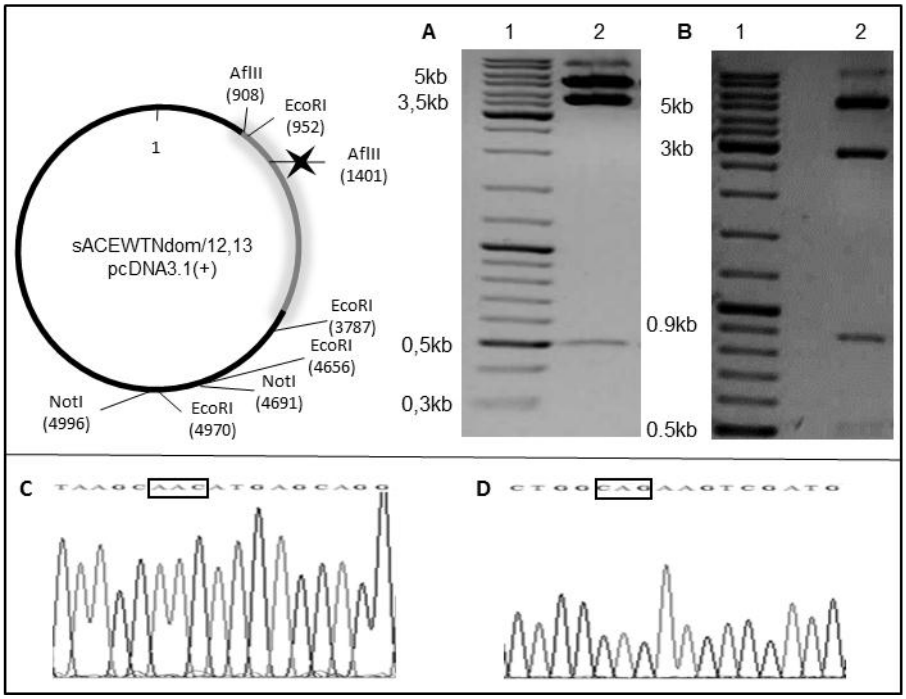

Figure 2.4: Vector diagram, restriction enzyme digests and electrophoretogram of sACEWTNdom/12,13pcDNA3.1(+). A) Construct was digested with AflII and NotI, with expected fragments of 5358 bp, 3783 bp and 305 bp. B) Construct was digested with EcoRI, with expected fragments of 5428 bp, 2835 bp, 869 bp, 314 bp. C) Electrophoretogram showing the presence of glycosylation site 5. D) Electrophoretogram showing the absence of glycosylation site 15. Black star indicates a mutated restriction site. 1 – O'generuler DNA ladder mix; 2 – sACEWTNdom/12,13pcDNA3.1(+).

2.3.1.2 Construction of sACE3,6,9/WTCdom

A MG C-domain was also substituted with a WT C-domain to generate sACE3,6,9/WTCdompcDNA3.1(+) using WTsACEpBSK(+) and sACE3,6,9/12,13pcDNA3.1(+) as templates. Constructs were digested as indicated in Figure 2.5.

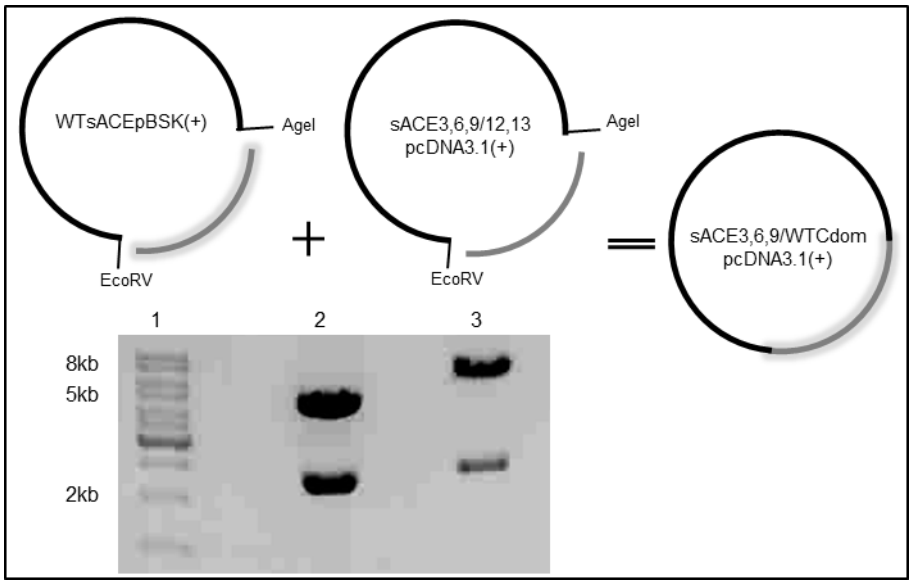

Figure 2.5 Schematic showing subcloning strategy of sACE3,6,9/WTCdompcDNA3.1(+). Restriction enzymes AgeI and EcoRV were used to cut out a 2329 bp WT C-domain insert and a 7117 bp vector fragment containing the N-domain and pcDNA3.1(+) with glycosylation sites 3, 6 and 9. 1 – O'generuler DNA ladder mix; 2 – WTsACEpBSK(+); 3 – sACE3,6,9/12,13pcDNA3.1(+).

Residual undigested DNA is observed migrating at approximately 10 kb (Figure 2.6 A, B). However, the expected banding pattern is observed indicating absence of site 5, evidenced by the presence of an AflII restriction site at position 1401 (Figure 2.6 A), and the presence of site 15 (Figure 2.6 B), evidenced by the absence of an EcoRI restriction site at position 3787. Furthermore, electrophoretograms in Figure 2.6 C and D indicate the presence/absence of the respective sites, thus confirming successful incorporation of a fully-glycosylated C-domain.

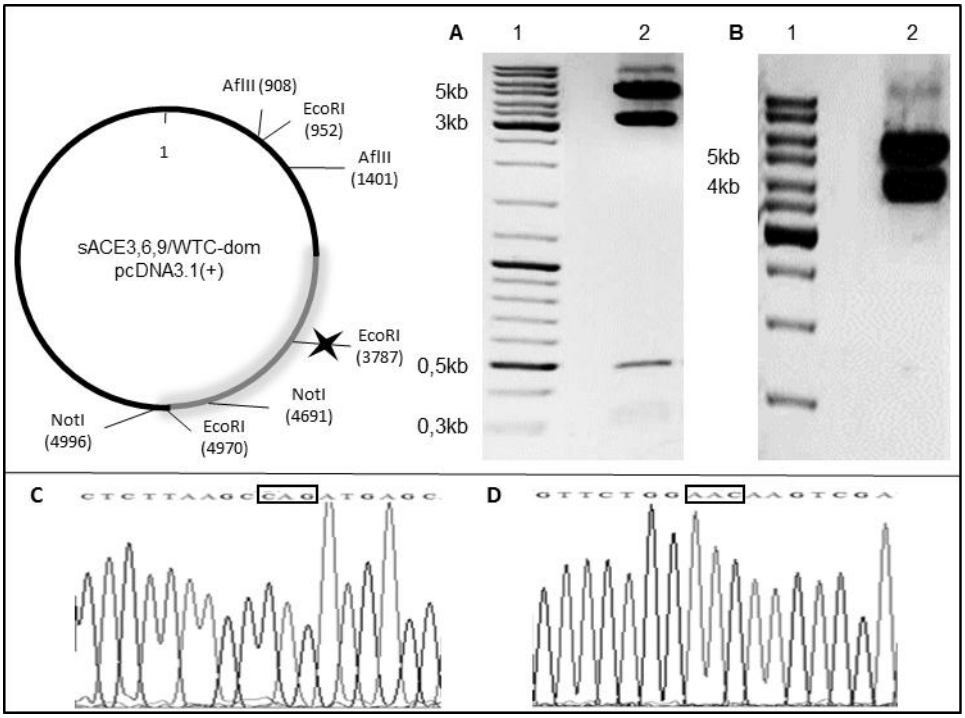

Figure 2.6: Vector diagram, restriction enzyme digests and electrophoretograms of sACE3,6,9/WTCdompcDNA3.1(+). A) Construct was digested with AflII and NotI, with expected fragments of 5358 bp, 3290 bp and 493 bp and 305 bp. B) Construct was digested with EcoRI, with expected fragments of 5428 bp, 4018 bp. C) Electrophoretogram showing the absence of glycosylation site 5. D) Electrophoretogram showing the presence of glycosylation site 15. Black star indicates a mutated restriction site. 1 – O'generuler DNA ladder mix; 2 – sACE3,6,9/WTCdom pcDNA3.1(+).

2.3.1.3 Construction of sACE3,8,9/12,13

Since a number of MG-sACE mutants with varying intact glycosylation sites proximal to the inter-domain linker region have been generated (see Figure 2.1), an additional mutant, sACE3,8,9/12,13pcDNA3.1(+), needed to be generated to investigate the effect of this combination of intact glycosylation sites on protection from linker proteolysis. This was generated using Ndom3,8,9pcDNA3.1(+) and sACE3,6,9/12,13pcDNA3.1(+) as templates. Constructs were digested as indicated Figure 2.7.

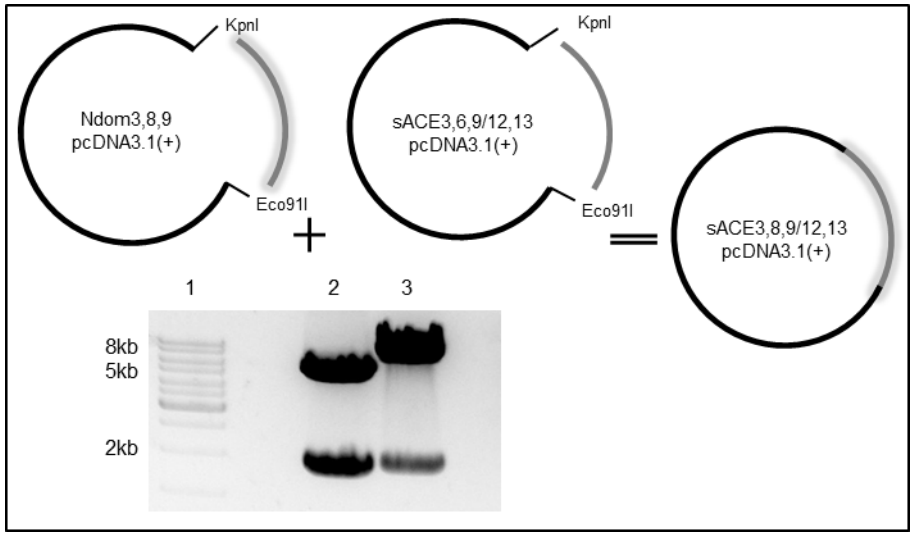

Figure 2.7 Schematic showing subcloning strategy of sACE3,8,9/12,13pcDNA3.1(+). Restriction enzymes KpnI and Eco91I were used to cut out a 1981 bp N-domain insert containing glycosylation sites 3, 8 and 9, and a 7465 bp vector fragment containing the C-domain and pcDNA3.1(+) with glycosylation sites 12 and 13. 1 – O'generuler DNA ladder mix; 2 – Ndom3,8,9pcDNA3.1(+); 3 – sACE3,6,9/12,13pcDNA3.1(+).

Restriction enzyme digests were conducted and the resultant banding pattern observed confirms that an RcaI digestion produces an additional fragment of 1270 bp (Figure 2.8 A). This is due to reintroduction of site 3 which results in the addition of an RcaI restriction site at position 1182. Similarly, digestion with PvuI produces a linearized plasmid (Figure 2.8 B) which is due to the reintroduction of site 8 that results in the removal a PvuI restriction site at position 2292. Furthermore, DNA sequencing confirmed the presence of both site 3 (Figure 2.8 C) and 8 (Figure 2.8 D).

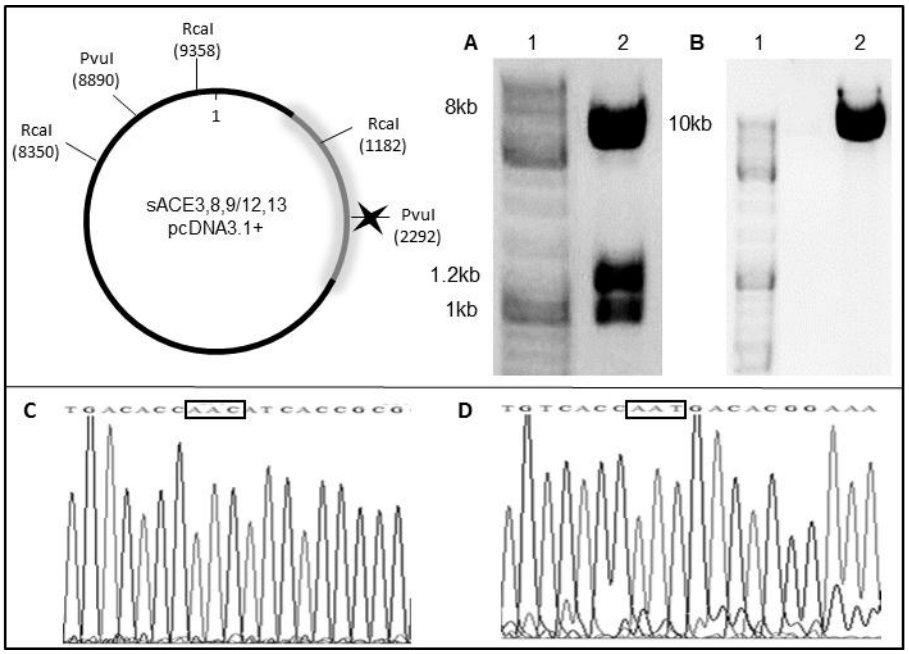

Figure 2.8: Vector diagram, restriction enzyme digests and eletrophoretograms of sACE3,8,9/12,13pcDNA3.1(+). A) Construct was digested with RcaI, with expected fragments of 7171 bp, 1270 bp and 1008 bp. B) Construct was digested with PvuI which resulted in the linearization of the construct. C) Electrophoretogram showing the presence of glycosylation site 3. D) Electrophoretogram showing the presence of glycosylation site 8. Black star indicates a mutated restriction site. 1 – O'generuler DNA ladder mix; 2 – sACE3,8,9/12,13pcDNA3.1(+).

2.3.1.4 Construction of sACE3,6,9/H600C/12,13

Due to the lack of compatible restriction sites for subcloning and technical difficulties encountered with PCR based SDM (see section 2.4), a more complex strategy was needed to be employed for generating sACE3,6,9/H600C/12,13pcDNA3.1(+). This involved a two-step subcloning strategy which allowed for the incorporation of a segment containing coding region for the H600C substitution. Constructs sACE3,6,9/12,13pcDNA3.1(+) and sACEH600CpcDNA3.1(+) (Gordon, 2011) were used as templates which were digested as indicated in Figure 2.9. Three bands of interest (V1, V2 and H600C) were excised, purified and ligated as described in section 2.2.2. Firstly, fragments of 7094 bp containing the N-domain with glycosylation sites 3, 6 and 9 and pcDNA3.1(+) (V1) and the H600C fragment from the AgeI/XhoI digestion of sACEH600CpcDNA3.1(+) were ligated (Figure 2.9).

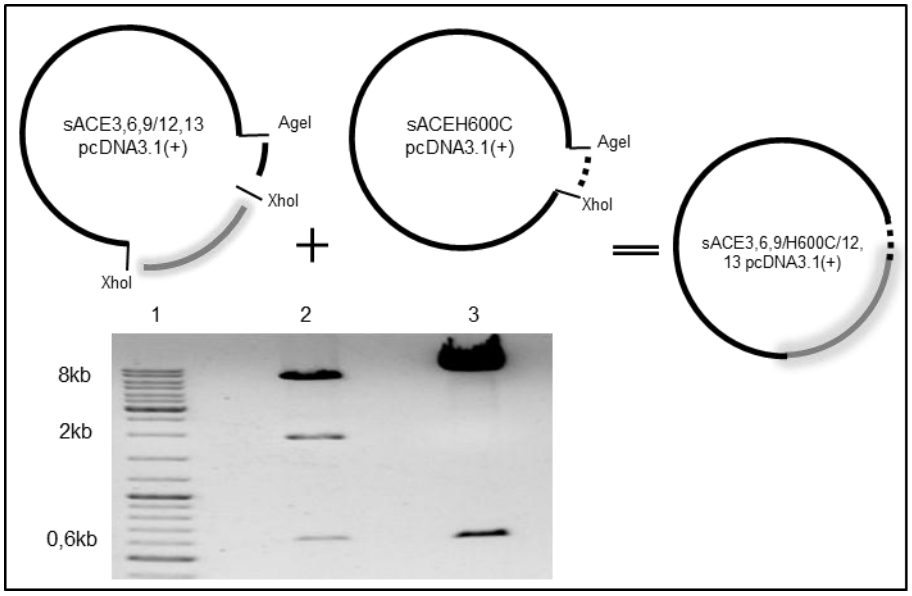

Figure 2.9 Schematic showing subcloning strategy of sACE3,6,9/H600C/12,13pcDNA3.1(+). Restriction enzymes AgeI and XhoI were used to cut out fragments of 7094 bp (containing the N-domain with glycosylation sites 3, 6 and 9 and pcDNA3.1(+) (V1)) and a 1735 bp fragment (containing the C-domain with glycosylation sites 12 and 13) (V2)) from sACE3,6,9/12,13pcDNA3.1(+). A 617 bp fragment containing the H600C substitution (dashed curve) was obtained from sACEH600CpcDNA3.1(+). 1 – O'generuler DNA ladder mix; 2 – sACE3,6,9/12,13pcDNA3.1(+); 3 – sACEH600CpcDNA3.1(+).

In Figure 2.10 A, a BsaXI digest showed some residual undigested DNA at approximately 10 kb, but the expected banding pattern resulting in the presence of an additional BsaXI restriction site is observed, indicating the successful incorporation of H600C. Double bands were noticeable at the 1893 bp, 724 bp and 471 bp sized fragments and this is likely due to a reduced efficiency of the restriction enzyme resulting in star activity (Selin *et al.*, 2013). The same pattern is noticed upon digest of negative controls sACEH600CpcDNA3.1(+) and sACE3,6,9/12,13pcDNA3.1(+) (Figure 2.11). Furthermore, DNA sequencing was done to confirm the sequence of the ligation product (Figure 2.10 B). V1/H600CpcDNA3.1(+) was then linearized with XhoI and ligated with V2 to yield sACE3,6,9/H600C/12,13pcDNA3.1(+).

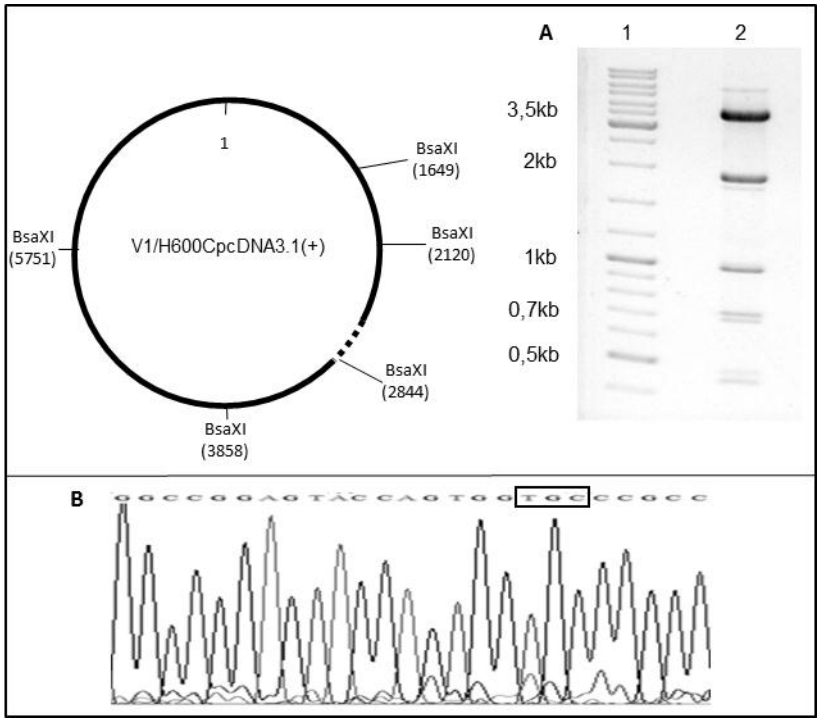

Figure 2.10: Vector diagram, restriction enzyme digest and electrophoretogram of V1/H600CpcDNA3.1(+). A) V1/H600CpcDNA3.1(+) was digested with BsaXI, with expected fragments of 3606 bp, 1893 bp, 1014 bp, 724 bp and 471 bp. B) Electrophoretogram showing the presence of the H600C substitution. 1 – O'generuler DNA ladder mix; 2 – V1/H600CpcDNA3.1(+).

Successful subcloning was then confirmed by digestion with BsaXI as indicated in Figure 2.11. The banding pattern clearly indicates that sACE3,6,9/H600C/12,13 is a combination of sACE3,6,9/12,13 and sACEH600C.

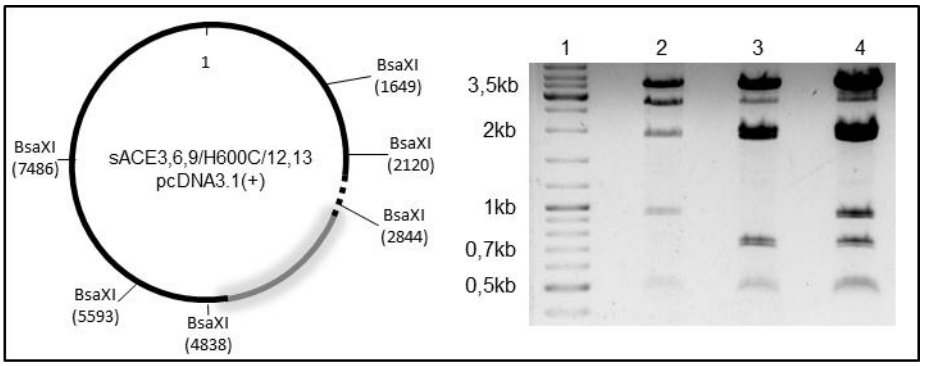

Figure 2.11: Vector diagram and restriction enzyme digest of sACE3,6,9/H600C/12,13pcDNA3.1(+) including negative controls sACE3,6,9/12,13pcDNA3.1(+) and sACEH600CpcDNA3.1(+). Constructs were digested with BsaXI, with expected fragments for sACE3,6,9/12,13pcDNA3.1(+) being at 3606 bp, 1994 bp, 1893 bp, 755 bp, 724 bp and 471 bp. 1 – O'generuler DNA ladder mix; 2 – sACE3,6,9/12,13pcDNA3.1(+); 2 – sACEH600CpcDNA3.1(+), 3 – sACE3,6,9/H600C/12,13pcDNA3.1(+).

2.3.2 Cloning of minimally glycosylated sACE mutants to investigate thermal stability

In order to assess the effect of *N*-glycan site occupancy on sACE expression and thermal stability, glycosylation sites had to be reintroduced into available MG-sACE mutants. To this end, sequential addition of specific glycosylation sites previously shown to be important for the expression of ACE was employed. A study on the N-domain revealed that removal of site 1 did not greatly alter the thermal stability while removal of site 2 caused a great loss in thermal stability (Anthony, 2011). Thus, reintroduction of site 2 to MG-sACE was employed to investigate its effect on full-length sACE.

2.3.2.1 Construction of sACE2,3,8,9/12,13

To generate sACE2,3,8,9/12,13pcDNA3.1(+), sites 2, 3, 8 and 9 were subcloned from sACE2,3,8,9/11,13pcDNA3.1(+) and ligated with sites 12 and 13 from sACE3,6,9/12,13pcDNA3.1(+). Constructs were digested as indicated in Figure 2.12.

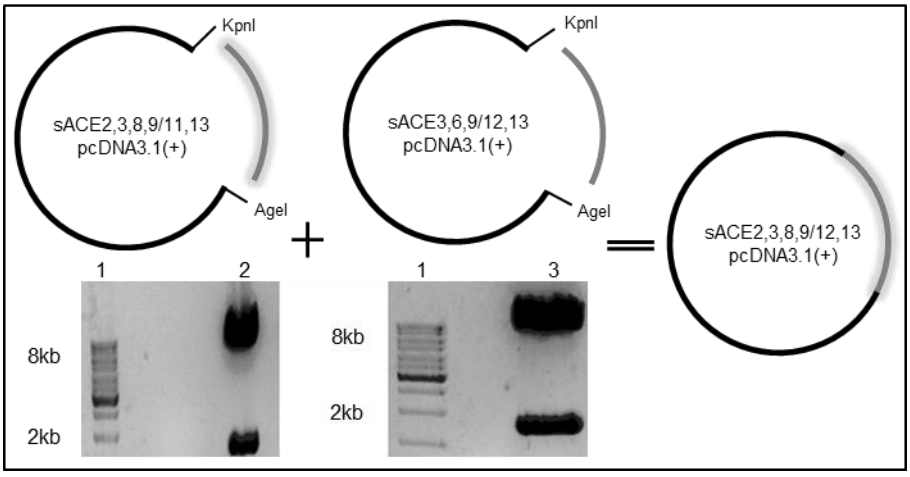

Figure 2.12 Schematic showing subcloning strategy of sACE2,3,8,9/12,13pcDNA3.1(+). Restriction enzymes KpnI and AgeI were used to cut out a 1747 bp N-domain insert containing glycosylation sites 2, 3, 8 and 9, and a 7712 bp vector fragment containing the C-domain and pcDNA3.1(+) with glycosylation sites 12 and 13. 1 – O'generuler DNA ladder mix; 2 – sACE2,3,8,9/11,13pcDNA3.1(+); 3 – sACE3,6,9/12,13pcDNA3.1(+).

Successful incorporation of site 2 was confirmed by the observed banding pattern from an Eco47III digest which produces two fragments of 8059 bp and 1357 bp (Figure 2.13 A). This is due to silent mutation resulting in the knock-out of an Eco47III restriction site at position 1138 when site 2 is reintroduced. The appropriate sequence for an intact glycosylation site 2 was also observed (Figure 2.13 B).

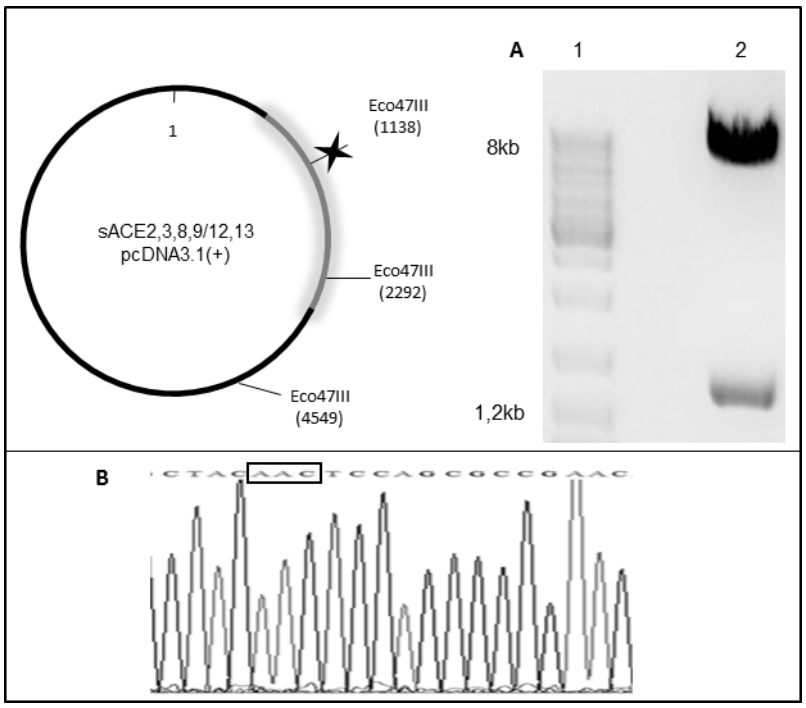

Figure 2.13: Vector diagram, restriction enzyme digest and electrophoretogram of sACE2,3,8,9/12,13pcDNA3.1(+). A) Construct was digested with Eco47III, with expected fragments of 8059 bp and 1387 bp. B) Electrophoretogram showing the presence site 2. Black star indicates a mutated restriction site. 1 – O'generuler DNA ladder mix; 2 – sACE2,3,8,9/12,13pcDNA3.1(+).

2.3.2.2 Construction of sACE2,3,6,8,9/12,13

A second mutant was generated similarly to the above-mentioned using sACE2,3,6,8,9/11,13pcDNA3.1(+) and sACE3,6,9/12,13pcDNA3.1(+). Constructs were digested as indicated in Figure 2.14 and sACE2,3,6,8,9 pcDNA3.1(+) and sACE12,13 were ligated yielding, sACE2,3,6,8,9/12,13pcDNA3.1(+).

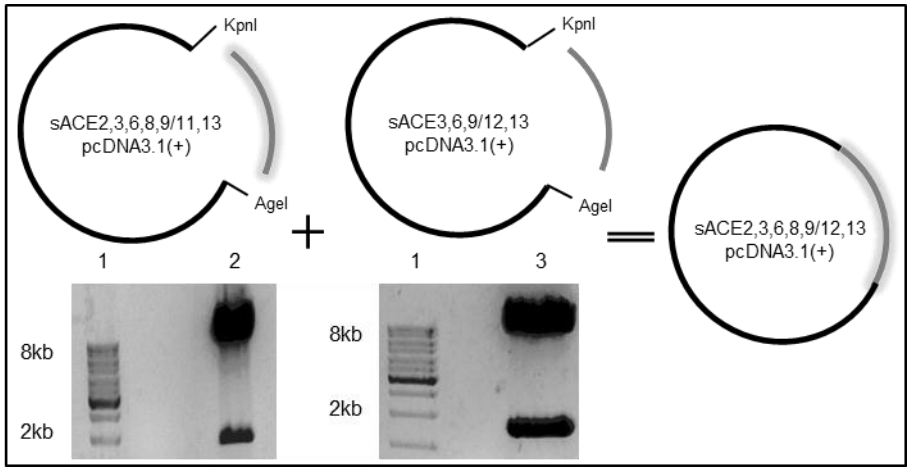

Figure 2.14 Schematic showing subcloning strategy of sACE2,3,6,8,9/12,13pcDNA3.1(+). Restriction enzymes KpnI and AgeI were used to cut out a 1747 bp N-domain insert containing glycosylation sites 2, 3, 6, 8 and 9, and a 7712 bp vector fragment containing the C-domain and pcDNA3.1(+) with glycosylation sites 12 and 13. 1 – O'generuler DNA ladder mix; 2 – sACE2,3,6,8,9/11,13pcDNA3.1(+); 3 – sACE3,6,9/12,13pcDNA3.1(+).

Subcloning was confirmed as with sACE2,3,6,8,9/12,13 where the successful incorporation of site 2 was evidenced by the appropriate DNA sequence (Figure 2.15 B) and the banding pattern (Figure 2.15 A), resultant from the absence of an Eco47III restriction site at position 1138.

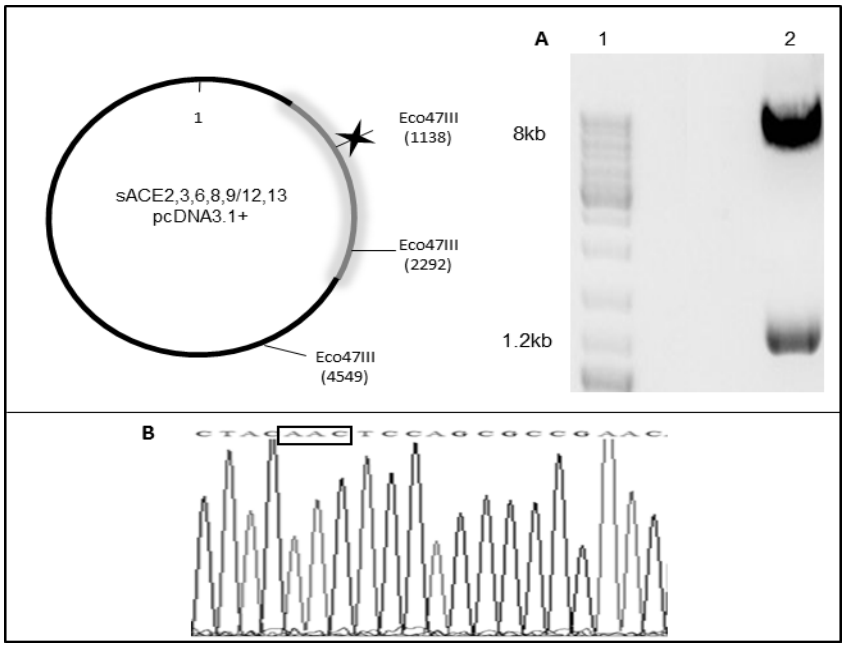

Figure 2.15: Vector diagram, restriction enzyme digest and electrophoretogram of sACE2,3,6,8,9/12,13pcDNA3.1(+). A) Construct was digested with Eco47III, with expected fragments of 8059 bp and 1387 bp. B) Electrophoretogram showing the presence site 2. Black star indicates a mutated restriction site. 1 – O'generuler DNA ladder mix; 2 – sACE2,3,6,8,9/12,13pcDNA3.1(+).

2.4 DISCUSSION

The aim of this study was to generate novel MG-sACE constructs geared towards investigating the effect of *N*-glycan site occupancy on protection from inter-domain linker proteolysis, expression and thermal stability. Furthermore, a disulphide bridge was engineered between the linker region and the N-domain by introducing the amino acid substitution H600C. The subcloning approach used was much more favourable than SDM (see section 2.4) due to its simplicity, efficiency and reliability. A detailed background discussion on the rationale behind the design of each mutant will be covered in Chapters 3 and 4. In brief, the design of these mutants was based on the preservation of previously described key glycosylation sites on the individual domains (Anthony *et al.*, 2010; Gordon *et al.*, 2003). This was important to avoid obtaining possibly misfolded and inactive sACE proteins during expression. The library of generated mutants (Figure 2.16) share a degree of overlap between the aims of this project. Meaning, constructs generated for addressing the role of *N*-glycan site occupancy on limited proteolysis were also required to assess the effect of site occupancy on the stability and expression, and vice versa (see Chapter 3 and 4).

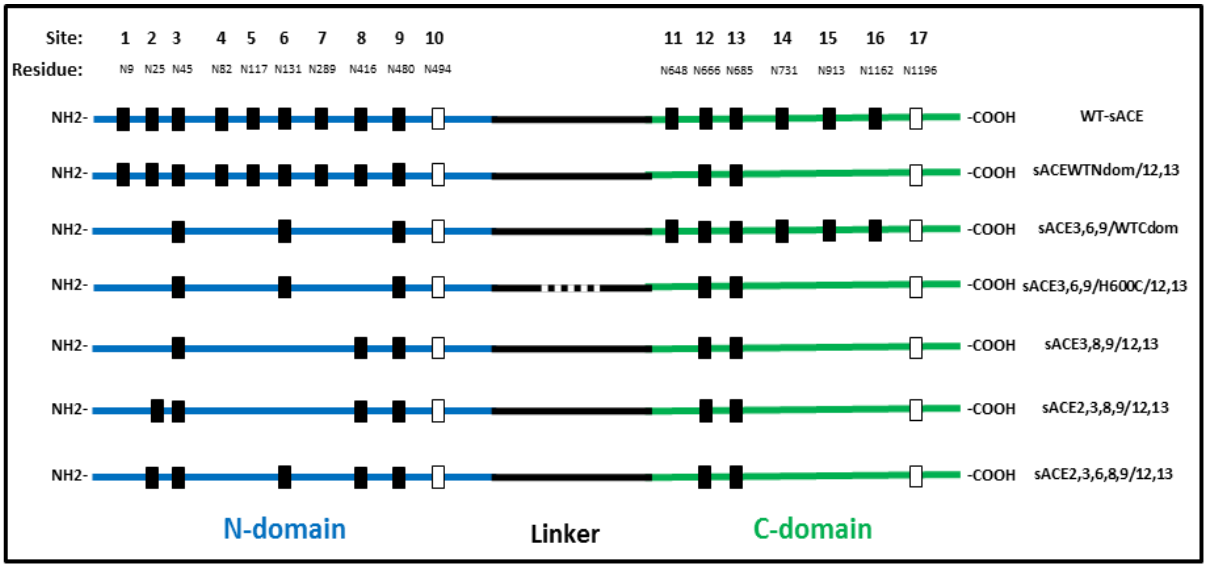

Figure 2.16: Diagrammatic representation of generated MG-sACE mutants. Black boxes indicate intact glycosylation sites and white boxes indicate sites that are not glycosylated. Dashed line indicates position of the H600C mutation. Numbers indicate glycosylation site positions.

A few anomalies were noticed in some agarose gels. In Figures 2.4, 2.6 and 2.10, residual undigested DNA was observed. Several factors may be responsible for this observation. Firstly, restriction enzymes may be less efficient due to suboptimal conditions caused by improper enzyme dilutions, excessive DNA content or less efficient buffering, especially during double digests where a certain buffer may be 100% optimal for one enzyme while only displaying 50-100% for another. Furthermore, contamination caused by impurities in the buffer, water and enzyme solution may be affecting enzyme activity. Additionally, reduced incubation time usually results in incomplete DNA digestion. Figure 2.4 A and B displayed an electrophoretic mobility shift of approximately 300 bp to approximately 500 bp. This phenomenon has been widely reported and forms the basis of the electrophoretic mobility shift assay used to study DNA-protein interactions (Makela *et al.*, 2012). Furthermore, RNase A, which is used to during DNA purification, has been shown to cause gel-shifts (Huhtanen *et al.*, 2012). Unexpected bands were observed migrating below bands of interest in Figures 2.10 A and 2.11. This was possibly due to BsaXI star activity caused by reduced enzyme efficiency due to improper storage and handling conditions. Six MG-sACE (Figure 2.16) mutants were successfully generated and found to contain no aberrant mutations from DNA sequencing data. Furthermore, the desired codons for Asn (AAC/T), Gln (CAG) and Cys600 (TGC) translation were observed.

Initial attempts to generate mutants using PCR based SDM were hindered by some technical difficulties;

Firstly, SDM yielded no product from several reactions using modified protocols of a standard PCR kit (Kapa HiFi PCR kit (Kapa Biosystems, Cape Town, South Africa)). This is usually a result of lack of primer annealing. Preferential annealing of mutagenic primers is essential for ensuring the incorporation of the desired mutation, and this usually requires optimization. Therefore an annealing temperature gradient PCR was done, however, no product was observed. Attempts to overcome this hurdle employed another method termed

Touch-down PCR which lowers the primer annealing temperature within a desired range after each cycle, thus increases reaction efficiency at lower annealing temperatures, while increasing the specificity at higher annealing temperatures. This too resulted in no product. This was possibly due to the cumbersome nature of the sACE gene in pcDNA3.1(+). The entire plasmid has a molecular weight of almost 10 kb, and it is known that large oligonucleotides may be problematic during the denaturing, annealing and extension steps (Ling *et al.*, 1997; B. Shen, 2002). Additionally, PCR on large plasmids is prone to increased spurious mutations that may occur due to slippage of *Taq* polymerase, especially with an increase in PCR cycles (Ling *et al.*, 1997). Due to these problems, PCR-based methods were abandoned. Subcloning on the other hand proved to be much more beneficial and less tedious with the exception of one difficulty encountered. Finding compatible restrictions sites proved to be challenging as sACE and individual domain constructs that have been generated previously lack some of the restriction sites in the multiple cloning site of the vectors in which they are inserted. This is due to the several sub/cloning experiments that have been carried out in the group, where some of the restriction sites were lost. Furthermore, considering the fact that MG-sACE constructs have restriction sites added/removed upon each glycosylation site alteration, some restriction sites that were engineered to facilitate subcloning for a particular study previously, were not compatible with this study. Thus, a degree of manoeuvring between constructs and multiple restriction enzyme digests had to be done in order to identify compatible sites for subcloning.

Chapter 3: Investigating the effect of *N*-glycan site occupancy on inter-domain linker proteolysis

3.1 INTRODUCTION

Great strides have been made in the rational drug design of domain selective ACE inhibitors. These have relied heavily on the availability of high resolution crystal structures of the N- and C-domain (see section 1.1.2). However, these structures provide little insight into the previously described cooperativity between the two domains of sACE (Binevski *et al.*, 2003; Friborg *et al.*, 2002; Woodman *et al.*, 2005). To date, the high resolution 3D structure of sACE has been elusive (see section 1.1.2). Solving the structure would aid in a better understanding of the functional and structural properties of the full-length sACE with regards to domain cooperativity, and the design of more potent and selective ACE inhibitors. As mentioned in Chapter 1, initial attempts to generate a suitable MG-sACE candidate for X-ray crystallography involved the combination of previously crystallized individual domains to yield sACE3,8,9/11,13 (Figure 3.1). Unfortunately, this glycosylation mutant was susceptible to limited proteolysis in the inter-domain linker region (Anthony, 2011), suggesting that removal of *N*-glycans rendered sACE susceptible to attack by an as yet unknown protease. Thus, a logical approach was to reintroduce *N*-glycans which are proximal to the inter-domain linker region in sACE3,8,9/11,13, in order to identify those crucial for preventing proteolysis. Identifying these key *N*-glycans is likely to aid in generating a stable MG-sACE construct with the least possible intact glycosylation sites, suitable for X-ray crystallography studies.

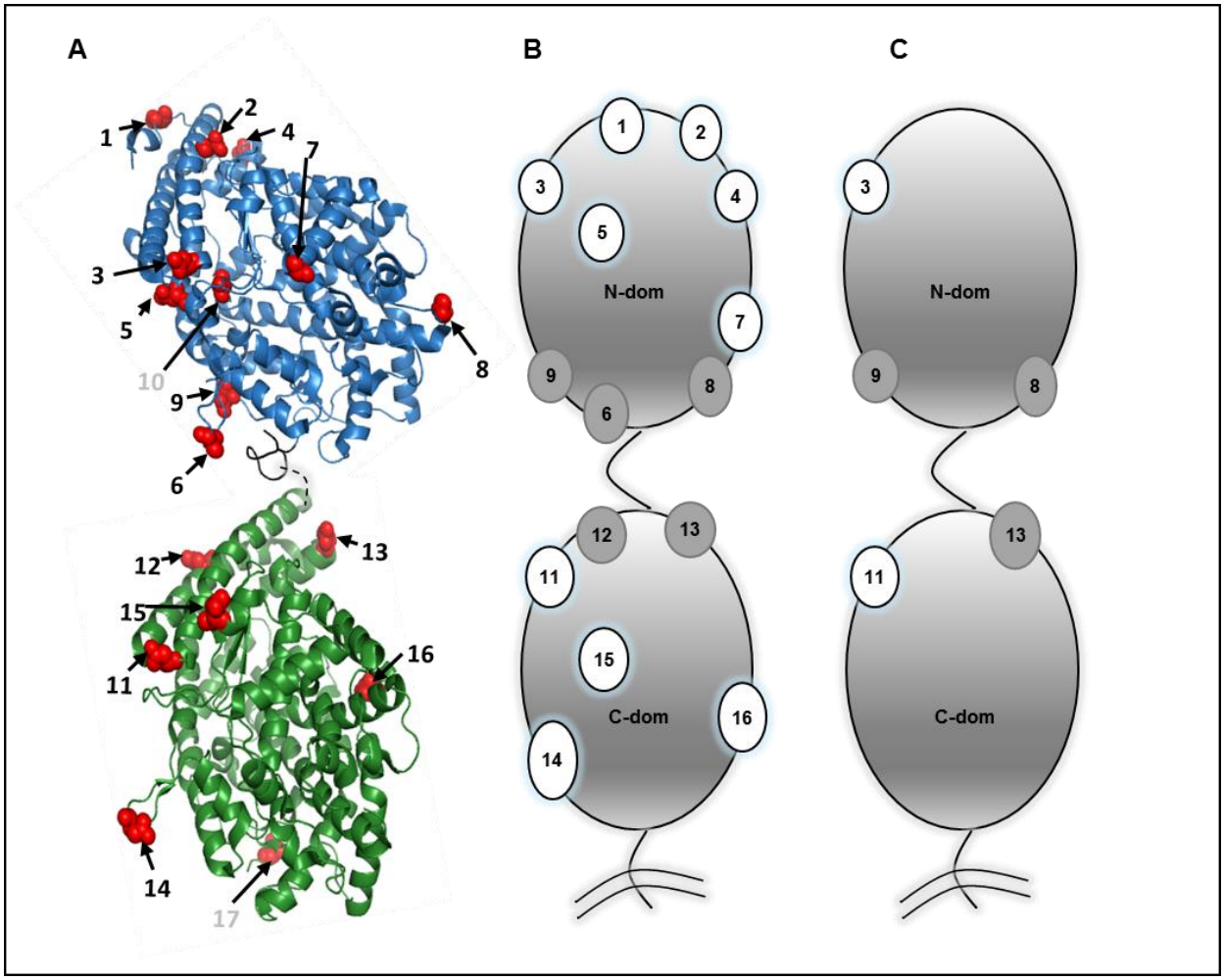

Figure 3.1: Two and three-dimensional representations of WT-sACE and sACE3,8,9/11,13 showing *N*-glycan site occupancy. A) Three-dimensional WT-sACE model of combined individual domain crystal structures. Glycosylation sites that are not glycosylated are faded. B) Two-dimensional WT-sACE model. C) Two-dimensional sACE3,8,9/11,13 model. Glycosylation sites are numbered starting from the N-domain. Glycosylation sites proximal the inter-domain linker region are indicated by grey circles. Dashed curve represents inter-domain linker connection.

Objective:

1) To determine the effect of *N*-glycan site occupancy on inter-domain linker proteolysis of minimally glycosylated somatic ACE.

3.2 EXPERIMENTAL METHODS

3.2.1 Transient transfection and expression of MG-sACE mutants in CHO cells

Chinese hamster ovary K1 (CHO-K1) cells were seeded into 6 well plates in complete growth medium (43% DMEM, 43% F-12 HAMS, 20 mM HEPES pH 7.5), supplemented with 10% fetal calf serum (FCS) which was heat inactivated at 56°C for 30 minutes, then incubated at 37°C in 5% CO_2 to reach approximately 50-80% confluence in 24 hours. Cells were transfected in triplicate or more with template DNA inserted in pCDNA3.1(+) (including a H_2O mock and a WT-sACE control) using the liposome method (GeneJuice® Transfection Reagent liposome method (Novagen)) as per manufacturer's instructions. Cell lysates and media were collected 24-72 hours post transfection for analysis.

3.2.2 Enzymatic activity determination via Z-Phe-His-Leu (Z-FHL) fluorimetric assay

To confirm successful transfection, ACE enzymatic activity was determined from harvested media and lysates using a Z-FHL fluorimetric assay, based on the Hippuryl-His-Leu (HHL) fluorimetric assay (Friedland and Silverstein in 1976). Assays were carried out using triplicate repeats for each sample collected from media and lysates. To 3 wells in a 96 well plate, 6 µl of each sample (in 2% FCS medium) was added. To these sample containing wells, 30 µl of a 1 mM Z-FHL working solution was then added, including an empty zero-blank-time (ZBT). These were incubated at 37°C for 15 – 30 minutes with shaking, to promote cleavage of Z-FHL. Following incubation, the reaction was stopped with 120 µl of 0.4 M NaOH per well. To the ZBT wells, 3 µl of medium/lysate was added and allowed to shake thoroughly. The cleaved product from the reaction was derivatized by the addition of 10 µl O-phthaldialdehyde (20 mg/ml of methanol) per well (including ZBT), followed by an

incubation for 10 minutes at room temperature with shaking in the dark. Derivitization was halted by the addition of 30 µl of a 3 M HCl solution. The fluorescence was measured at the excitation wavelength of λ_{Ex}=360nm and the emission wavelength of λ_{Em}=485nm in the Cary Eclipse Fluorimeter (Varian CA, USA). The fluorescent units (FU) were converted to enzyme activity in mU/ml/min using the HHL standard curve (Appendix A3), representative of the nmols of HL produced per ml of sample, per minute. Each of the activity values were calculated accordingly, considering both incubation period and the volume of sample added.

3.2.3 Sample preparation using lisinopril affinity resin

Samples displaying ACE activity were concentrated using Lisinopril-Sepharose beads (Lisinopril is a strong non-domain selective competitive inhibitor of sACE). Briefly, 60 µl of a Lisinopril-Sepharose resin prepared in wash buffer (20 mM HEPES, 800 mM NaCl (pH 7.5)) was added to 250 µl of media/lysates and vortexed for 30 minutes. Samples were then centrifuged at 12000xg for 5 minutes. The resultant supernatant was promptly discarded and the ACE-lisinopril pellet was resuspened with 20 µl wash buffer.

3.2.4 Western blotting and densitometry

Samples were electrophoresed in sodium dodecyl sulphate polyacrylamide gel using standard lab protocol (Appendix A4). Following electrophoresis, the protein was transferred from the gel to Hybond-ECL nitrocellulose membranes (Amersham, Buckinghamshire, UK) in blotting buffer (0.5 M Tris, 1.44% (w/v) glycine, and 0.2% (v/v) methanol) at 100 V for 1 hour. Membranes were then incubated in blocking buffer (5% (w/v) skim milk, 0.1% (v/v) Tween-20, 0.2 M NaCl, 0.05 M Tris-HCl (pH7.4)) overnight at 4°C, to prevent non-specific binding upon antibody incubation. Membranes were then incubated for 1.5 hours with the monoclonal rat anti-ACE primary antibody 4G6 (Balyasnikova *et al.*, 2003; Balyasnikova *et al.*, 2005) (1/250 dilution in blocking buffer), which detects a linear epitope on the N-domain of sACE. This was followed by a 1 hour incubation in anti-rat antibody (1/2000 dilution in blocking buffer). The membrane was then washed with blocking buffer three times for 5 minutes to remove any residual unbound antibody. Detection was carried out using the

Immun-Star™ WesternC™ Chemiluminescent Kit (BioRad, (Hercules, CA, USA)) as per manufacturer's instructions and visualized on a G:Box iChemi™ chemiluminescence imager (Syngene, Cambridge, UK) for quantification using ImageJ software (http://rsbweb.nih.gov/ij). The percentage cleavage was calculated as a function of the percentage of full-length sACE detected, by determining the ratio of full-length sACE remaining to the individual domain in the entire mixed population sACE isoforms present on the blot.

3.3 RESULTS

In order to understand the effect of glycosylation on the cleavage of the inter-domain linker region of sACE, a panel of MG-sACE mutants with varying *N*-glycan site occupancy proximal to the inter-domain linker were generated (see Chapter 2) (Figure 3.2).

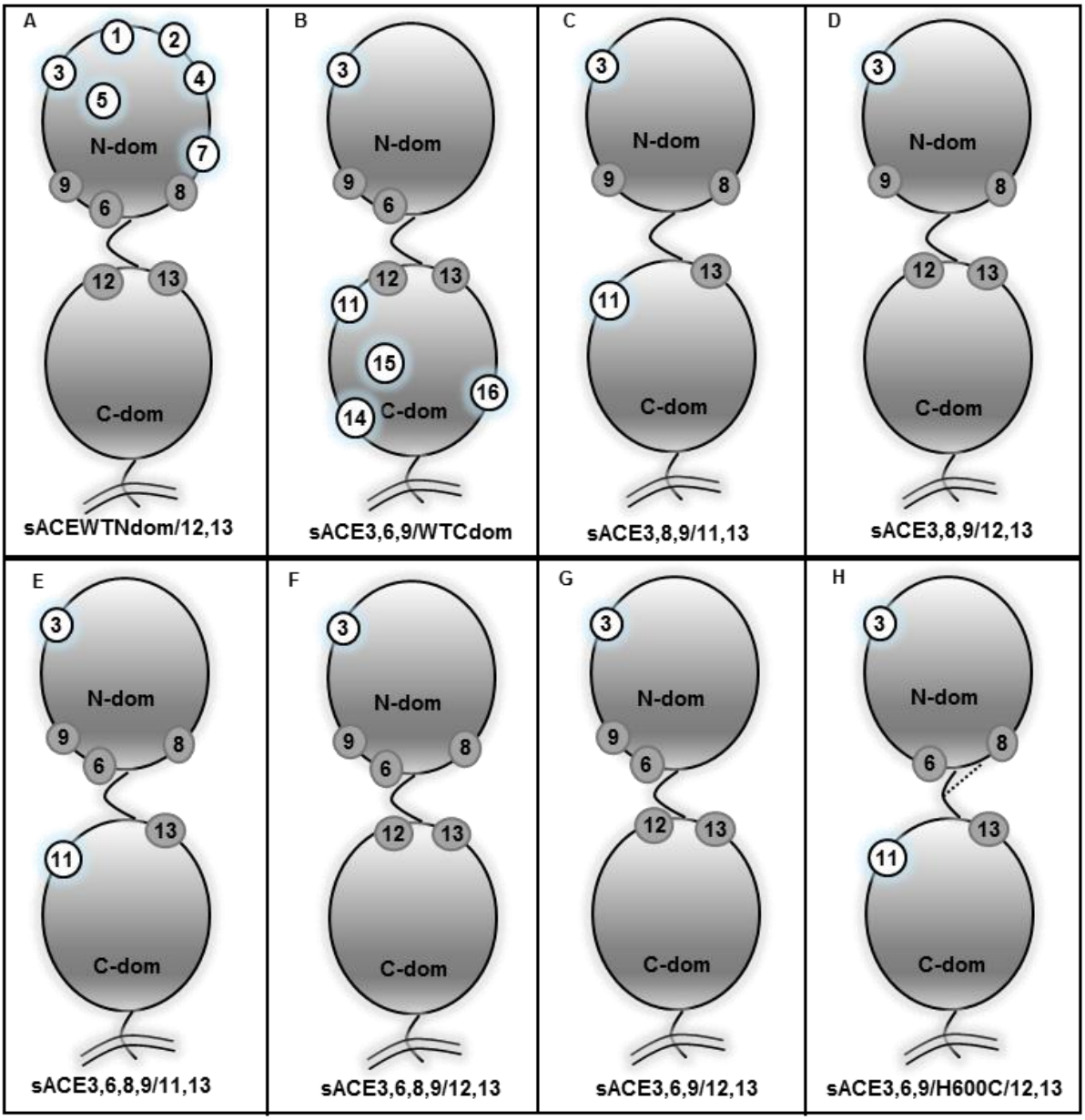

Figure 3.2: Diagrammatic representation of MG-sACE mutants showing respective *N*-glycan site occupancy. Glycosylation sites are numbered starting from the N-domain. Glycosylation sites proximal the inter-domain linker region are indicated by grey circles. Dotted line indicates disulphide bridge between C600 and C474.

These were transiently expressed in CHO cells, assayed for enzymatic activity, concentrated and Western blotted as previously described (see section 3.2). Protection from inter-domain linker proteolysis was first investigated by reintroducing the *N*-glycan at site 6 (N131). When comparing sACE3,8,9/11,13 and sACE3,6,8,9/11,13, it was noted that reintroduction of site 6 resulted in a small, but not significant, reduction in the cleavage (Figure 3.3).

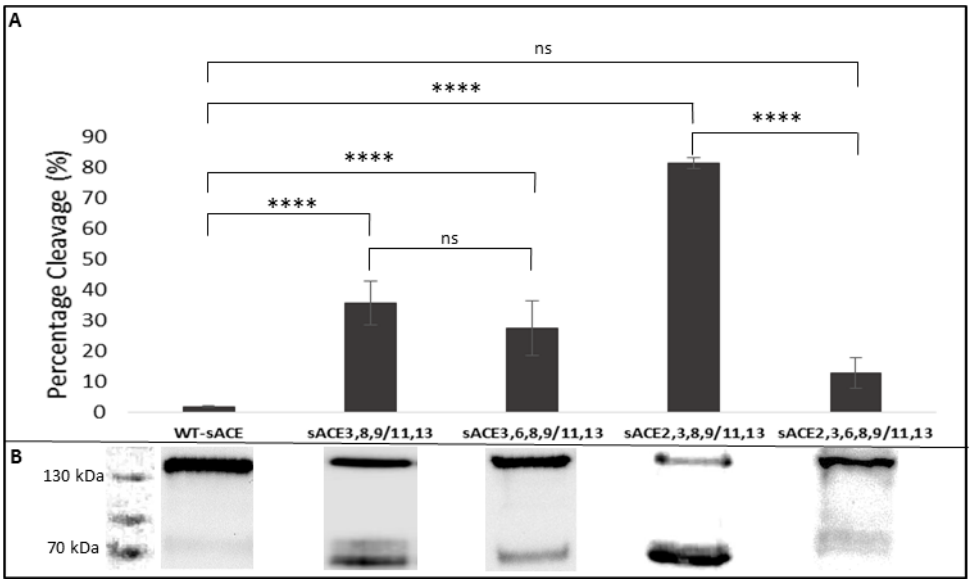

Figure 3.3: Percentage cleavage graph of MG-sACE mutants with and without glycosylation site 6 (N131) intact. A) Bar graph indicating percentage cleavage values of the respective MG-sACE mutants from triplicate or more experiments. The percentage cleavage was calculated as a function of the percentage of full-length sACE detected. B) Representative Western blots for each MG-sACE mutant. ****P ≤ 0.0001, ns = Not significant. Molecular weight marker – PageRuler™ Plus Prestained Protein Ladder. Error bars indicate mean ±SD.

Interestingly, addition of site 2 (N25) to sACE3,8,9/11,13 resulted in a 2-fold increase in the cleavage, which was significantly blunted by the addition of site 6 (Figure 3.3). Furthermore, sACE2,3,6,8,9/11,13's level of cleavage was not significantly different to that of WT sACE (Figure 3.3). This suggests that site 6 may be important in preventing, or at least limiting inter-domain linker proteolysis. Additionally, site 2 appears to increase MG-sACE's susceptibility to proteolysis, possibly by inducing a conformational change that exposes the linker region making it more susceptible to proteolysis (Figure 3.7). Substitution of site 11 (N648) with 12 (N666) revealed a striking result as there was a significant increase in the cleavage of sACE3,8,9/12,13 when compared to both WT-sACE and sACE3,8,9/11,13 (Figure 3.4).

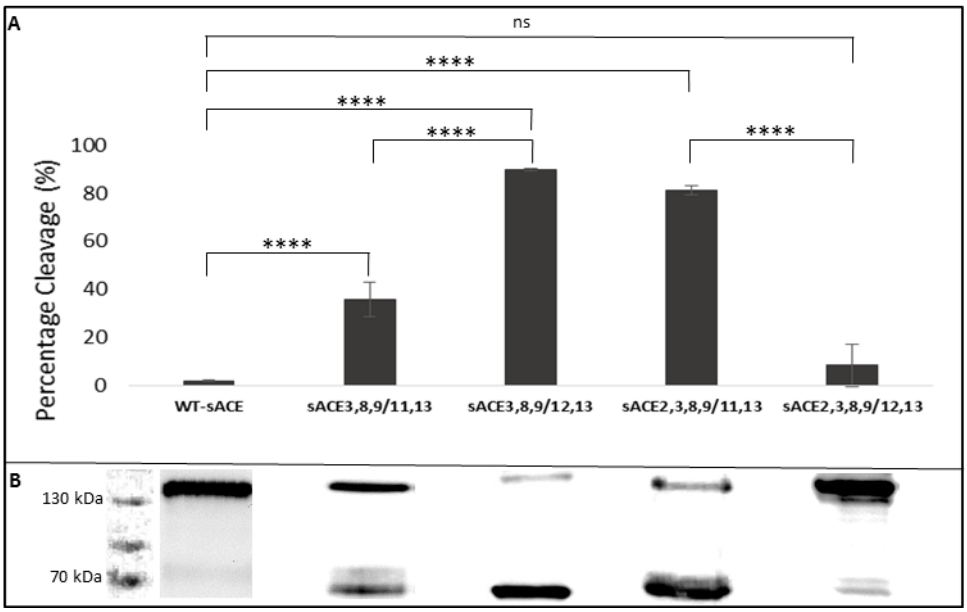

Figure 3.4: Percentage cleavage graph of MG-sACE mutants with and without glycosylation site 12 (N666) intact. A) Bar graph indicating percentage cleavage values of the respective MG-sACE mutants from triplicate or more experiments. The percentage cleavage was calculated as a function of the percentage of full-length sACE detected. B) Representative Western blots for each MG-sACE mutant. ****P ≤ 0.0001, ns = Not significant. Molecular weight marker – PageRuler™ Plus Prestained Protein Ladder. Error bars indicate mean ±SD.

This was unexpected as site 12 is proximal to the inter-domain linker region. Interestingly, when site 2 was reintroduced in the presence of site 12 (N666), the cleavage levels were reduced dramatically and cleavage was not significantly different to WT-sACE (Figure 3.4). This trend between sACE2,3,8,9/11,13 and sACE2,3,8,9/,12,13 is similar to that noticed with the reintroduction of site 2 and 6 in a single mutant (Figure 3.3), suggesting that site 12 may be playing a role in limiting cleavage but requires the presence of site 2 to cause a conformational change or steric hindrance that affects cleavage. When both site 6 and 12 are intact in MG-sACE, cleavage is reduced by 65% or more (Figure 3.5).

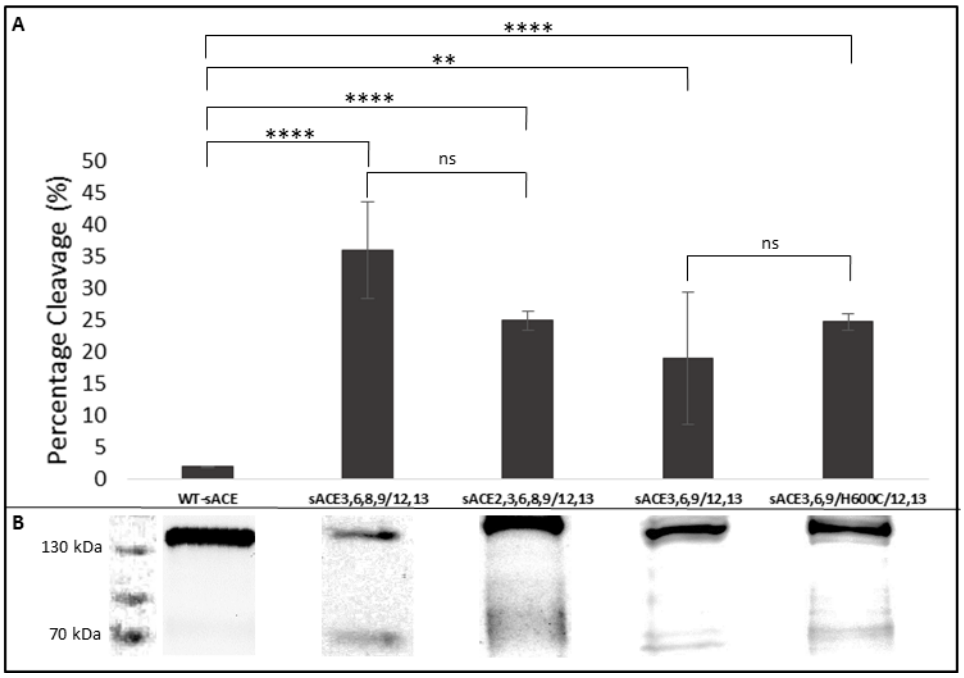

Figure 3.5: Percentage cleavage graph of MG-sACE mutants with a combination of glycosylation sites 6 (N131) and 12 (N666) intact and sACE3,6,9/H600C/12,13. A) Bar graph indicating percentage cleavage values of the respective MG-sACE mutants from triplicate or more experiments. The percentage cleavage was calculated as a function of the percentage of full-length sACE detected. B) Representative Western blots for each MG-sACE mutant. **P ≤ 0.01, ****P ≤ 0.0001, ns = Not significant. Molecular weight marker – PageRuler™ Plus Prestained Protein Ladder. Error bars indicate mean ±SD.

With the mutant sACE2,3,6,8,9/12,13, the detrimental effect of site 2 is again blunted by the presence of both site 6 and 12. The most striking result is noticed with sACE3,6,9/12,13 which is the least susceptible to proteolysis (Figure 3.5). This suggests that glycosylation sites 3, 6, 9, 12 and 13 are crucial for protecting against proteolysis, although the cleavage is still significantly higher than that of WT-sACE (Figure 3.5). Furthermore, the presence of a disulphide bridge through the H600C substitution did not have a significant effect on reducing proteolysis (Figure 3.5). WT domain substitutions in MG-sACE revealed that the presence of a fully-glycosylated N-domain resulted in a 10-fold increase in the percentage cleavage when compared to WT-sACE. In contrast, the presence of a fully-glycosylated C-domain caused an increase in the cleavage when compared to WT-sACE that was not significant (Figure 3.6). This suggests that C-domain glycans are more important in protecting the inter-domain linker from proteolysis.

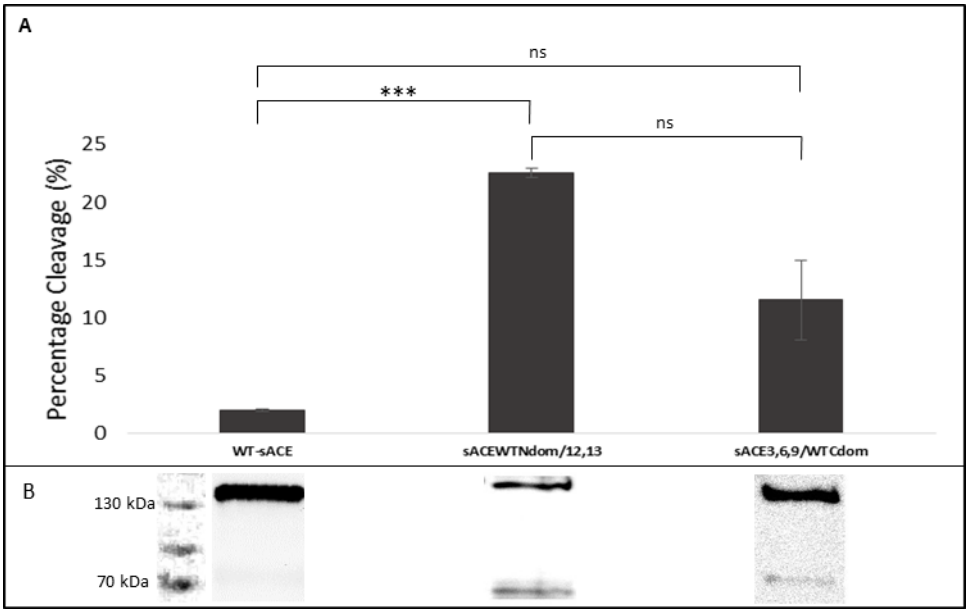

Figure 3.6: Percentage cleavage graph of domain substitution MG-sACE mutants. A) Bar graph indicating percentage cleavage values of the respective MG-sACE mutants from triplicate or more experiments. The percentage cleavage was calculated as a function of the percentage of full-length sACE detected. B) Representative western blots for each MG-sACE mutant. ***P ≤ 0.001, ns = Not significant. Molecular weight marker – PageRuler™ Plus Prestained Protein Ladder. Error bars indicate mean ±SD.

3.3 DISCUSSION

This study investigates the effect of *N*-glycan site occupancy on the proteolysis of the ACE inter-domain linker. The first MG-sACE that was previously generated in our research group had three *N*-glycans proximal to the inter-domain linker (site 8 (N416), 9 (N480) and 13 (N685)) (Figure 3.1). However, this site occupancy did not prevent inter-domain linker proteolysis. Therefore, two additional sites (6 (N131) and 12 (N666)) were reintroduced. A striking observation was made upon the reintroduction site 2. It resulted in a significant increase in linker proteolysis (Figures 3.3 and 3.4). It is unclear why the reintroduction of site 2 has this detrimental effect site 2 is located on the lid region of the N-domain (see section 1.1.2), which is a substantial distance from inter-domain linker region (approximately 60 Å). However, differences in *N*-glycan site occupancy in the lid region have been shown to result in local conformational changes within the ACE protein structure, evidenced by reduced binding of monoclonal antibodies raised to the epitope in this region of WT-sACE (Taasoli *et al.*, 2008). Additionally, site 2 is known to be important in the expression and thermal

stability of the N-domain (Anthony, 2011), therefore it is possible that it may have different functions within sACE. Furthermore, glycosylation has been implicated in inter-domain interactions such as homodimerization of ACE (Corradi *et al.*, 2006; Gordon, 2011). Before evaluating these data, it is important to note that both the *N*-glycans and the inter-domain linker region display a high degree of flexibility. Therefore, *in vitro*, MG-sACE may assume different conformations depending on these two factors. The presence of some *N*-glycans may favour a conformation that rarely allows access to the linker region by the protease responsible for the cleavage, while other *N*-glycans may favour the opposite. Thus, it is possible that N25 at site 2 may induce a conformational change which renders the inter-domain linker region more susceptible to proteolytic attack (Figure 3.7).

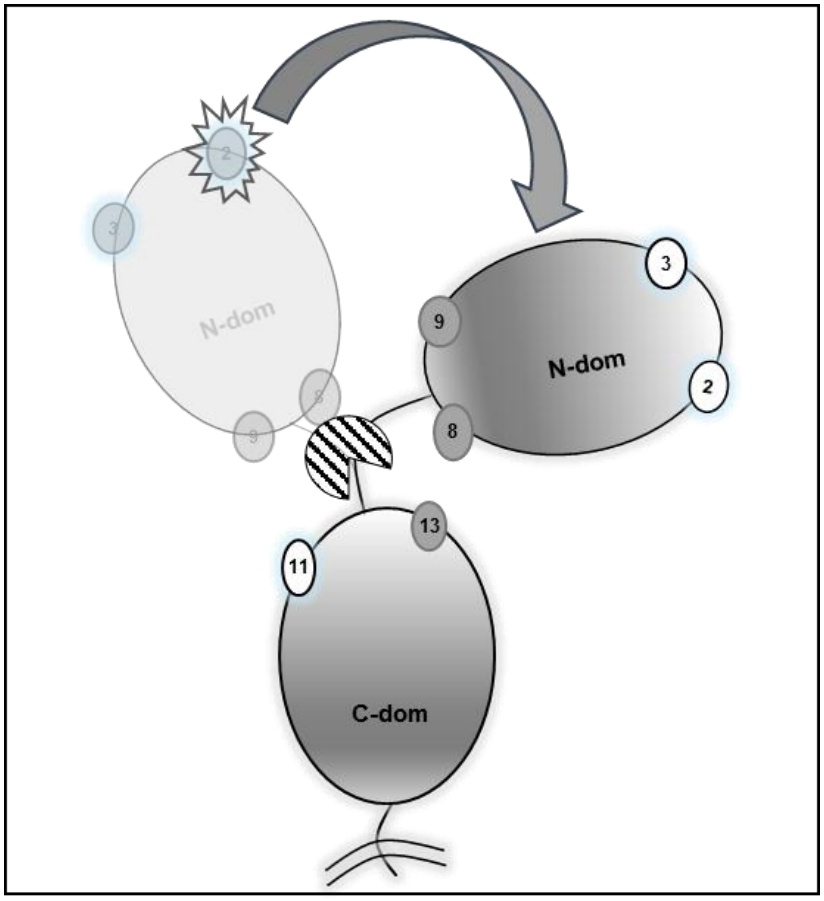

Figure 3.7: Proposed mechanism of increased susceptibility to proteolysis in the presence of glycosylation site 2 in sACE2,3,8,9/11,13. Site 2 may induce a conformational change, leaving the inter-domain linker region susceptible to proteolytic attack. Glycosylation sites are numbered starting from the N-domain. Sites proximal the inter-domain linker region are indicated by grey circles. Proteolytic enzyme is indicated by a striped pacman cartoon.

Interestingly, reintroduction of site 6 abolished this increase in susceptibility to proteolysis induced by site 2 and this might be due to the following;

1) N131 might be reversing the N25 induced conformational change in MG-sACE (Figure 3.8 A), therefore making the inter-domain linker region less susceptible to proteolysis; or 2) The presence of a sugar at site 6 may be physically shielding the inter-domain linker region from proteolytic attack, even in the glycan 2-induced conformation (Figure 3.8 B). The protective effect of site 6 is observed with every MG-sACE mutant in which it is intact, suggesting that site 6 is crucial for protecting against inter-domain linker proteolysis.

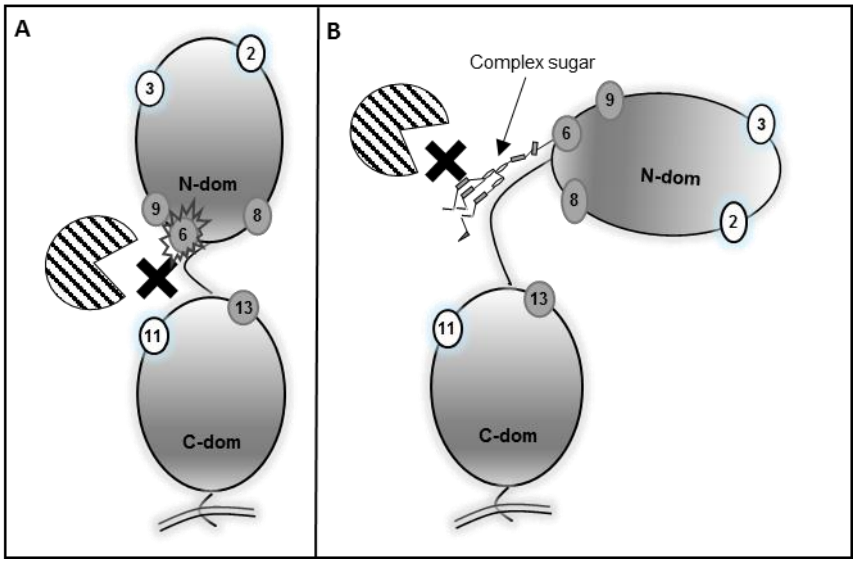

Figure 3.8: Proposed mechanisms of site 6 protection from inter-domain linker proteolysis in the presence of glycosylation site 2 using sACE2,3,8,9/11,13, and sACE2,3,6,8,9/11,13 as models. A) Site 6 may reverse the site 2 induced conformational change, resulting in a conformation of sACE which limits access of the responsible protease to the inter-domain linker region. B) Site 6 may physically prevent access of the responsible protease to the inter-domain linker region, even in the site 2 induced conformation. The complex sugar represents the possible type of glycan attachment to N131 at site 6. Glycosylation sites are numbered starting from the N-domain. Sites proximal the inter-domain linker region are indicated by grey circles. Proteolytic enzyme is indicated by a striped pacman cartoon.

Replacing a glycan at site 11 with one at site 12 (sACE3,8,9/12,13) had a similar effect to the introduction of a glycan at site 2 (Figure 3.4), which was unexpected as site 12 is in close proximity to the inter-domain linker region. Previously, *N*-glycans in the lid subdomain of the C-domain (site 11 (N648) and site 12 (N666)) have been proposed to be involved in inter-domain interactions (Corradi *et al.*, 2006).

Thus, a glycan at site 12 may be interacting with the nearest glycan (N685) at site 13, limiting its flexibility and exposing the last few residues of the linker region (see section 1.1.2) which are the most flexible, and thus more likely to undergo proteolysis. Interestingly, reintroduction of the detrimental site 2 resulted in a striking decrease in the linker proteolysis, similar to that seen with WT-sACE (Figure 3.4). This unexpected observation may be explained by the fact that a glycan at N666 (site 12) is thought to be involved in inter-domain interactions. Therefore, a strong interaction between it and a glycan at N131 (site 6) may be occurring, and thus physically shielding the linker region from proteolysis. Alternatively, the presence of both N131 and N666 may favour a more stable conformation of sACE which is less susceptible to proteolytic attack. Here, an interesting dynamic is observed in the presence of two glycans that have synergistic properties when both are present, but have detrimental effects when either is absent. This is reminiscent the redundant nature of *N*-glycans, where the importance of one may only be noticed when the other is absent/present. However, additional work needs to be done to verify the proposed effect of the possible interaction between glycans at sites 6 and 12.

A clear synergistic effect is noticed when glycosylation sites 6 and 12 are present in MG-sACE (Figure 3.5). Interestingly, when only sites 3, 6, 9, 12 and 13 are present, the cleavage is dramatically reduced. This suggests that site 8 may not be involved in protecting the linker from proteolysis, albeit a glycan that is in close proximity to the linker region. This observation paves the way for identifying the least possible intact glycosylation sites required for a stable MG-sACE. Stabilization of the linker region through the H600C substitution made no significant difference, suggesting that limiting flexibility by the introduction of an additional disulphide (Cys474 – Cys600) in the linker does not confer protection from proteolysis (Figure 3.5). A construct with a minimally glycosylated N-domain fused to a wild-type C-domain (sACE3,6,9/WTCdom) revealed similar linker cleavage to that of wild-type sACE. In contrast, a wild-type N-domain fused to a minimally glycosylated C-domain

(sACEWTNdom/12,13) resulted in an approximate 10-fold increase in proteolysis (Figure 3.6). This suggests that *N*-glycans on the C-domain are more important in protecting from inter-domain linker proteolysis. As mentioned previously, the stability of sACE is affected by both temperature (thermal stability (see Chapter 4)) and proteolysis. It is well known that the N-domain is responsible for most of sACEs thermal stability through extensive N-glycosylation (Anthony, 2011; O'Neill *et al.*, 2008; Voronov *et al.*, 2002). Thus, it is likely that the C-domain may be important in conferring stability, evidenced by its ability to limit inter-domain linker proteolysis.

Chapter 4: The effect of glycosylation on the expression and stability of sACE

4.1 INTRODUCTION

sACE is a membrane-bound protein that is exported to the cell surface in its mature form and is also shed from the cell surface (Cannon *et al.*, 2007; Danilov *et al.*, 2011; Friborg *et al.*, 2002; Kost *et al.*, 2003; Taastrom *et al.*, 2004; Woodman *et al.*, 2005). Although truncated soluble constructs of sACE have been engineered, the membrane-bound form is also cleaved and released into the medium as a soluble form. Furthermore, individual domains of cleaved membrane-bound MG-sACE mutants are also found in culture medium. This prompts the following questions: 1) does inter-domain linker proteolysis occur intracellularly or extracellularly? and 2) does it occur during synthesis, post-translationally? Thus, determining the location of linker proteolysis will aid in understanding the process of proteolysis as well as serve as a stepping stone towards identifying the protease(s) responsible.

It is well known that protein glycosylation affects the expression and thermal stability of sACE and its individual domain isoforms (Anthony *et al.*, 2010; O'Neill *et al.*, 2008; Voronov *et al.*, 2002). Previous work has determined that two N-terminal glycosylation sites are required for the expression of functional C-domain (Gordon *et al.*, 2003), while three C-terminal or two C- and one N-terminal glycosylation sites are required for the N-domain (Anthony *et al.*, 2010). An MG-sACE protein (sACE3,8,9/11,13) comprised of these hypo-glycosylated domains suggests that the same glycosylation sites are sufficient for the expression of sACE. However, the effect of additional glycosylation sites on the expression of MG-sACE has not been investigated. As previously mentioned, glycosylation site 2 is important in both the expression and thermal stability of the N-domain (Anthony *et al.*, 2010), therefore, reintroduction of this site into MG-sACE was used as the starting point for this

study. Furthermore, available MG-sACE mutants were assessed for differences in expression and stability profiles (Figure 4.1), with the exception of sACE3,6,8,9/11,13 due to its oligosaccharide site occupancy similarity to sACE3,6,8,9/12,13. Expression of MG-sACE has proven to be problematic as some mutants are expressed at levels which are insufficient for downstream purification. Hence, only a few of the MG-sACE mutants were successfully expressed and purified. These were used to investigate the effect of glycosylation on the thermal stability.

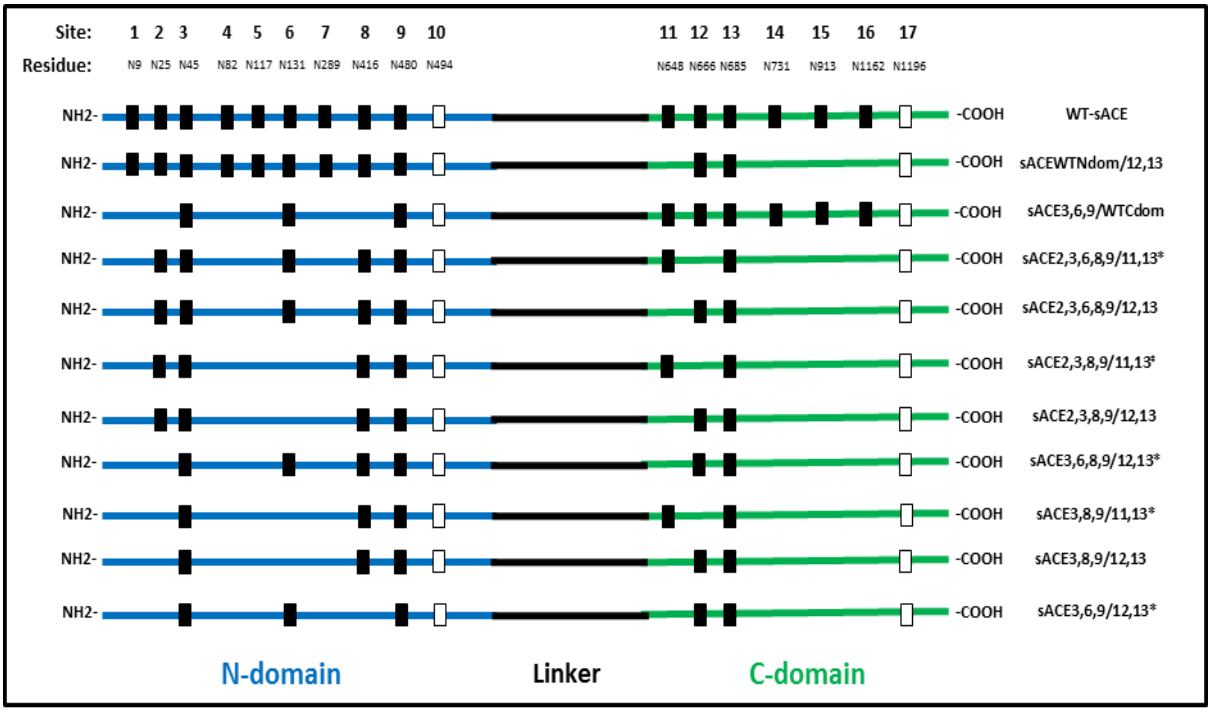

Figure 4.1: Diagrammatic representation of MG-sACE mutants assessed for differences in expression and stability profiles. Black boxes indicate intact glycosylation sites and white boxes indicate sites that are not glycosylated. Numbers indicate glycosylation site positions.
*Mutants generated by C.S. Anthony (2011).
‡Mutant generated for Honours Thesis (2011).

Objectives:

1) To determine the cellular localization of the inter-domain linker proteolysis.
2) To investigate the effect of *N*-glycosylation on the expression of sACE.
3) To investigate the effect of *N*-glycosylation on the thermal stability of sACE.

4.2 EXPERIMENTAL METHODS

4.2.1 Transfection and expression

MG-sACE mutants were initially transiently transfected and mutants displaying high enzymatic activity from these experiments were stably transfected for selection and purification (Table 4.1).

Table 4.1: Summary of transfection method for each MG-sACE.

MG-sACE	Transient	Stable
sACEWTNdom/12,13	✓	×
sACE3,6,9/WTCdom	✓	✓
sACE2,3,6,8,9/11,13	✓	×
sACE2,3,6,8,9/12,13	✓	×
sACE2,3,8,9/11,13	✓	×
sACE2,3,8,9/12,13	✓	×
sACE3,6,8,9/12,13	✓	✓
sACE3,8,9/11,13	✓	✓
sACE3,8,9/12,13	✓	×
sACE3,6,9/12,13	✓	×

4.2.1.1 Transient transfection of MG-sACE in CHO cells

All transient transfections were carried out as described in section 3.2.1. For determining the cellular localization of proteolysis, complete growth medium was replaced with serum-free medium (Gibco Opti-MEM, Invitrogen, USA) 24 hours post analysis.

4.2.1.2 Stable transfection, selection and expression of high expressing recombinant MG-sACE in CHO cells

High expressing recombinant MG-sACE constructs were stably transfected into CHO cells as follows. Cells were seeded into 10 cm^3 plates in complete growth medium (10% FCS, 43% DMEM, 43% F-12 HAMS, 20 mM HEPES pH 7.5) at 37°C with 5% CO_2, until 50%

confluency was reached. These were then transfected with template DNA inserted in pCDNA3.1(+) using the $CaPO_4$ method (ProFection® Mammalian Transfection Systems kit - Promega, WI, USA) as per manufacturer's instructions. Cells were incubated with complete growth medium overnight, which was then replaced with selective medium containing 0.8 mg/ml of Geneticin (G418, Sigma, MO, USA). Geneticin resistant colonies were picked from the mixed culture using sterile toothpicks and seeded in duplicate into 24-well plates. For cells expressing transmembrane constructs, one well was lysed using lysis buffer (1% (v/v) Triton X-100, 50 mM HEPES, 500 mM NaCl, 1 mM phenylmethylsulfonyl fluoride (PMSF)) and assayed for enzymatic activity. Cells expressing soluble constructs were incubated in 2% FCS for 24 hours and assayed for activity. Clones having high activity were lifted using trypsin-EDTA (0.5% (w/v) Trypsin, 0.5 mM EDTA, PBS pH 7.4). And grown further for stocks (Appendix A6). This was repeated until cells were transferred into two T75 tissue culture flasks. Cells expressing transmembrane constructs were sorted. FACS was carried out at the Institute of Infectious Disease and Molecular Medicine (IDM, University Of Cape Town). Cells in a T75 were washed three times with 1x PBS and lifted with trypsin-EDTA, then resuspended in 1 ml 1x PBS. Cells were labelled with 10 µg/ml of primary monoclonal antibody 1D8 raised to an epitope on the central part of the C-domain (Balyasnikova *et al.*, 2005; Nikolaeva *et al.*, 2006), for 30 minutes at room temperature. These were centrifuged and washed with 1x PBS three times. Cells were then incubated with 5 µl Alexa Fluor® 488 Goat Anti-Mouse IgG (H+L) antibody (Sigma, MO, USA) for 30 minutes on ice in the dark. Cells were washed as mentioned above and resuspended in 1 ml 10% FCS and transferred to a falcon tube. Sorted cells were added to a T25 culture flask with 10% FCS containing 1% (v/v) Penicillin Streptomycin and allowed to grow to confluency. Cells were then lifted and transferred into multiple T175 culture flasks. These were lysed with lysis buffer and lysates were collected in sterile 50 ml tubes. Cell lysates were centrifuged at 4000xg at 4˚C for 15 minutes. The resultant supernatants were collected in sterile 50 ml tubes and stored at -20˚C until purification. Cells expressing soluble constructs were grown until confluent in multiple

T175 flasks and incubated with 2% FCS at standard conditions. Medium was harvested after 48 to 72 hours into sterile 50 ml tubes and stored at -20˚C until used.

4.2.2 Sample preparation for using lisinopril affinity resin

Samples for determining the cellular localization of inter-domain linker proteolysis were prepared as described in section 3.2.3.

4.2.3 Western blotting and densitometry

Western blotting and densitometry was carried out as described in section 3.2.4. There was a variation in the primary antibody used to determine the cellular localization of proteolysis. Here, an antibody cocktail of two monoclonal anti-ACE antibodies (4G6 and 1D8 (Balyasnikova *et al.*, 2003; Balyasnikova *et al.*, 2005; Nikolaeva *et al.*, 2006)) was used to detect both the N- and the C-domain.

4.2.4 Enzymatic activity determination via Z-Phe-His-Leu (Z-FHL) fluorimetric assay

Enzymatic activity was determined as described in section 3.2.2.

4.2.5 Purification of MG-sACE proteins

Expressed proteins were purified using lisinopril-sepharose affinity chromatography (Ehlers *et al.*, 1991). Medium/lysate harvests were allowed to flow through the column at a speed of 1.0 ml/min. Once the medium/lysate was loaded onto the column, wash buffer was allowed to flow through at a speed of 0.25 ml/min overnight to wash off unbound protein. Bound protein was pH eluted with degassed 50 mM borate at pH 9.5 and 2 ml fractions were collected. Fractions showing ACE activity were pooled and dialysed in 2x 2 litres 50 mM HEPES with 0.1 mM PMSF at 4˚C. Protein was concentrated to approximately 500 µl using 30000 kDa Amicon® Ultra-4 centrifugal filter units (Millipore, Cork, Ireland). The optical density, at a wavelength 280 nm (OD280), was read using NanoDrop™ 1000 spectrophotometer to determine the concentration of the final protein using a calculated extinction coefficient of 309815 M^{-1} cm^{-1}.

4.2.6 Protein Purity Determination via SDS-PAGE

Protein purity was assessed using a standard SDS-PAGE protocol (Appendix A4). Proteins were then stained with Coomassie (0.2% (w/v) Coomassie Blue, 7% (v/v) glacial acetic acid, 50% (v/v) ethanol) overnight and destained in destain solution (7% (v/v) glacial acetic acid, 25% (v/v) ethanol) for visualization

4.2.7 Determination of kinetic constants for Z-FHL hydrolysis

Kinetic parameters for Z-FHL (Bachem, Budendorf, Switzerland) hydrolysis were determined using the abovementioned fluorimetric assay. Initial reaction rates were calculated using Z-FHL concentration range of 0.00 to 2.5 mM. Assays were done at least three times in triplicate. Data was fitted in GraphPad Prism (GraphPad Software Inc., USA) and Michaelis-Menten constants (K_m, V_{max}, k_{cat} and k_{cat}/K_m) were calculated accordingly. Kinetic values were normalized according to the specific activities of each protein.

4.2.8 Thermal denaturation assay

Purified MG-ACE proteins were incubated at 55°C for up to 90 min in 50 mM HEPES, pH 7.4. Residual enzymatic activity was determined at different time points as described in section 3.2.2.

4.3 RESULTS

4.3.1 Determining cellular localization of inter-domain linker proteolysis

To determine the cellular location of inter-domain linker proteolysis, cell lysate and medium were harvested from cells expressing sACE3,6,8,9/12,13 and analysed using Western blotting (Figure 4.2). Full-length MG-sACE corresponding to the band at 160 kDa was observed in both the cell lysate and the medium. Similarly, the N-domain corresponding to the band at 90 kDa was also found in both lysate and medium. In contrast, the C-domain that ran with a higher mobility than the N-domain due to its lower content of oligosaccharides, was only found in the cell lysate.

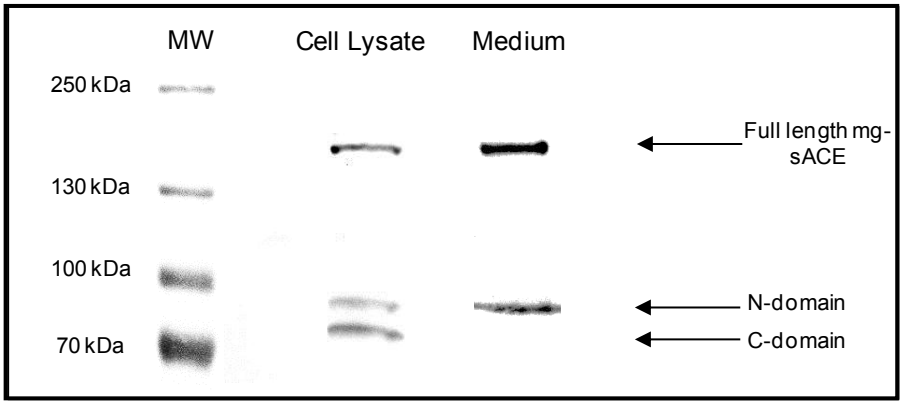

Figure 4.2: Western blot of sACE3,6,8,9/12,13 medium and lysate samples with a cocktail of monoclonal antibodies directed towards the N-domain (4G6) and the C-domain (1D8). Full-length MG-sACE, N-domain and C-domain are indicated with black arrows. MW - PageRuler™ Plus Prestained Protein Ladder.

4.3.2 The effect of glycosylation on the expression of unpurified MG-sACE proteins

To assess the effect of glycosylation on the expression of MG-sACE, constructs were transiently expressed and assayed for enzymatic activity as described in sections 4.2.1.1 and 4.2.4. Western blotting and densitometry were then used to obtain the full-length MG-sACE pixel density (PD) (total peak area) of the bands from each blot. This was then normalized by calculating ACE activity over PD ratio (mU/ml/PD). This value gives an indication of the total active protein per transient transfection, similar to the specific activity. This was done due to the fact that the specific activities of some MG-sACE could not be determined as expression levels were too low for protein purification and characterization. As seen in Figure 4.3, MG-sACE variants with only five intact glycosylation sites (sites 3 (N45), 6 (N131) or 8 (N416), 9 (N480), 12 (N666) and 13 (N689)) displayed an approximately 4-fold lower mean activity/PD ratio in comparison to WT-sACE.

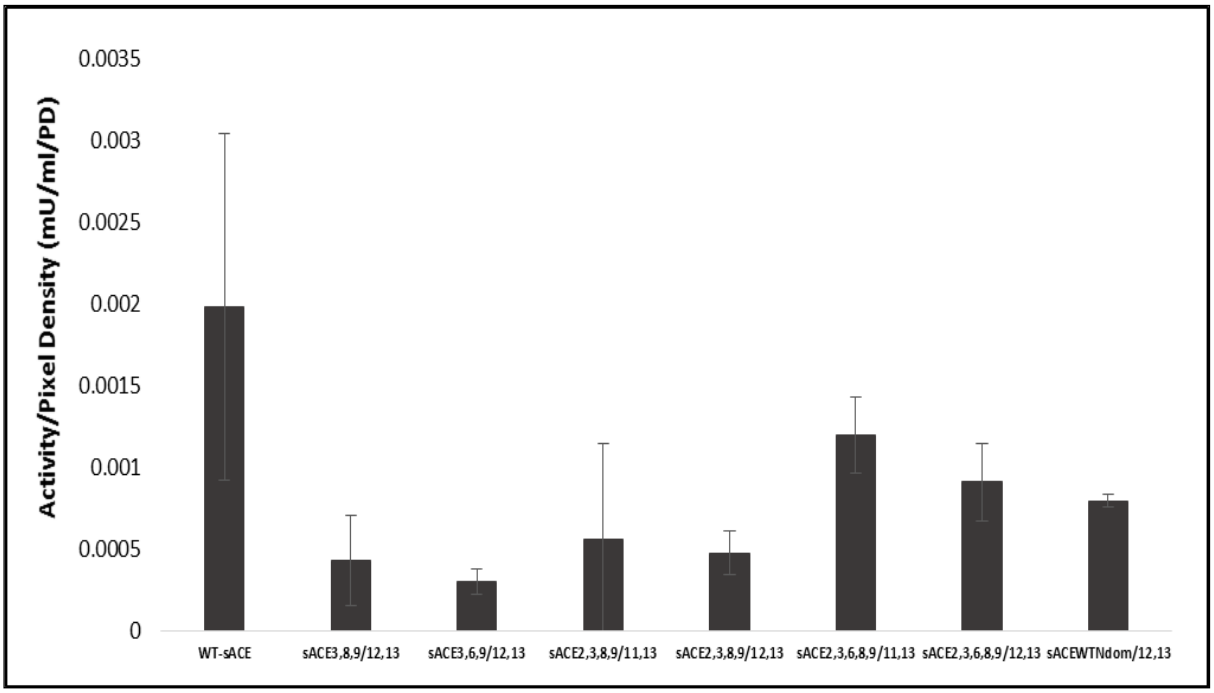

Figure 4.3: Graph indicating total active protein per transient transfection. The activity/pixel density ratio was determined using western blotting, densitometry and the activity in mU/ml of each sample. Transfections were done in duplicate. Error bars indicate mean ±SD.

Furthermore, addition of site 2 (N25) did not have a notable effect on the abovementioned variants, suggesting that this site is not important in the expression of sACE. Interestingly, MG-sACE variants that have both sites 6 and 2 intact have an overall higher activity/PD ratio, suggesting that these sites, in combination, are important in maintaining a high expression profile. When site 12 is substituted with site 11 (N648), the activity/PD ratio is increased slightly (Figure 4.3). Surprisingly, an MG-sACE with a fully glycosylated N-domain that has 12 potential glycosylation sites has a slightly lower activity/PD ratio compared to those with six intact sites (Figure 4.3), highlighting the fact that there is some redundancy of the *N*-glycosylation sites in sACE.

4.3.3 The effect of glycosylation on the expression of purified MG-sACE proteins

Relatively high expressing MG-sACE variants were purified as described in section 4.2.5. Purification yields were 381 mg/L for sACE3,8,9/,11,13; 122 mg/L for sACE3,6,8,9/12,13; and 381 mg/L for sACE3,6,9/WTCdom. To determine the effect of glycosylation on ACE expression, the specific activity was calculated promptly after purification and the degree of purity was assessed by SDS-PAGE as described in section 4.2.6. The specific activities of sACE3,8,9/11,13 and sACE3,6,9/WTCdom were found to be almost 6-fold lower than that of WT-sACE (Figure 4.4 A). Interestingly, a sharp increase in the specific activity was noticed with sACE3,6,8,9/12,13, further highlighting the importance of site 6 (Figure 4.4 A) (see section 4.3.2). Furthermore, minor changes in the electrophoretic mobility of the hypo-glycosylated constructs sACE3,8,9/11,13 and sACE3,6,8,9/12,13 were noticed (Figure 4.4 B), correlating with the decrease in the number of intact glycosylation site and thus, in the *N*-glycan content of each mutant.

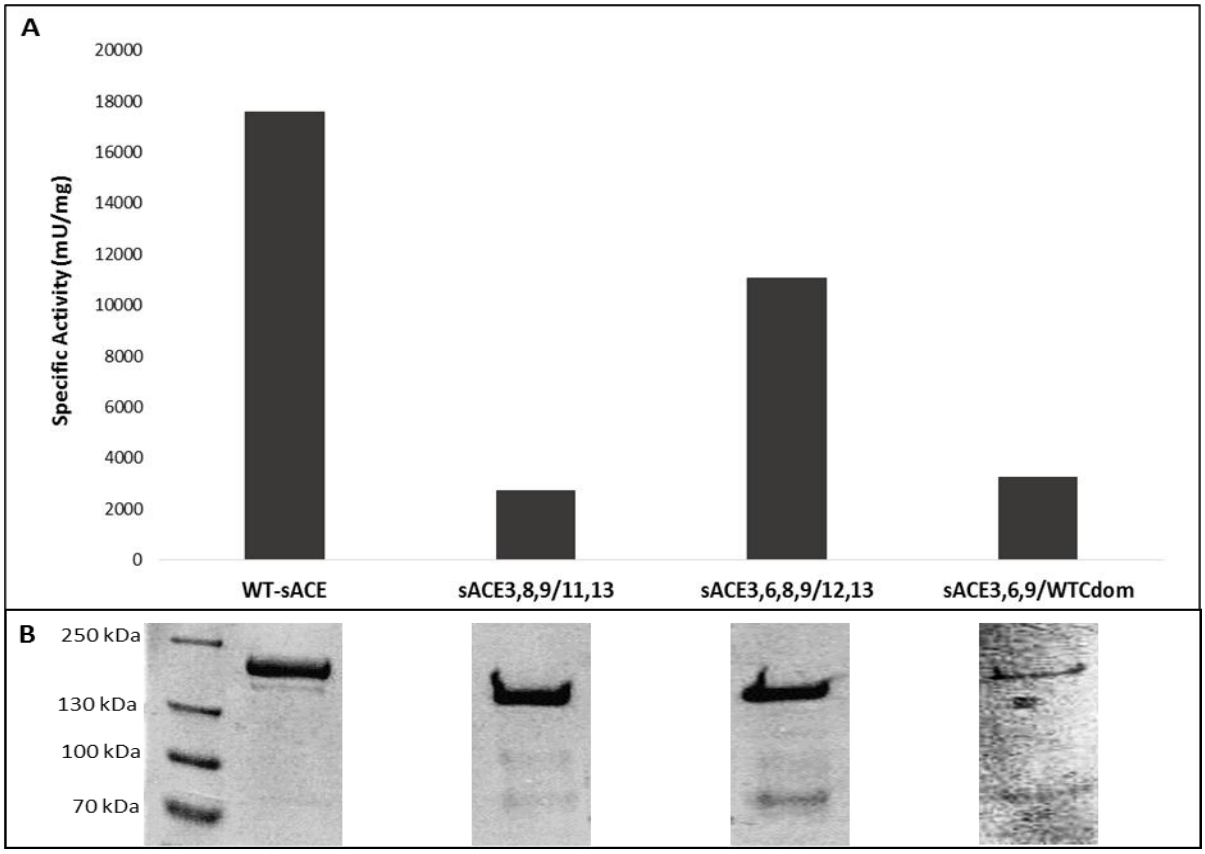

Figure 4.4: Expression of WT-sACE and MG-sACE mutants. A) Calculated specific activities of WT-sACE, sACE3,8,9/11,13, sACE3,6,8,9/12,13 and sACE3,6,9/WTCdom are shown, B) Representative SDS=PAGE gels of each sACE variant stained with Coomassie, indicating successful purification. Molecular weight marker – PageRuler™ Plus Prestained Protein Ladder.

Purified MG-sACE samples are comprised of a population of three sACE isoforms (full-length sACE and the proteolytically cleaved N- and C-domains). The individual domains are known to be active which may have an effect on the enzymatic activity readings. However, the amount of the individual domains in each sample is unlikely to have a significant effect on MG-sACE functionality. To address this issue, MG-sACE mutants were kinetically characterized and compared with WT-sACE to ensure that the functional integrity of the minimally glycosylated constructs had not been compromised. Kinetic constants for sACE3,8,9/11,13 have previously been determined and were found to be similar to those of WT-sACE (Anthony, 2011). Michaelis-Menten curves for the hydrolysis of Z-FHL were plotted for each purified mutant and the K_m values for WT-sACE, sACE3,6,8,9/12,13 and sACE3,6,9/WTCdom were found to be very similar at 0.33 mM, 0.32 mM and 0.31 mM respectively. Similarly the K_{cat} values and the catalytic efficiencies (K_{cat}/K_m) were found to be

comparable (Figure 4.5). These data suggest that MG-sACE is functioning with a similar efficiency to WT-sACE.

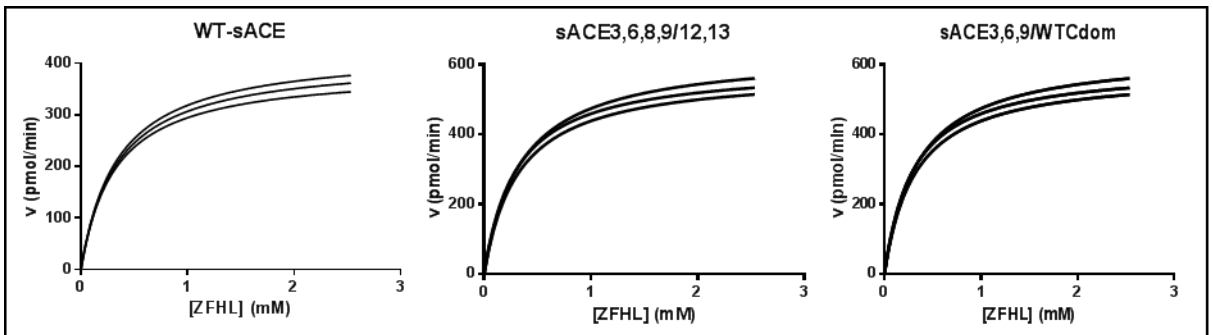

	k_{cat}/K_m	K_m (mM)	k_{cat} (s^{-1})
WT-sACE	28.74 (±0.21)	0.33 (±0.0071)	9.51 (±0.26)
sACE3,6,8,9/12,13	31.73 (±0.94)	0.32 (±0.027)	10.21 (±0.28)
sACE3,6,9/WTCdom	28.18 (±0.85)	0.31 (±0.012)	8.99 (±0.25)

Figure 4.5: Michaelis-Menten curve of WT-SACE, sACE3,6,8,9/12,13 and sACE3,6,9/WTCdom with k_{cat}/K_m, K_m and k_{cat} indicated. Kinetic constants were determined as described in section 4.2.7. Curves were plotted in GraphPad Prism.

4.3.4 The effect of glycosylation on the thermal stability of purified MG-sACE proteins

For investigating the effect of *N*-glycan site occupancy on the thermal stability of purified MG-sACE mutants, thermal denaturation experiments were carried out. This method is based on the transformation of a well-defined, folded structure of a protein formed under physiological conditions to an unfolded state under conditions of increased temperature. The residual enzymatic activity of each mutant is determined at 55ºC over 90 minutes, giving an indication of how much active protein remains and thus, how thermally stable each protein is. The thermal stability was then determined and plotted as shown in Figures 4.6 and 4.7. As previously mentioned, the N-domain has been shown to be the major contributing factor towards the thermal stability of sACE. This is evident in Figure 4.6 where the WTNdom retains 60% activity after 15 minutes at 55°C followed by WT-sACE and sACE3,6,9/WTNdom at approximately 15%, sACE3,6,8,9/12,13 at 10%, WTCdom at 6% and sACE3,8,9/11,13 at only 2% remaining activity.

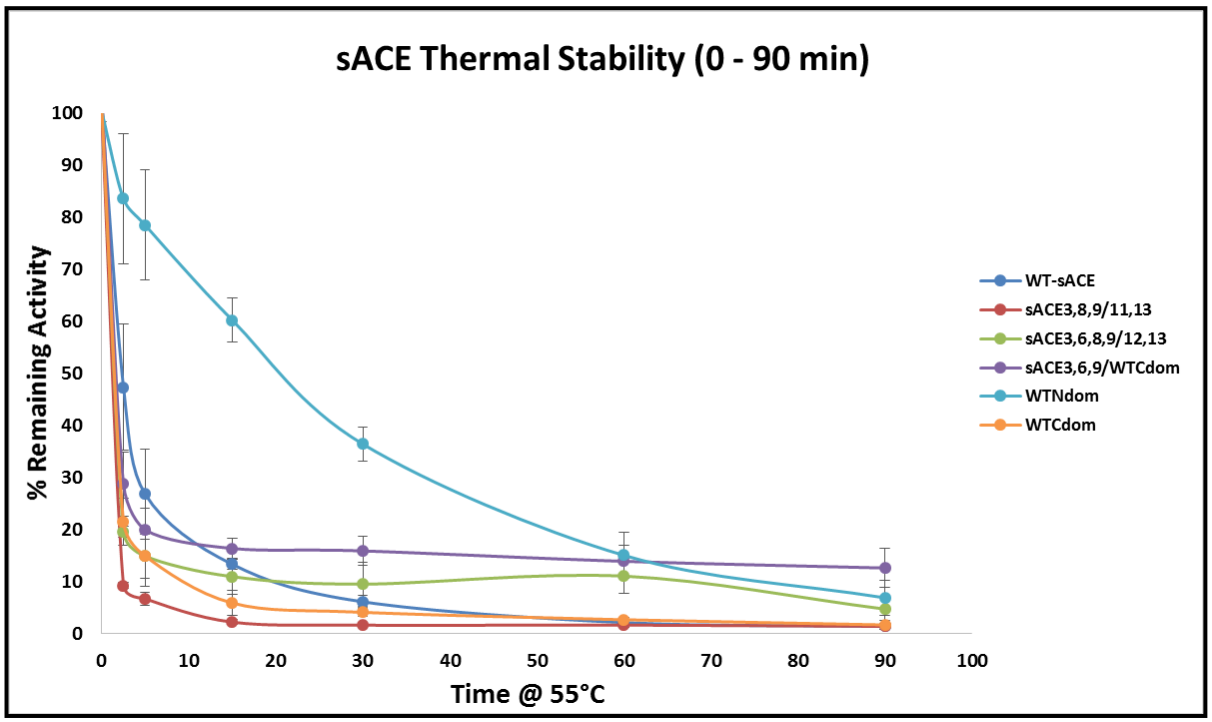

Figure 4.6: The effect of glycosylation on sACE thermal stability. Thermal denaturation assays were done as described in section 4.2.8. Percentage remaining activity was plotted as a function of time at 55°C from 0 – 90 minutes. Error bars indicate mean ±SD.

The most notable difference between the percentage remaining activities is seen at after 2.5 minutes (Figure 4.7), where WTNdom retains a remarkable 84%, followed by WT-sACE retaining 47%, sACE3,6,9/WTCdom retaining 28%, WTCdom and sACE3,6,8,9/12,13 retaining approximately 20% and sACE3,8,9/11,13 only retaining 9%. After 90 minutes WT-sACE and all glycosylation mutants had less than 20% remaining enzymatic activity.

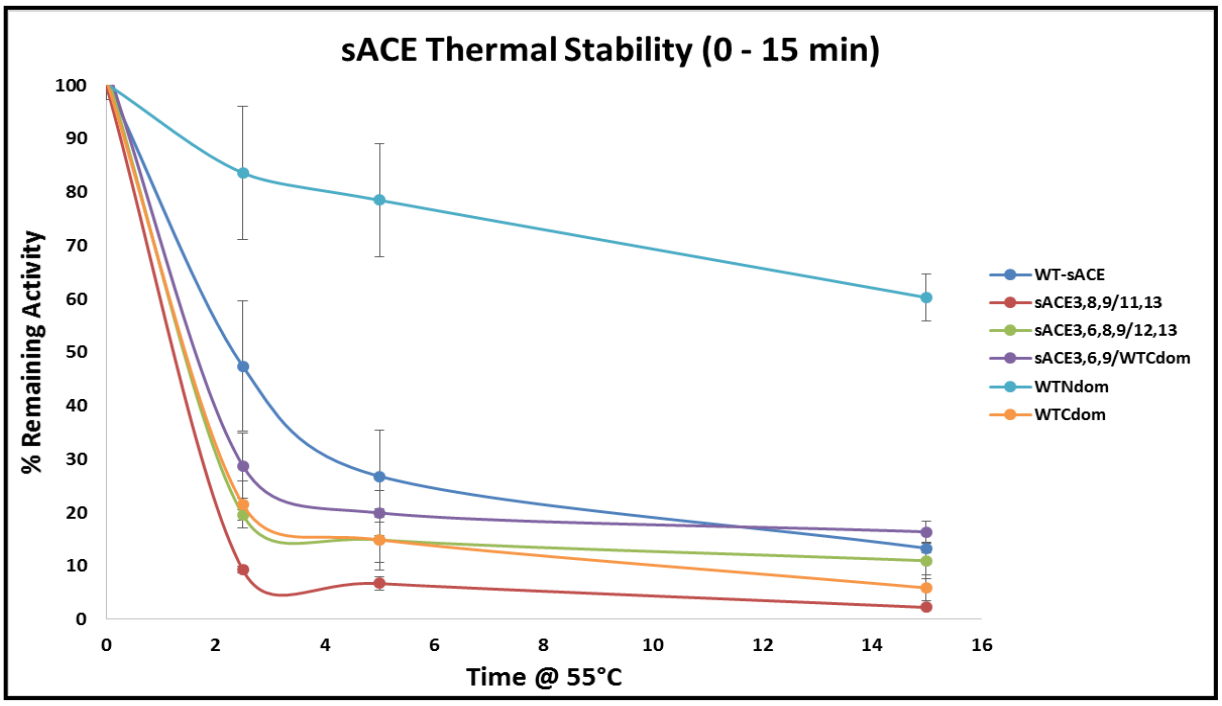

Figure 4.7: The effect of glycosylation on sACE thermal stability. Thermal denaturation assays were done as described in section 4.2.8. Percentage remaining activity was plotted as a function of time at 55°C from 0 – 15 minutes. Error bars indicate mean ±SD.

4.4 DISCUSSION

This investigation was aimed at determining the cellular localization of the inter-domain proteolytic event and the effect of *N*-glycan site occupancy on the expression and thermal stability of somatic ACE. Interestingly, only N-domain and full-length MG-sACE were found in the cell lysate and medium samples (Figure 4.2), while the C-domain was only found in the lysate, suggesting that proteolysis occurs in the intracellular milieu. As mentioned in Chapter 1, sACE has a signal peptide that is required to initiate exportation to the cell surface. This signal peptide is located at the N-terminus of sACE, i.e. on the N-domain. Therefore, after inter-domain linker proteolysis, there are two possible fates of MG-sACE (Figure 4.8).

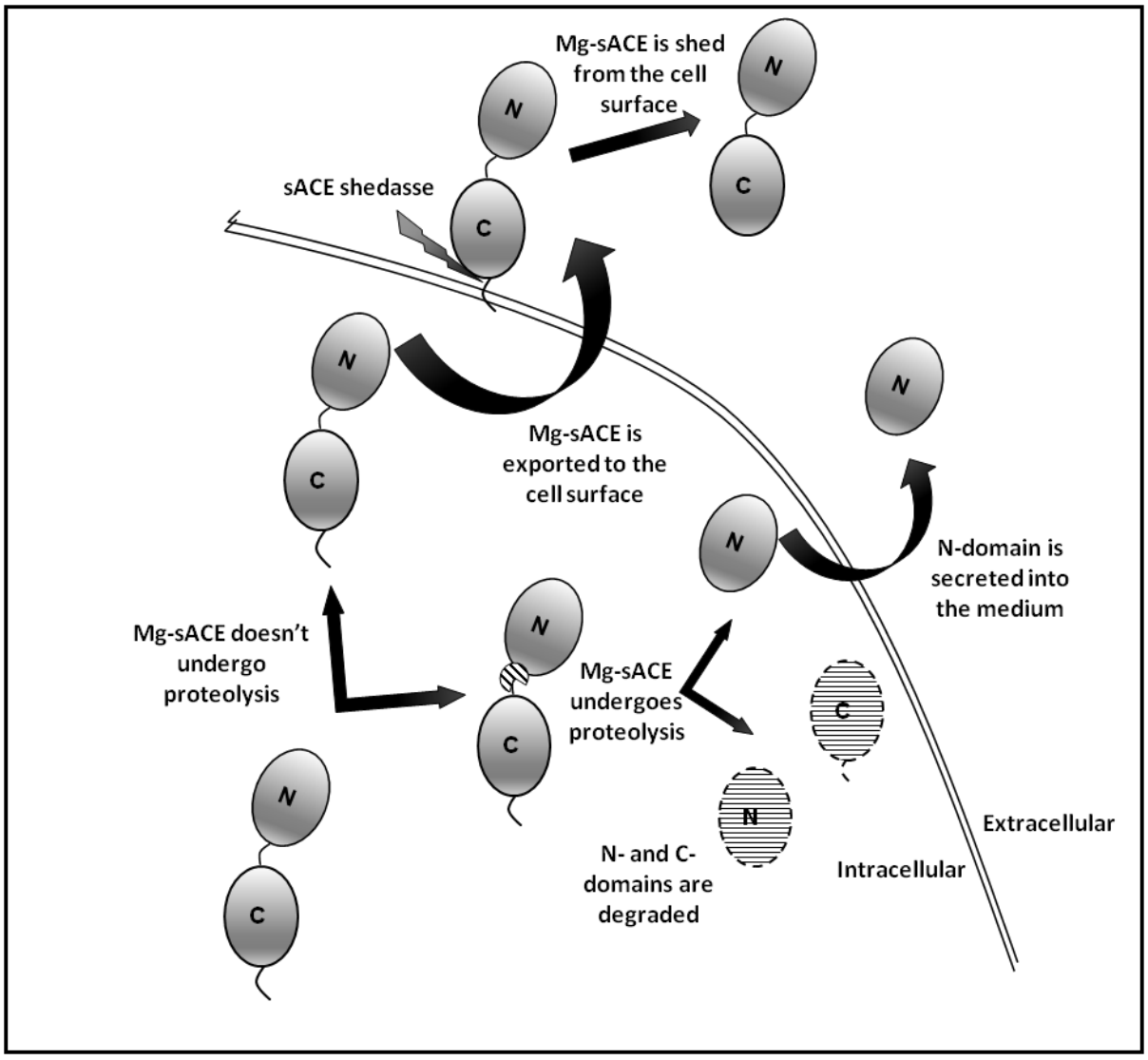

Figure 4.8: Diagrammatic representation of the fates of MG-sACE intra- and extracellular.

Firstly, the MG-sACE population that does not undergo proteolysis is successfully exported to the cell surface where it undergoes ectodomain shedding. Secondly, the population of MG-sACE that undergoes linker proteolysis results in some N-domain being exported to the cell surface while another batch is retained and degraded intracellularly. Due to the fact that the N-domain lacks the stalk and transmembrane region of sACE, it is not anchored to the cell membrane and is secreted into the medium (Figure 4.8). Furthermore, the C-domain, is retained within the cell as it lacks the signal peptide required for exportation to the cell surface. Interestingly, low levels of the C-domain are noticed in the cell lysate in Figure 4.2,

suggesting that it may be degraded within the cell to avoid accumulation of an obsolete intracellular C-domain.

As previously mentioned, *N*-glycans play a crucial role during the folding and processing of sACE. A decrease in expression is noticed when *N*-glycosylation sites are removed. Therefore, expressing MG-sACE mutants at sufficient levels for purification is difficult. Thus, a qualitative study was done to explore the effect of glycosylation on expression for MG-sACE mutants that could not be expressed in sufficient quantities for purification. It was found that MG-sACE mutants with only five glycosylation sites intact had a very low expression profile, while those with an additional site 6 (N131) fared better (Figure 4.3), suggesting that this site might be important during the *in vitro* processing of sACE. Furthermore, site 2, has been shown to be important in maintaining the expression profile of the individual N-domain (Anthony *et al.*, 2010). However, in contrast to the effect of a glycan at site 6, site 2 did not seem to have a significant effect on the expression of MG-sACE. It is important to note that the effect of each glycosylation site on sACE has not been fully investigated and the rationale behind the design of MG-sACE mutants is based on what is available in literature about the individual truncated domains. Therefore, sites that may be important in the expression of the individual domains may not necessarily be as important in sACE. This is reminiscent of the differences in the glycosylation requirements for each domain where the C-domain relies on N-terminal glycans (Gordon *et al.*, 2003), while with the N-domain three C-terminal glycans were necessary and sufficient for expression (Anthony *et al.*, 2010). Interestingly, a fully glycosylated N-domain within MG-sACE did not have a significantly different effect on expression compared to a MG N-domain (Figure 4.3). Thus, it is possible that for sACE, a unique combination of glycosylation sites on both domains may be required for appropriate processing of sACE. This may be due to differences in the secondary and tertiary structures of sACE which may require glycans located at key sites in order to facilitate multiple protein folding cycles (see section 1.2.3). However, further investigation is needed to confirm this.

Mutants that were expressed at levels sufficient for expression confirmed three points:

Firstly, MG-sACE mutants with five glycosylation sites intact have the lowest expression profile (Figures 4.3 and 4.4 A). This may be because a combination of glycosylation sites 3, 6 or 8, 9, 11 or 12 and 13 does not allow for optimal *in vitro* processing or additional site(s) may be required. This is in contrast to the tACE (C-domain), where only one or two glycans were necessary and sufficient for correct processing and enzymatic activity of this isoform (Gordon *et al.*, 2003).

Secondly, a fully glycosylated domain (C-domain) within MG-sACE does not have a marked effect on the expression of sACE (Figures 4.3 and 4.4 A). Again, this suggests that a particular combination of glycans on both domains is required for optimal processing.

Thirdly, site 6 has the most notable effect on the expression of MG-sACE (Figures 4.3 and 4.4 A). Therefore, in addition to its role in preventing inter-domain linker proteolysis, this site may also be crucial for the expression of sACE.

There exist several quantitative methods for investigating the degree of protein thermal stability, including differential scanning calorimetry and circular dichroism spectroscopy. However, these methods require a high concentration of protein, which poses a problem for MG-sACE mutants which have low protein purification yields. Therefore, thermal denaturation, a simpler and timeous semi-quantitative method that requires minimal protein amounts was used. ACE thermal denaturation assays rely on the functional integrity of proteins under investigation. As previously mentioned, purified MG-sACE samples essentially have three different populations of sACE isoforms, therefore caution has to be taken when analysing enzymatic activity data. To address this, kinetic analyses were carried out to determine whether each minimally glycosylated mutant has a similar catalytic efficiency to WT-sACE. Indeed, kinetic constants of the purified mutant proteins were comparable to those of WT-sACE (Figure 4.5). These findings confirm that full-length MG-

sACE is mostly responsible for the enzymatic activity from each sample, even in the presence of traces of the individual domains.

Investigating the effect of glycosylation on the thermal stability revealed that the most thermally stable MG-sACE mutant is sACE3,6,9/WTCdom (Figures 4.6 and 4.7), which is expected as the bulk of sACE's thermal stability is mediated by *N*-glycans and this MG-sACE mutant has the highest site occupancy (Anthony *et al.*, 2010; O'Neill *et al.*, 2008). Interestingly, reintroduction of 6 site along with a site 11 to 12 substitution was able to rescue the stability of the least stable mutant (sACE3,8,9/11,13) from 9% to 20% (similar to the WT C-domain value) after 2.5 minutes (Figure 4.7), further highlighting the importance of site 6. These data suggest that a complex combination of glycosylation sites within sACE is important in maintaining adequate expression and thermal stability. However, this effect needs to be investigated more quantitatively to corroborate these findings.

Conclusions and future work

We determined the minimum glycosylation requirements for a stable MG-sACE to be combinations of glycans attached to residues N25, N45, N131, N416, N480, N648 and N685 (sACE2,3,6,8,9/11,13) or N25, N45, N416, N480, N666 and N685 (sACE2,3,8,9/12,13). Interestingly, addition of N25 (site 2) to sACE3,8,9/11,13 resulted in a sharp increase in inter-domain linker proteolysis, likely due to a conformational change caused by this site occupation. This effect was blunted by the presence of N131 (site 6) and/or N666 (site 12). Also, N416 at site 8 was found to have no protective effect in terms of inter-domain linker proteolysis, evidenced by protection conferred by N45, N131, N480, N666 and N685 in sACE3,6,9/12,13 in comparison to sACE3,8,9/12,13. Limiting inter-domain linker flexibility by disulphide bridge formation had no notable effect on protection from proteolysis. Furthermore, we identified C-domain *N*-glycans as being crucial in maintaining adequate protection from proteolysis. Although MG-sACE constructs that are the least susceptible to linker proteolysis have been identified, these are still relatively highly glycosylated, which is problematic for X-ray crystallography. Thus, steps need to be taken to inhibit linker proteolysis. This could be done by identifying the linker cleavage site(s). Identified residue(s) at the cleavage site(s) could then be converted to more rigid amino acids such as proline which might be less susceptible to linker proteolysis. Initial attempts to do this using limited proteolysis and mass spectrometry were unsuccessful due to the nature of the peptides generated. Here, limited proteolysis using trypsin was conducted, however, predicted inter-domain linker peptide fragment masses could not be identified. It would thus be beneficial to consider different digest agents such as Glu-C or Lys-C. Additionally, another technique such as N-terminal sequencing could be employed.

Inter-domain linker proteolysis was found to occur intracellularly. An interesting occurrence was noticed in this study. Mature MG-sACE was successfully exported to the cell surface,

while some N-domain was secreted to the extracellular milieu and both the N- and C-domain were retained and degraded intracellularly. This limits the range of protease candidates to intracellular enzymes, serving as a step closer to identifying the protease(s) responsible for the cleavage of the linker in MG-sACE.

Glycosylation site 6 (N131) was found to be important in protection from proteolysis, high expression and thermal stability. In contrast, site 2 (N25), which is known to play a role in maintaining a high expression and thermal stability profile of the individual N-domain (Anthony *et al.*, 2010), had no notable effect on MG-sACE's expression and thermal stability. Surprisingly, a fully-glycosylated N- or C-domain fused with their minimally glycosylated counterparts had no dramatic effect on the expression of MG-sACE. This indicates that a unique combination of glycans on both domains is required to maintain adequate expression of sACE unlike the tACE isoform which only requires one or two glycans (Gordon *et al.*, 2003). Due to low expression levels displayed by MG-sACE mutants, expression systems with the appropriate glycosylation machinery such as yeast could be better options. Previous studies have described the different glycosylation requirements for minimally glycosylated sACE and tACE isoforms in yeast (Sadhukhan *et al.*, 1996; Williams *et al.*, 1996) and differences in glycosylation requirements for recombinant proteins in mammalian cells (Croset *et al.*, 2012). Interestingly, glycoforms which were not sufficiently expressed in mammalian cells, were expressed in yeast cells and vice versa, with a certain level of overlap. Thus, exploring yeast expression could be beneficial in obtaining MG-sACE at sufficient amounts for purification. Wild-type sACE was successfully cloned into two yeast expression vectors (data not included in this thesis). These could be used as subcloning templates for generating MG-sACE constructs in yeast vectors.

We determined that MG-sACE proteins were functionally comparable to WT-sACE at 37ºC, however, glycosylation had a significant effect on temperature stability. The most thermally stable mutant was sACE3,6,9/WTCdom, which is not surprising as it has nine potential oligosaccharides, which are known to confer sACE thermal stability (Anthony *et al.*, 2010;

O'Neill *et al.*, 2008; Voronov *et al.*, 2002). Additionally, reintroduction of glycosylation site 6 (N131) and substitution of site 11 (N648) with site 12 (N666) was able to rescue the thermal stability of sACE3,8,9/11,13 from 9% to 20% after 2.5 minutes. Additional work needs to be done on purified MG-sACE constructs to further investigate the role of *N*-glycans on the thermal stability and expression of sACE.

Overall, this work resulted in production of a number sACE constructs with varying degrees glycan site occupancy. Previous studies have successfully generated individual domain mutants of similar *N*-glycan site occupancy variation, which led to the solution the N- and C-domain crystal structures (Anthony *et al.*, 2010; Gordon *et al.*, 2003). These newly generated sACE glycoforms could be used as tools to further identify key *N*-glycans which could potentially lead to acquiring the high resolution 3D structure of sACE, the importance of which cannot be overstated, as this will aid in understanding the complexities of ACE's functionality and involvement in a variety of non-traditional roles mentioned in Chapter 1. More importantly, the structure of sACE could drive the design of potent inhibitors with much improved side effect profiles for the treatment of cardiovascular disease.

Appendix

A1) sACE protein sequence and internal sequencing primers

A set of internal sACE primers were used for DNA sequencing.

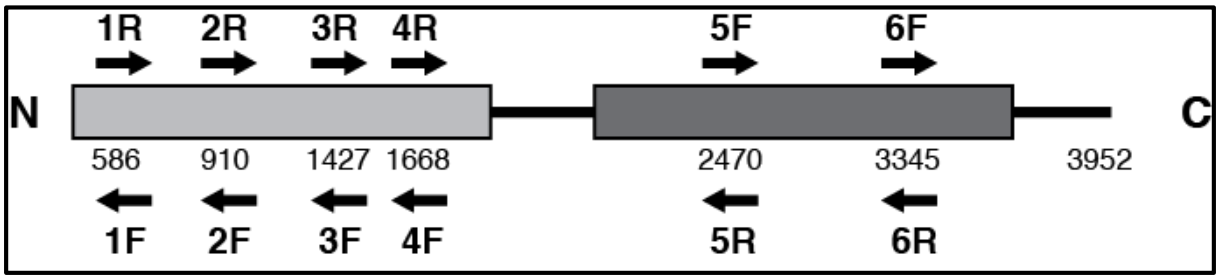

Figure A1. Schematic representation of the sACE gene with forward primers indicated above the gene and reverse primers indicated below. The nucleotide position of the beginning of the forward primer is indicated. Adapted from Gordon, 2011.

```
1     MGAASGRRGPGLLLPLPLLLLLPPQPALALDPGLQPGNFS[1]ADEAGAQLFAQSYNSS[2]AEQV
61    LFQSVAASWAHDTNIT[3]AENARRQEEAALLSQEFAEAWGQKAKELYEPIWQNFT[4]DPQLRRI
121   IGAVRTLGSANLPLAKRQQYNALLSNMS[5]RIYSTAKVCLPNKT[6]ATCWSLDPDLTNILASSR
181   SYAMLLFAWEGWHNAAGIPLKPLYEDFTALSNEAYKQDGFTDTGAYWRSWYNSPTFEDDL
241   EHLYQQLEPLYLNLHAFVRRALHRRYGDRYINLRGPIPAH LLGDMWAQSWENIYDMVVPF
301   PDKPNLDVTSTMLQQGWNAT[7]HMFRVAEEFFTSLELSPMPPEFWEGSMLEKPADGREVVCH
361   ASAWDFYNRKDFRIKQCTRVTMDQLSTVHHEMGHIQYYLQYKDLPVSLRRGANPGFHEAI
421   GDVLALSVSTPEHLHKIGLLDRVTNDT[8]ESDINYLLKMALEKIAFLPFGYLVDQWRWGVFS
481   GRTPPSRYNFDWWYLRTKYQGICPPVTRNET[9]HFDAGAKFHVPNVT[10]PYIRYFVSFVLQFQF
541   HEALCKEAGYEGPLHQCDIYRSTKAGAKLRKVLQAGSSRPWQEVLKDMVGLDALDAQPLL
601   KYFQPVTQWLQEQNQQNGEVLGWPEYQWHPPLPDNYPEGIDLVTDEAEASKFVEEYDRTS
661   QVVWNEYAEANWNYNTN[11]ITTETSKILLQKNMQIANHT[12]LKYGTQARKFDVNQLQNTT[13]IKRI
721   IKKVQDLERAALPAQELEEYNKILLDMETTYSVATVCHPNGS[14]CLQLEPDLTNVMATSRKY
781   EDLLWAWEGWRDKAGRAILQFYPKYVELINQAARLNGYVDAGDSWRSMYETPSLEQDLER
841   LFQELQPLYLNLHAYVRRALHRHYGAQHINLEGPIPAHLLGNMWAQTWSNIYDLVVPFPS
901   APSMDTTEAMLKQGWTPRRMFKEADDFFTSLGLLPVPPEFWNKS[15]MLEKPTDGREVVCHAS
961   AWDFYNGKDFRIKQCTTVNLEDLVVAHHEMGHIQYFMQYKDLPVALREGANPGFHEAIGD
1021  VLALSVSTPKHLHSLNLLSSEGGSDEHDINFLMKMALDKIAFIPFSYLVDQWRWRVFDGS
1081  ITKENYNQEWWSLRLKYQGLCPPVPRTQGDFDPGAKFHIPSSVPYIRYFVSFIIQFQFHE
1141  ALCQAAGHTGPLHKCDIYQSKEAGQRLATAMKLGFSRPWPEAMQLITGQPNMS[16]ASAMLSY
1201  FKPLLDWLRTENELHGEKLGWPQYNWT[17]PNSARSEGPLPDSGRVSFLGLDLDAQQARVGQW
1261  LLLFLGIALLVATLGLSQRLFSIRHRSLHRHSHGPQFGSEVELRHS
```

Figure A2. Amino acid sequence of sACE. Signal peptide targeting the enzyme for secretion is underlined (not present in the mature form of the enzyme). *N*-linked glycosylation motifs numbered and highlighted in bold.

A2) Expression vectors

Vectors used for the expression of sACE in bacterial and mammalian cells are indicated below.

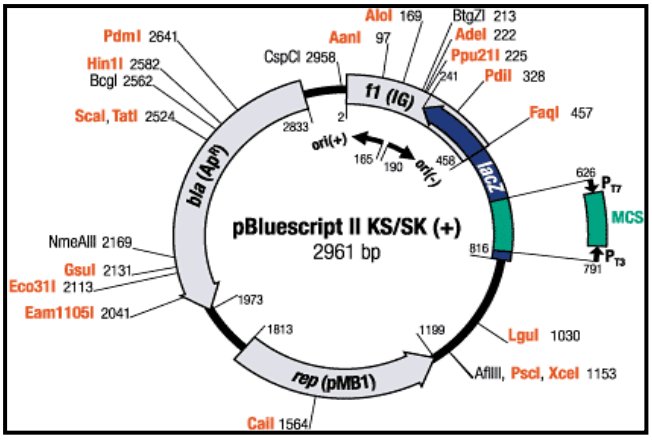

Figure A2: pBSK II KS/SK + plasmid. For bacterial cell transformation.

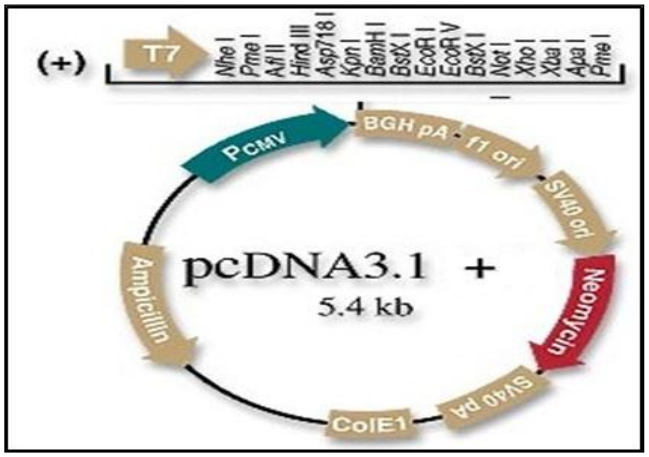

Figure A3: pCDNA3.1 (+). For mammalian cell transfection.

A3) Hippuryl-His-Leu standard curve

Hippuryl-His-Leu (HL) standards were prepared from a 5.7 mM stock solution in 1x phosphate buffer, pH 8.3, at concentrations of 0; 0.037; 0.074; 0.148; 0.296; 0.592 mM.

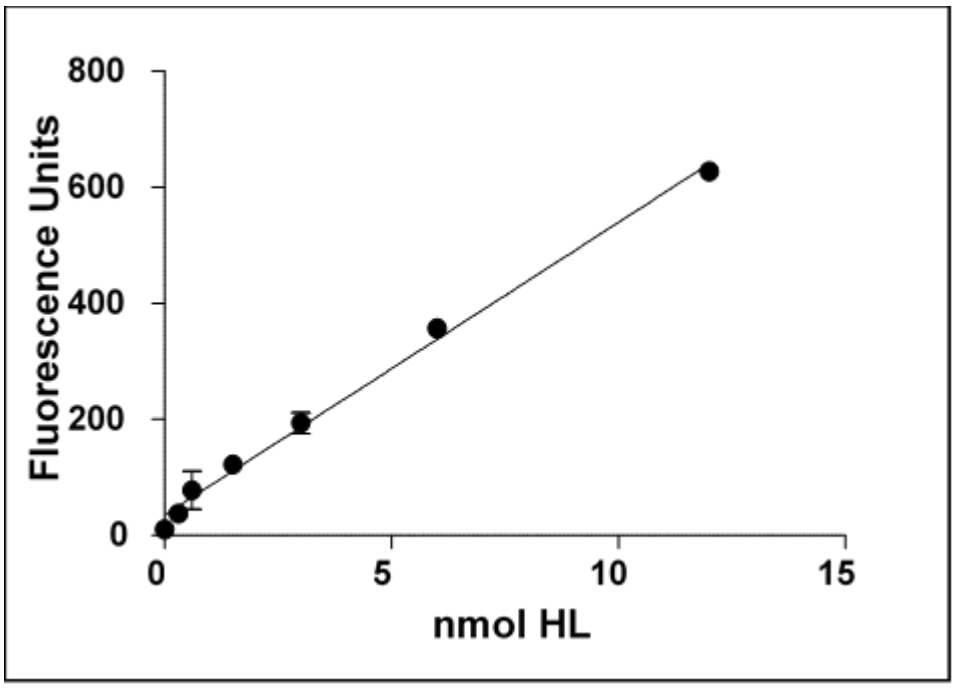

Figure A4: HL standard curve for enzyme activity calculation, showing correlation between fluorescence intensity and varying nmol of HL (Generated using GraphPad Prism).

The fluorescence intensity is converted to mU/ml using the formula;

$$mU\ ACE = \frac{FU\ x\ (\mu l\ of\ total\ reaction\ volume) x\ (sample\ dilution\ factor)}{(HL\ standard\ curve\ slope) x\ (reaction\ time) x\ (volume\ of\ diluted\ sample\ assayed)}$$

Where FU is the fluorescence intensity.

A4) SDS-polyacrylamide gel electrophoresis (SDS-PAGE)

SDS-polyacrylamide gel electrophoresis (SDS-PAGE) was carried out as per standard laboratory protocols. Here, 20 µl of sample was mixed with 5 µl 5x sample buffer (50% (v/v) glycerol, 25% (v/v) β-mercaptoethanol, 15% (w/v) SDS, 0.31 M Tris, 0.25% (w/v) bromophenol blue) and denatured at 100˚C for 5 minutes. Denatured samples were separated on 10% polyacrylamide gels (0.1% SDS, 375 mM Tris buffer, pH 8.8) and 3% stacking (0.1% SDS, 125 mM Tris buffer, pH 6.8) with 0.1% (w/v) ammonium persulphate (AMPS) and 10 µl tetramethylethylenediamine (TEMED) in a Tris-glycine tank buffer (pH 8.3).. Electrophoresis was carried out at 25 mA/gel for 1 hour.

A5) Z-FHL working solution

A 20 mM stock solution of Z-FHL was prepared by dissolving 110 mg Z-FHL in 1 mL 0.28 M NaOH, and made up to 10 mL with dH_2O. The 1 mM Z-FHL working solution was prepared by adding 15 ml dH_2O to 4 ml 5x phosphate buffer (0.5 M potassium phosphate, pH 8.3, 1.5 M NaCl) with 20 µl 10 mM $ZnSO_4$, and 1 ml of 20 mM Z-FHL.

A6) Freezing of CHO cells for storage in liquid nitrogen

Cells from a confluent T75 were lifted using trypsin-EDTA into a 10 ml blue cap tube which was centrifuged for 30 seconds at 4000xg. The supernatant was removed and cells were resuspended with 3 ml of ice cold 10% Dimethyl sulfoxide (DMSO) prepared in FCS. Cells were kept on ice for 20-30 minutes and aliquoted into six vials. These were promptly transferred to liquid N_2 tanks.

References

Acharya, K. R., Sturrock, E. D., Riordan, J. F., & Ehlers, M. R. (2003). Ace revisited: a new target for structure-based drug design. *Nat Rev Drug Discov, 2*(11), 891-902. doi: 10.1038/nrd1227

Adam, A., Cugno, M., Molinaro, G., Perez, M., Lepage, Y., & Agostoni, A. (2002). Aminopeptidase P in individuals with a history of angio-oedema on ACE inhibitors. *Lancet, 359*(9323), 2088-2089. doi: 10.1016/S0140-6736(02)08914-6

Akif, M., Masuyer, G., Schwager, S. L., Bhuyan, B. J., Mugesh, G., Isaac, R. E., . . . Acharya, K. R. (2011). Structural characterization of angiotensin I-converting enzyme in complex with a selenium analogue of captopril. *FEBS J, 278*(19), 3644-3650. doi: 10.1111/j.1742-4658.2011.08276.x

Akif, M., Schwager, S. L., Anthony, C. S., Czarny, B., Beau, F., Dive, V., . . . Acharya, K. R. (2011). Novel mechanism of inhibition of human angiotensin-I-converting enzyme (ACE) by a highly specific phosphinic tripeptide. *Biochem J, 436*(1), 53-59. doi: 10.1042/BJ20102123

An, H. J., & Lebrilla, C. B. (2011). Structure elucidation of native N- and O-linked glycans by tandem mass spectrometry (tutorial). *Mass Spectrom Rev, 30*(4), 560-578. doi: 10.1002/mas.20283

Anthony, C. S. (2011). *The Importance of N-linked Glycosylation on the N-domain of Angiotensin-I Converting Enzyme.* (Doctor of Philosophy Ph.D.), University of Cape Town.

Anthony, C. S., Corradi, H. R., Schwager, S. L., Redelinghuys, P., Georgiadis, D., Dive, V., . . . Sturrock, E. D. (2010). The N domain of human angiotensin-I-converting enzyme: the role of N-glycosylation and the crystal structure in complex with an N domain-specific phosphinic inhibitor, RXP407. *J Biol Chem, 285*(46), 35685-35693. doi: 10.1074/jbc.M110.167866

Apweiler, R., Hermjakob, H., & Sharon, N. (1999). On the frequency of protein glycosylation, as deduced from analysis of the SWISS-PROT database. *Biochim Biophys Acta, 1473*(1), 4-8.

Balyasnikova, I. V., Metzger, R., Franke, F. E., & Danilov, S. M. (2003). Monoclonal antibodies to denatured human ACE (CD 143), broad species specificity, reactivity on paraffin sections, and detection of subtle conformational changes in the C-terminal domain of ACE. *Tissue Antigens, 61*(1), 49-62.

Balyasnikova, I. V., Sun, Z. L., Franke, F. E., Berestetskaya, Y. V., Chubb, A. J., Albrecht, R. F., . . . Danilov, S. M. (2005). Monoclonal antibodies 1B3 and 5C8 as probes for monitoring the integrity of the C-terminal end of soluble angiotensin-converting enzyme. *Hybridoma (Larchmt), 24*(1), 14-26. doi: 10.1089/hyb.2005.24.14

Beckham, G. T., Dai, Z., Matthews, J. F., Momany, M., Payne, C. M., Adney, W. S., . . . Himmel, M. E. (2012). Harnessing glycosylation to improve cellulase activity. *Curr Opin Biotechnol, 23*(3), 338-345. doi: 10.1016/j.copbio.2011.11.030

Bergman, L. W., & Kuehl, W. M. (1979). Formation of an intrachain disulfide bond on nascent immunoglobulin light chains. *J Biol Chem, 254*(18), 8869-8876.

Bernard, B. A., Yamada, K. M., & Olden, K. (1982). Carbohydrates selectively protect a specific domain of fibronectin against proteases. *J Biol Chem, 257*(14), 8549-8554.

Bernstein, K. E., Ong, F. S., Blackwell, W. L., Shah, K. H., Giani, J. F., Gonzalez-Villalobos, R. A., . . . Touyz, R. M. (2013). A modern understanding of the traditional and nontraditional biological functions of angiotensin-converting enzyme. *Pharmacol Rev, 65*(1), 1-46. doi: 10.1124/pr.112.006809

Bernstein, K. E., Shen, X. Z., Gonzalez-Villalobos, R. A., Billet, S., Okwan-Duodu, D., Ong, F. S., & Fuchs, S. (2011). Different in vivo functions of the two catalytic domains of

angiotensin-converting enzyme (ACE). *Curr Opin Pharmacol, 11*(2), 105-111. doi: 10.1016/j.coph.2010.11.001

Bicket, D. P. (2002). Using ACE inhibitors appropriately. *Am Fam Physician, 66*(3), 461-468.

Binevski, P. V., Sizova, E. A., Pozdnev, V. F., & Kost, O. A. (2003). Evidence for the negative cooperativity of the two active sites within bovine somatic angiotensin-converting enzyme. *FEBS Lett, 550*(1-3), 84-88.

Bumpus, F. M., Schwarz, H., & Page, I. H. (1957). Synthesis and pharmacology of the octapeptide angiotonin. *Science, 125*(3253), 886-887.

Butters, T. D., Sparks, L. M., Harlos, K., Ikemizu, S., Stuart, D. I., Jones, E. Y., & Davis, S. J. (1999). Effects of N-butyldeoxynojirimycin and the Lec3.2.8.1 mutant phenotype on N-glycan processing in Chinese hamster ovary cells: application to glycoprotein crystallization. *Protein Sci, 8*(8), 1696-1701. doi: 10.1110/ps.8.8.1696

Campbell, Duncan J. (2001). The Kallikrein–Kinin System In Humans. *Clinical and Experimental Pharmacology and Physiology, 28*(12), 1060-1065. doi: 10.1046/j.1440-1681.2001.03564.x

Cannon, W. R., Taasevigen, D., Baxter, D. J., & Laskin, J. (2007). Evaluation of the influence of amino acid composition on the propensity for collision-induced dissociation of model peptides using molecular dynamics simulations. *J Am Soc Mass Spectrom, 18*(9), 1625-1637. doi: 10.1016/j.jasms.2007.06.005

Chen, H. L., Lunsdorf, H., Hecht, H. J., & Tsai, H. (2010). Porcine pulmonary angiotensin I-converting enzyme--biochemical characterization and spatial arrangement of the N- and C-domains by three-dimensional electron microscopic reconstruction. *Micron, 41*(6), 674-685. doi: 10.1016/j.micron.2010.01.005

Cheng, Z. (2010). Protein translocation through the Sec61/SecY channel. *Biosci Rep, 30*(3), 201-207. doi: 10.1042/BSR20090158

Coates, D. (2003). The angiotensin converting enzyme (ACE). *Int J Biochem Cell Biol, 35*(6), 769-773.

Corradi, H. R., Schwager, S. L., Nchinda, A. T., Sturrock, E. D., & Acharya, K. R. (2006). Crystal structure of the N domain of human somatic angiotensin I-converting enzyme provides a structural basis for domain-specific inhibitor design. *J Mol Biol, 357*(3), 964-974. doi: 10.1016/j.jmb.2006.01.048

Coulter, D. M., & Edwards, I. R. (1987). Cough associated with captopril and enalapril. *Br Med J (Clin Res Ed), 294*(6586), 1521-1523.

Croset, A., Delafosse, L., Gaudry, J. P., Arod, C., Glez, L., Losberger, C., . . . Antonsson, B. (2012). Differences in the glycosylation of recombinant proteins expressed in HEK and CHO cells. *J Biotechnol, 161*(3), 336-348. doi: 10.1016/j.jbiotec.2012.06.038

Csala, M., Kereszturi, E., Mandl, J., & Banhegyi, G. (2012). The endoplasmic reticulum as the extracellular space inside the cell: role in protein folding and glycosylation. *Antioxid Redox Signal, 16*(10), 1100-1108. doi: 10.1089/ars.2011.4227

Daniels, R., Kurowski, B., Johnson, A. E., & Hebert, D. N. (2003). N-linked glycans direct the cotranslational folding pathway of influenza hemagglutinin. *Mol Cell, 11*(1), 79-90.

Danilov, S. M., Gordon, K., Nesterovitch, A. B., Lunsdorf, H., Chen, Z., Castellon, M., . . . Sturrock, E. D. (2011). An angiotensin I-converting enzyme mutation (Y465D) causes a dramatic increase in blood ACE via accelerated ACE shedding. *PLoS One, 6*(10), e25952. doi: 10.1371/journal.pone.0025952

Deddish, P. A., Wang, J., Michel, B., Morris, P. W., Davidson, N. O., Skidgel, R. A., & Erdos, E. G. (1994). Naturally occurring active N-domain of human angiotensin I-converting enzyme. *Proc Natl Acad Sci U S A, 91*(16), 7807-7811.

Dickstein, K., & Kjekshus, J. (2002). Effects of losartan and captopril on mortality and morbidity in high-risk patients after acute myocardial infarction: the OPTIMAAL randomised trial. Optimal Trial in Myocardial Infarction with Angiotensin II Antagonist Losartan. *Lancet, 360*(9335), 752-760.

Douglas, R. G., Sharma, R. K., Masuyer, G., Lubbe, L., Zamora, I., Acharya, K. R., . . . Sturrock, E. D. (2014). Fragment-based design for the development of N-domain-

selective angiotensin-1-converting enzyme inhibitors. *Clin Sci (Lond), 126*(4), 305-313. doi: 10.1042/CS20130403

Ehlers, M. R., Abrie, J. A., & Sturrock, E. D. (2013). C domain-selective inhibition of angiotensin-converting enzyme. *J Renin Angiotensin Aldosterone Syst, 14*(2), 189-192. doi: 10.1177/1470320313489206

Ehlers, M. R., Chen, Y. N., & Riordan, J. F. (1991). Purification and characterization of recombinant human testis angiotensin-converting enzyme expressed in Chinese hamster ovary cells. *Protein Expr Purif, 2*(1), 1-9.

Ehrt, S., & Schnappinger, D. (2003). Isolation of plasmids from E. coli by boiling lysis. *Methods Mol Biol, 235*, 79-82. doi: 10.1385/1-59259-409-3:79

Elliott, D. F., & Peart, W. S. (1956). Amino-acid sequence in a hypertensin. *Nature, 177*(4507), 527-528.

Erdos, E. G. (2006). The ACE and I: how ACE inhibitors came to be. *FASEB J, 20*(8), 1034-1038. doi: 10.1096/fj.06-0602ufm

Erdos, E. G., & Yang, H. Y. (1967). An enzyme in microsomal fraction of kidney that inactivates bradykinin. *Life Sci, 6*(6), 569-574.

Erdos, G., Sayeed, S., Hu, F. Z., Antalis, P. T., Shen, K., Hayes, J. D., . . . Ehrlich, G. D. (2006). Construction and characterization of a highly redundant Pseudomonas aeruginosa genomic library prepared from 12 clinical isolates: application to studies of gene distribution among populations. *Int J Pediatr Otorhinolaryngol, 70*(11), 1891-1900. doi: 10.1016/j.ijporl.2006.06.016

Esther, C. R., Jr., Marino, E. M., & Bernstein, K. E. (1997). The role of Angiotensin-converting enzyme in blood pressure control, renal function, and male fertility. *Trends Endocrinol Metab, 8*(5), 181-186.

Fleming, I. (2006). Signaling by the angiotensin-converting enzyme. *Circ Res, 98*(7), 887-896. doi: 10.1161/01.RES.0000217340.40936.53

Frenkel, Z., Shenkman, M., Kondratyev, M., & Lederkremer, G. Z. (2004). Separate roles and different routing of calnexin and ERp57 in endoplasmic reticulum quality control revealed by interactions with asialoglycoprotein receptor chains. *Mol Biol Cell, 15*(5), 2133-2142. doi: 10.1091/mbc.E03-12-0899

Friborg, J. T., Taastrom, A., Andersen, I. B., Schultz-Larsen, P., & Andreasen, P. B. (2002). [Can emergency admissions to departments of internal medicine be replaced by planned admissions?]. *Ugeskr Laeger, 164*(40), 4660-4663.

Fuchs, S., Xiao, H. D., Cole, J. M., Adams, J. W., Frenzel, K., Michaud, A., . . . Bernstein, K. E. (2004). Role of the N-terminal catalytic domain of angiotensin-converting enzyme investigated by targeted inactivation in mice. *J Biol Chem, 279*(16), 15946-15953. doi: 10.1074/jbc.M400149200

Fuchs, S., Xiao, H. D., Hubert, C., Michaud, A., Campbell, D. J., Adams, J. W., . . . Bernstein, K. E. (2008). Angiotensin-converting enzyme C-terminal catalytic domain is the main site of angiotensin I cleavage in vivo. *Hypertension, 51*(2), 267-274. doi: 10.1161/HYPERTENSIONAHA.107.097865

Fujihara, J., Yasuda, T., Kunito, T., Fujii, Y., Takatsuka, H., Moritani, T., & Takeshita, H. (2008). Two N-linked glycosylation sites (Asn18 and Asn106) are both required for full enzymatic activity, thermal stability, and resistance to proteolysis in mammalian deoxyribonuclease I. *Biosci Biotechnol Biochem, 72*(12), 3197-3205.

Fujihara, Y., Tokuhiro, K., Muro, Y., Kondoh, G., Araki, Y., Ikawa, M., & Okabe, M. (2013). Expression of TEX101, regulated by ACE, is essential for the production of fertile mouse spermatozoa. *Proc Natl Acad Sci U S A, 110*(20), 8111-8116. doi: 10.1073/pnas.1222166110

Fyhrquist, F., & Saijonmaa, O. (2008). Renin-angiotensin system revisited. *Journal of Internal Medicine, 264*(3), 224-236. doi: 10.1111/j.1365-2796.2008.01981.x

Georgiadis, D., Cuniasse, P., Cotton, J., Yiotakis, A., & Dive, V. (2004). Structural determinants of RXPA380, a potent and highly selective inhibitor of the angiotensin-converting enzyme C-domain. *Biochemistry, 43*(25), 8048-8054. doi: 10.1021/bi049504q

Gill, D. J., Chia, J., Senewiratne, J., & Bard, F. (2010). Regulation of O-glycosylation through Golgi-to-ER relocation of initiation enzymes. *J Cell Biol, 189*(5), 843-858. doi: 10.1083/jcb.201003055

Gonzalez-Villalobos, R. A., Shen, X. Z., Bernstein, E. A., Janjulia, T., Taylor, B., Giani, J. F., . . . Bernstein, K. E. (2013). Rediscovering ACE: novel insights into the many roles of the angiotensin-converting enzyme. *J Mol Med (Berl), 91*(10), 1143-1154. doi: 10.1007/s00109-013-1051-z

Gordon, K. (2011). *Protein-Protein Interactions of Human Somatic Angiotensin-Converting Enzyme.* (Doctor Of Philosophy PhD), University Of Cape Town.

Gordon, K., Redelinghuys, P., Schwager, S. L., Ehlers, M. R., Papageorgiou, A. C., Natesh, R., . . . Sturrock, E. D. (2003). Deglycosylation, processing and crystallization of human testis angiotensin-converting enzyme. *Biochem J, 371*(Pt 2), 437-442. doi: 10.1042/BJ20021842

Guimaraes, P. B., Alvarenga, E. C., Siqueira, P. D., Paredes-Gamero, E. J., Sabatini, R. A., Morais, R. L. T., . . . Pesquero, J. B. (2011). Angiotensin II Binding to Angiotensin I-Converting Enzyme Triggers Calcium Signaling. *Hypertension, 57*(5), 965-U200. doi: 10.1161/hypertensionaha.110.167171

Hagaman, J. R., Moyer, J. S., Bachman, E. S., Sibony, M., Magyar, P. L., Welch, J. E., . . . O'Brien, D. A. (1998). Angiotensin-converting enzyme and male fertility. *Proc Natl Acad Sci U S A, 95*(5), 2552-2557.

Hakkarainen, P., Kiianmaa, K., Kuoppasalmi, K., & Tigerstedt, C. (2012). Addiction research centres and the nurturing of creativity: the Department of Alcohol, Drugs and Addiction at the National Institute for Health and Welfare in Finland: diverse problems, diverse perspectives. *Addiction, 107*(10), 1741-1746. doi: 10.1111/j.1360-0443.2011.03594.x

Helenius, A. (1994). How N-linked oligosaccharides affect glycoprotein folding in the endoplasmic reticulum. *Mol Biol Cell, 5*(3), 253-265.

Helenius, A., & Aebi, M. (2001). Intracellular functions of N-linked glycans. *Science, 291*(5512), 2364-2369.

Helenius, A., & Aebi, M. (2004). Roles of N-linked glycans in the endoplasmic reticulum. *Annu Rev Biochem, 73*, 1019-1049. doi: 10.1146/annurev.biochem.73.011303.073752

Helenius, J., & Aebi, M. (2002). Transmembrane movement of dolichol linked carbohydrates during N-glycoprotein biosynthesis in the endoplasmic reticulum. *Semin Cell Dev Biol, 13*(3), 171-178.

Hsiao, C. C., Cheng, K. F., Chen, H. Y., Chou, Y. H., Stacey, M., Chang, G. W., & Lin, H. H. (2009). Site-specific N-glycosylation regulates the GPS auto-proteolysis of CD97. *FEBS Lett, 583*(19), 3285-3290. doi: 10.1016/j.febslet.2009.09.001

Huhtanen, P., & Tigerstedt, C. (2012). Women and young adults suffer most from other people's drinking. *Drug Alcohol Rev, 31*(7), 841-846. doi: 10.1111/j.1465-3362.2012.00480.x

Imperiali, B., & O'Connor, S. E. (1999). Effect of N-linked glycosylation on glycopeptide and glycoprotein structure. *Curr Opin Chem Biol, 3*(6), 643-649.

Imperiali, B., & Rickert, K. W. (1995). Conformational implications of asparagine-linked glycosylation. *Proc Natl Acad Sci U S A, 92*(1), 97-101.

Jaspard, E., Wei, L., & Alhenc-Gelas, F. (1993). Differences in the properties and enzymatic specificities of the two active sites of angiotensin I-converting enzyme (kininase II). Studies with bradykinin and other natural peptides. *J Biol Chem, 268*(13), 9496-9503.

Jokubaitis, V. J., Sinka, L., Driessen, R., Whitty, G., Haylock, D. N., Bertoncello, I., . . . Simmons, P. J. (2008). Angiotensin-converting enzyme (CD143) marks hematopoietic stem cells in human embryonic, fetal, and adult hematopoietic tissues. *Blood, 111*(8), 4055-4063. doi: 10.1182/blood-2007-05-091710

Jones, J., Krag, S. S., & Betenbaugh, M. J. (2005). Controlling N-linked glycan site occupancy. *Biochim Biophys Acta, 1726*(2), 121-137. doi: 10.1016/j.bbagen.2005.07.003

Junot, C., Gonzales, M. F., Ezan, E., Cotton, J., Vazeux, G., Michaud, A., . . . Dive, V. (2001). RXP 407, a selective inhibitor of the N-domain of angiotensin I-converting enzyme, blocks in vivo the degradation of hemoregulatory peptide acetyl-Ser-Asp-Lys-Pro with no effect on angiotensin I hydrolysis. *J Pharmacol Exp Ther, 297*(2), 606-611.

Kohlstedt, K., Brandes, R. P., Muller-Esterl, W., Busse, R., & Fleming, I. (2004). Angiotensin-converting enzyme is involved in outside-in signaling in endothelial cells. *Circ Res, 94*(1), 60-67. doi: 10.1161/01.RES.0000107195.13573.E4

Kohlstedt, K., Gershome, C., Trouvain, C., Hofmann, W. K., Fichtlscherer, S., & Fleming, I. (2009). Angiotensin-converting enzyme (ACE) inhibitors modulate cellular retinol-binding protein 1 and adiponectin expression in adipocytes via the ACE-dependent signaling cascade. *Mol Pharmacol, 75*(3), 685-692. doi: 10.1124/mol.108.051631

Kohlstedt, K., Shoghi, F., Muller-Esterl, W., Busse, R., & Fleming, I. (2002). CK2 phosphorylates the angiotensin-converting enzyme and regulates its retention in the endothelial cell plasma membrane. *Circ Res, 91*(8), 749-756.

Kost, Olga A., Balyasnikova, Irina V., Chemodanova, Elena E., Nikolskaya, Irina I., Albrecht, Ronald F., 2nd, & Danilov, Sergei M. (2003). Epitope-dependent blocking of the angiotensin-converting enzyme dimerization by monoclonal antibodies to the N-terminal domain of ACE: possible link of ACE dimerization and shedding from the cell surface. *Biochemistry, 42*(23), 6965-6976.

Kozlowski, S., Corr, M., Takeshita, T., Boyd, L. F., Pendleton, C. D., Germain, R. N., . . . Margulies, D. H. (1992). Serum angiotensin-1 converting enzyme activity processes a human immunodeficiency virus 1 gp160 peptide for presentation by major histocompatibility complex class I molecules. *J Exp Med, 175*(6), 1417-1422.

Kretz, K. A., Carson, G. S., Morimoto, S., Kishimoto, Y., Fluharty, A. L., & O'Brien, J. S. (1990). Characterization of a mutation in a family with saposin B deficiency: a glycosylation site defect. *Proc Natl Acad Sci U S A, 87*(7), 2541-2544.

Kroger, W. L., Douglas, R. G., O'Neill, H. G., Dive, V., & Sturrock, E. D. (2009). Investigating the domain specificity of phosphinic inhibitors RXPA380 and RXP407 in angiotensin-converting enzyme. *Biochemistry, 48*(35), 8405-8412. doi: 10.1021/bi9011226

Lambert, D. W., Clarke, N. E., & Turner, A. J. (2010). Not just angiotensinases: new roles for the angiotensin-converting enzymes. *Cell Mol Life Sci, 67*(1), 89-98. doi: 10.1007/s00018-009-0152-x

Langford, K. G., Shai, S. Y., Howard, T. E., Kovac, M. J., Overbeek, P. A., & Bernstein, K. E. (1991). Transgenic mice demonstrate a testis-specific promoter for angiotensin-converting enzyme. *J Biol Chem, 266*(24), 15559-15562.

Lederkremer, G. Z., & Glickman, M. H. (2005). A window of opportunity: timing protein degradation by trimming of sugars and ubiquitins. *Trends Biochem Sci, 30*(6), 297-303. doi: 10.1016/j.tibs.2005.04.010

Lentz, K. E., Skeggs, L. T., Jr., Woods, K. R., Kahn, J. R., & Shumway, N. P. (1956). The amino acid composition of hypertensin II and its biochemical relationship to hypertensin I. *J Exp Med, 104*(2), 183-191.

Li, P., Xiao, H. D., Xu, J., Ong, F. S., Kwon, M., Roman, J., . . . Fuchs, S. (2010). Angiotensin-converting enzyme N-terminal inactivation alleviates bleomycin-induced lung injury. *Am J Pathol, 177*(3), 1113-1121. doi: 10.2353/ajpath.2010.081127

Lin, C., Datta, V., Okwan-Duodu, D., Chen, X., Fuchs, S., Alsabeh, R., . . . Shen, X. Z. (2011). Angiotensin-converting enzyme is required for normal myelopoiesis. *FASEB J, 25*(4), 1145-1155. doi: 10.1096/fj.10-169433

Ling, M. M., & Robinson, B. H. (1997). Approaches to DNA mutagenesis: an overview. *Anal Biochem, 254*(2), 157-178. doi: 10.1006/abio.1997.2428

Lucero, H. A., Kintsurashvili, E., Marketou, M. E., & Gavras, H. (2010). Cell signaling, internalization, and nuclear localization of the angiotensin converting enzyme in smooth muscle and endothelial cells. *J Biol Chem, 285*(8), 5555-5568. doi: 10.1074/jbc.M109.074740

Makela, P., Tigerstedt, C., & Mustonen, H. (2012). The Finnish drinking culture: change and continuity in the past 40 years. *Drug Alcohol Rev, 31*(7), 831-840. doi: 10.1111/j.1465-3362.2012.00479.x

Marin, M. B., Ghenea, S., Spiridon, L. N., Chiritoiu, G. N., Petrescu, A. J., & Petrescu, S. M. (2012). Tyrosinase degradation is prevented when EDEM1 lacks the intrinsically disordered region. *PLoS One, 7*(8), e42998. doi: 10.1371/journal.pone.0042998

Masuyer, G., Schwager, S. L., Sturrock, E. D., Isaac, R. E., & Acharya, K. R. (2012). Molecular recognition and regulation of human angiotensin-I converting enzyme (ACE) activity by natural inhibitory peptides. *Sci Rep, 2*, 717. doi: 10.1038/srep00717

Mitra, N., Sinha, S., Ramya, T. N., & Surolia, A. (2006). N-linked oligosaccharides as outfitters for glycoprotein folding, form and function. *Trends Biochem Sci, 31*(3), 156-163. doi: 10.1016/j.tibs.2006.01.003

Nachon, F., Nicolet, Y., Viguie, N., Masson, P., Fontecilla-Camps, J. C., & Lockridge, O. (2002). Engineering of a monomeric and low-glycosylated form of human butyrylcholinesterase: expression, purification, characterization and crystallization. *Eur J Biochem, 269*(2), 630-637.

Natesh, R., Schwager, S. L., Sturrock, E. D., & Acharya, K. R. (2003). Crystal structure of the human angiotensin-converting enzyme-lisinopril complex. *Nature, 421*(6922), 551-554. doi: 10.1038/nature01370

Nikolaeva, M. A., Balyasnikova, I. V., Alexinskaya, M. A., Metzger, R., Franke, F. E., Albrecht, R. F., 2nd, . . . Danilov, S. M. (2006). Testicular isoform of angiotensin I-converting enzyme (ACE, CD143) on the surface of human spermatozoa: revelation and quantification using monoclonal antibodies. *Am J Reprod Immunol, 55*(1), 54-68. doi: 10.1111/j.1600-0897.2005.00326.x

O'Connor, S. E., & Imperiali, B. (1996). Modulation of protein structure and function by asparagine-linked glycosylation. *Chem Biol, 3*(10), 803-812.

O'Neill, H. G., Redelinghuys, P., Schwager, S. L., & Sturrock, E. D. (2008). The role of glycosylation and domain interactions in the thermal stability of human angiotensin-converting enzyme. *Biol Chem, 389*(9), 1153-1161. doi: 10.1515/BC.2008.131

Olden, K., Parent, J. B., & White, S. L. (1982). Carbohydrate moieties of glycoproteins. A re-evaluation of their function. *Biochim Biophys Acta, 650*(4), 209-232.

Ong, F. S., Lin, C. X., Campbell, D. J., Okwan-Duodu, D., Chen, X., Blackwell, W. L., . . . Bernstein, K. E. (2012). Increased angiotensin II-induced hypertension and inflammatory cytokines in mice lacking angiotensin-converting enzyme N domain activity. *Hypertension, 59*(2), 283-290. doi: 10.1161/HYPERTENSIONAHA.111.180844

Osborne, A. R., Rapoport, T. A., & van den Berg, B. (2005). Protein translocation by the Sec61/SecY channel. *Annu Rev Cell Dev Biol, 21*, 529-550. doi: 10.1146/annurev.cellbio.21.012704.133214

Papakyriakou, Athanasios, Spyroulias, Georgios A., Sturrock, Edward D., Manessi-Zoupa, Evy, & Cordopatis, Paul. (2007). Simulated Interactions between Angiotensin-Converting Enzyme and Substrate Gonadotropin-Releasing Hormone: Novel Insights into Domain Selectivity†. *Biochemistry, 46*(30), 8753-8765. doi: 10.1021/bi700253q

Ripka, J. E., Ryan, J. W., Valido, F. A., Chung, A. Y., Peterson, C. M., & Urry, R. L. (1993). N-glycosylation of forms of angiotensin converting enzyme from four mammalian species. *Biochem Biophys Res Commun, 196*(2), 503-508. doi: 10.1006/bbrc.1993.2278

Rittel, W.B., Iselin, B., Kappeler, H., Riniker, B., and Schwyzer, R. (1957). Synthese eines hochwirksamen hypertensin II-amids (L-asparagynl-L-arginyl-L-valyl-L-tyrosyl-Lisoleucyl-L-histidyl-L-prolyl-L-phenylalanin). *Helvetica Chimica Acta*(40), 614-624.

Ron, E., Shenkman, M., Groisman, B., Izenshtein, Y., Leitman, J., & Lederkremer, G. Z. (2011). Bypass of glycan-dependent glycoprotein delivery to ERAD by up-regulated EDEM1. *Mol Biol Cell, 22*(21), 3945-3954. doi: 10.1091/mbc.E10-12-0944

Sadhukhan, R., & Sen, I. (1996). Different glycosylation requirements for the synthesis of enzymatically active angiotensin-converting enzyme in mammalian cells and yeast. *J Biol Chem, 271*(11), 6429-6434.

Selin, J., Hakkarainen, P., Partanen, A., Tammi, T., & Tigerstedt, C. (2013). From political controversy to a technical problem? Fifteen years of opioid substitution treatment in Finland. *Int J Drug Policy, 24*(6), e66-72. doi: 10.1016/j.drugpo.2013.08.007

Shen, B. (2002). PCR approaches to DNA mutagenesis and recombination. An overview. *Methods Mol Biol, 192*, 167-174. doi: 10.1385/1-59259-177-9:167

Shen, X. Z., Billet, S., Lin, C., Okwan-Duodu, D., Chen, X., Lukacher, A. E., & Bernstein, K. E. (2011). The carboxypeptidase ACE shapes the MHC class I peptide repertoire. *Nat Immunol, 12*(11), 1078-1085. doi: 10.1038/ni.2107

Shen, X. Z., Lukacher, A. E., Billet, S., Williams, I. R., & Bernstein, K. E. (2008). Expression of angiotensin-converting enzyme changes major histocompatibility complex class I peptide presentation by modifying C termini of peptide precursors. *J Biol Chem, 283*(15), 9957-9965. doi: 10.1074/jbc.M709574200

Sherman, L. A., Burke, T. A., & Biggs, J. A. (1992). Extracellular processing of peptide antigens that bind class I major histocompatibility molecules. *J Exp Med, 175*(5), 1221-1226.

Sinka, L., Biasch, K., Khazaal, I., Peault, B., & Tavian, M. (2012). Angiotensin-converting enzyme (CD143) specifies emerging lympho-hematopoietic progenitors in the human embryo. *Blood, 119*(16), 3712-3723. doi: 10.1182/blood-2010-11-314781

Skeggs, L. T., Jr. (1993). Discovery of the two angiotensin peptides and the angiotensin converting enzyme. *Hypertension, 21*(2), 259-260.

Skeggs, L. T., Jr., Kahn, J. R., & Shumway, N. P. (1956). The preparation and function of the hypertensin-converting enzyme. *J Exp Med, 103*(3), 295-299.

Skeggs, L. T., Jr., Lentz, K. E., Kahn, J. R., Shumway, N. P., & Woods, K. R. (1956). The amino acid sequence of hypertensin. II. *J Exp Med, 104*(2), 193-197.

Skeggs, L. T., Jr., Marsh, W. H., Kahn, J. R., & Shumway, N. P. (1954). The existence of two forms of hypertensin. *J Exp Med, 99*(3), 275-282.

Slater, E. E., Merrill, D. D., Guess, H. A., Roylance, P. J., Cooper, W. D., Inman, W. H., & Ewan, P. W. (1988). Clinical profile of angioedema associated with angiotensin converting-enzyme inhibition. *JAMA, 260*(7), 967-970.

Soffer, R. L., & Sonnenblick, E. H. (1978). Physiologic, biochemical, and immunologic aspects of angiotensin-converting enzyme. *Prog Cardiovasc Dis, 21*(3), 167-175.

Soubrier, F., Alhenc-Gelas, F., Hubert, C., Allegrini, J., John, M., Tregear, G., & Corvol, P. (1988). Two putative active centers in human angiotensin I-converting enzyme revealed by molecular cloning. *Proc Natl Acad Sci U S A, 85*(24), 9386-9390.

Speirs, C., Wagniart, F., & Poggi, L. (1998). Perindopril postmarketing surveillance: a 12 month study in 47,351 hypertensive patients. *Br J Clin Pharmacol, 46*(1), 63-70.

Sturrock, E. D., Danilov, S. M., & Riordan, J. F. (1997). Limited proteolysis of human kidney angiotensin-converting enzyme and generation of catalytically active N- and C-terminal domains. *Biochem Biophys Res Commun, 236*(1), 16-19. doi: 10.1006/bbrc.1997.6841

Taaseh, N., Yaron, A., & Nelken, I. (2011). Stimulus-specific adaptation and deviance detection in the rat auditory cortex. *PLoS One, 6*(8), e23369. doi: 10.1371/journal.pone.0023369

Taasoli, G., & Kafilzadeh, F. (2008). Effects of dried and ensiled apple pomace from puree making on performance of finishing lambs. *Pak J Biol Sci, 11*(2), 294-297.

Taastrom, A., & Sondergaard, I. (2004). [Histamine poisoning after eating tuna burger]. *Ugeskr Laeger, 166*(38), 3307-3308.

Tigerstedt, N. M., Aavik, E., Lehti, S., Hayry, P., & Savolainen-Peltonen, H. (2009). Mechanisms behind the synergistic effect of sirolimus and imatinib in preventing restenosis after intimal injury. *J Vasc Res, 46*(3), 240-252. doi: 10.1159/000167272

Tigerstedt, N. M., Savolainen-Peltonen, H., Lehti, S., & Hayry, P. (2010). Vascular cell kinetics in response to intimal injury ex vivo. *J Vasc Res, 47*(1), 35-44. doi: 10.1159/000231719

Towler, P., Staker, B., Prasad, S. G., Menon, S., Tang, J., Parsons, T., . . . Pantoliano, M. W. (2004). ACE2 X-ray structures reveal a large hinge-bending motion important for inhibitor binding and catalysis. *J Biol Chem, 279*(17), 17996-18007. doi: 10.1074/jbc.M311191200

Trombetta, E. S., & Helenius, A. (1998). Lectins as chaperones in glycoprotein folding. *Curr Opin Struct Biol, 8*(5), 587-592.

van Berkel, P. H., Geerts, M. E., van Veen, H. A., Kooiman, P. M., Pieper, F. R., de Boer, H. A., & Nuijens, J. H. (1995). Glycosylated and unglycosylated human lactoferrins both bind iron and show identical affinities towards human lysozyme and bacterial lipopolysaccharide, but differ in their susceptibilities towards tryptic proteolysis. *Biochem J, 312 (Pt 1)*, 107-114.

Varki, A. (1993). Biological roles of oligosaccharides: all of the theories are correct. *Glycobiology, 3*(2), 97-130.

Voronov, S., Zueva, N., Orlov, V., Arutyunyan, A., & Kost, O. (2002). Temperature-induced selective death of the C-domain within angiotensin-converting enzyme molecule. *FEBS Lett, 522*(1-3), 77-82.

Watermeyer, J. M., Kroger, W. L., O'Neill, H. G., Sewell, B. T., & Sturrock, E. D. (2010). Characterization of domain-selective inhibitor binding in angiotensin-converting enzyme using a novel derivative of lisinopril. *Biochem J, 428*(1), 67-74. doi: 10.1042/BJ20100056

Wei, L., Alhenc-Gelas, F., Corvol, P., & Clauser, E. (1991). The two homologous domains of human angiotensin I-converting enzyme are both catalytically active. *J Biol Chem, 266*(14), 9002-9008.

Williams, T. A., Michaud, A., Houard, X., Chauvet, M. T., Soubrier, F., & Corvol, P. (1996). Drosophila melanogaster angiotensin I-converting enzyme expressed in Pichia pastoris resembles the C domain of the mammalian homologue and does not require glycosylation for secretion and enzymic activity. *Biochem J, 318 (Pt 1)*, 125-131.

Withka, J. M., Wyss, D. F., Wagner, G., Arulanandam, A. R., Reinherz, E. L., & Recny, M. A. (1993). Structure of the glycosylated adhesion domain of human T lymphocyte glycoprotein CD2. *Structure, 1*(1), 69-81.

Woodman, Z. L., Schwager, S. L., Redelinghuys, P., Carmona, A. K., Ehlers, M. R., & Sturrock, E. D. (2005). The N domain of somatic angiotensin-converting enzyme negatively regulates ectodomain shedding and catalytic activity. *Biochem J, 389*(Pt 3), 739-744. doi: 10.1042/BJ20050187

Wormald, M. R., & Dwek, R. A. (1999). Glycoproteins: glycan presentation and protein-fold stability. *Structure, 7*(7), R155-160.

Yamaguchi, D., Kawasaki, N., Matsuo, I., Totani, K., Tozawa, H., Matsumoto, N., . . . Yamamoto, K. (2007). VIPL has sugar-binding activity specific for high-mannose-type N-glycans, and glucosylation of the alpha1,2 mannotriosyl branch blocks its binding. *Glycobiology, 17*(10), 1061-1069. doi: 10.1093/glycob/cwm074

Yan, A., & Lennarz, W. J. (2005). Unraveling the mechanism of protein N-glycosylation. *J Biol Chem, 280*(5), 3121-3124. doi: 10.1074/jbc.R400036200

Yang, H. Y., & Erdos, E. G. (1967). Second kininase in human blood plasma. *Nature, 215*(5108), 1402-1403.

Zambidis, E. T., Park, T. S., Yu, W., Tam, A., Levine, M., Yuan, X., . . . Peault, B. (2008). Expression of angiotensin-converting enzyme (CD143) identifies and regulates primitive hemangioblasts derived from human pluripotent stem cells. *Blood, 112*(9), 3601-3614. doi: 10.1182/blood-2008-03-144766

Zou, K., Maeda, T., Watanabe, A., Liu, J., Liu, S., Oba, R., . . . Michikawa, M. (2009). Abeta42-to-Abeta40- and angiotensin-converting activities in different domains of angiotensin-converting enzyme. *J Biol Chem, 284*(46), 31914-31920. doi: 10.1074/jbc.M109.011437

Zou, K., Yamaguchi, H., Akatsu, H., Sakamoto, T., Ko, M., Mizoguchi, K., . . . Michikawa, M. (2007). Angiotensin-converting enzyme converts amyloid beta-protein 1-42 (Abeta(1-42)) to Abeta(1-40), and its inhibition enhances brain Abeta deposition. *J Neurosci, 27*(32), 8628-8635. doi: 10.1523/JNEUROSCI.1549-07.2007